NOTICE

The quality of this microform is heavily dependent upon the quality of the original thesis submitted for microfilming. Every effort has been made to ensure the highest quality of reproduction possible.

If pages are missing, contact the university which granted the degree.

Some pages may have indistinct print especially if the original pages were typed with a poor typewriter ribbon or if the university sent us an inferior photocopy.

Reproduction in full or in part of this microform is governed by the Canadian Copyright Act, R.S.C. 1970, c. C-30, and subsequent amendments.

AVIS

La qualité de cette microforme dépend grandement de la qualité de la thèse soumise au microfilmage. Nous avons tout fait pour assurer une qualité supérieure de reproduction.

S'il manque des pages, veuillez communiquer avec l'université qui a conféré le grade.

La qualité d'impression de certaines pages peut laisser à désirer, surtout si les pages originales ont été dactylographiées à l'aide d'un ruban usé ou si l'université nous a fait parvenir une photocopie de qualité inférieure.

La reproduction, même partielle, de cette microforme est soumise à la Loi canadienne sur le droit d'auteur, SRC 1970, c. C-30, et ses amendements subséquents.

ION/RADICAL AND ION/MOLECULE COMPLEXES AND ION STRUCTURE ASSIGNMENTS IN THE GAS PHASE

By Martine C. Bissonnette

A Thesis
Presented to the University of Ottawa
in fulfillment of the
thesis requirement for the degree of
Master in Science
in
the Department of Chemistry

University of Ottawa

January 1991

ISBN 0-315-68029-6

UNIVERSITÉ D'OTTAWA
UNIVERSITY OF OTTAWA

A Papa et Maman

&

Steve

REMERCIEMENTS

Après avoir fini de rédiger ma thèse dans la langue de Shakespeare, je me suis permise d'y glisser quelques paragraphes dans la langue de Molière, ma langue maternelle.

A mon arrivée à Ottawa, jamais je ne me serais doutée que j'y passerais les deux prochaines années car je n'y étais que pour un emploi d'été. Ma curiosité pour la spectrométrie de masse et ma première rencontre avec mon superviseur, Dr John L. Holmes, ont contribué à ma visite "allongée" de la capitale nationale.

Je voudrais particulièrement remercier Dr Holmes pour m'avoir accueillie dans son laboratoire les bras ouverts et pour avoir été toujours disponible pour répondre à mes mille et une questions et pour discuter des derniers résultats souvent imprévus! Ses conseils, qu'ils soient reliés à mon projet de recherche, à une présentation ou à la recherche d'un emploi futur ont toujours été très appréciés. Je tiens à souligner la patience de mon superviseur lors de la correction des épreuves de cette thèse, l'écriture d'un ouvrage de cette taille en anglais étant une tâche assez ardue pour une francophone. Un gros merci au Dr A.A. Mommers, Sander, pour m'avoir permis d'apprendre la "mécanique" du spectromètre de masse et pour ses bons trucs d'informatique. Merci d'avoir branché l'imprimante au laser à l'ordinateur de ma table de travail, ça m'a sauvé un temps fou! Il ne faudrait surtout pas que j'oublie le Dr John Krause (John pour les intimes) qui m'a permis d'avoir une expérience inoubliable en me faisant participer aux ateliers organisés pour les étudiants(tes) du secondaire. Merci John, j'ai adoré participer à "Kiddie-Chem" avec les jeunes. J'allais oublier, merci d'avoir acheté les petites choses qui rendent le travail plus agréable: manuels, logiciels d'informatique, etc... Un gros

merci au Dr Fred P. Lossing pour toutes les analyses thermochimiques et pour ses bonnes blagues. Sans oublier, le Dr Clem Kazakoff pour avoir effectué plusieurs analyses par chromatographie gazeuse-spectrométrie de masse (GC-MS) à la dernière minute et pour ses excellents conseils concernant les films à voir et à ne pas voir...

Je ne pourrais pas arrêter les remerciements sans mentionner le support et l'encouragement de mes collègues étudiants et post-doc. Tout d'abord, Dr George Mathai sans qui je serais probablement encore en train de me demander comment remplacer des atomes d'hydrogène par des deuteriums dans les molécules dont j'avais besoin. Martin Sirois, "vieille" connaissance de l'Université de Montréal, avec qui les conversations sont souvent plus ou moins scientifiques, merci pour l'encouragement et pour ton amitié. Merci à David Harnish, Hongwen Chen et au Dr Jian-Ru Cao pour les conseils et les discussions. Dave, merci pour les billets d'aérobique!

J'aimerais encore une fois remercier le Dr John Holmes pour m'avoir permis de présenter un poster à la conférence de l'ASMS à Tucson, Arizona. C'est une conférence et un voyage que je n'oublierai jamais, merci!

Finalement, j'aimerais remercier Steve, mes parents et les gens qui m'entourent pour leur encouragement, leur patience et leur support continuel.

Janvier 1991.

ABSTRACT

In the past few years, many "new" ion structures have been identified in gas the phase. Amongst these "new" ions are proton-bridged complexes, yild and distonic ions and ion-dipole complexes. They are often involved in fragmentation mechanisms as intermediate species. Their idendification is based on the thermochemistry and dissociation behaviour.

The fragmentation mechanism of ionized neopentanol, $(CH_3)_3CCH_2OH^{+\cdot}$, has been studied in great detail along with other $C_5H_{12}H^{+\cdot}$ isomers. Thermochemical and dissociation characteristics were extremely useful to compare the various isomers. The use of ^{13}C and D labelling was found an essential tool to establish the relation between the other species involved in the dissociation of neopentanol. The involvement of $(CH_3)_2C^{\cdot}CH_2{}^{+}(O)HCH_3$, $(CH_3)_3C^{+\cdot}(O)HCH_2$ and $(CH_3)_2(^{\cdot}CH_2)CCH_2{}^{+\cdot}OH_2$ was essential to explain the H/D label exchange occuring upon fragmentation of neopentyl alcohol. An ion-dipole complex between methanol and ionized methyl propene is proposed as the final intermediate which leads directly to the products, methanol and ionized methyl propene.

The results of the investigation of $C_7H_5^+$ ions from various precursor molecules are also described. Using the thermochemistry, estimations were made to obtain the relative stability of a number of structural isomers. It was found that the majority of these structures are thermodynamically possible. The following compounds, which all produce $C_7H_5^+$ ions, were studied: benzyl acetate, benzyl formate, benzyl alcohol, 2-bromocyclopropabenzene, 1,6-heptadiyne and 1,5-decadiyne. The $C_7H_5^+$ ions produced from the three benzyl compounds seem to have identical behaviour i.e. the thermochemical and dissociative properties are the same. Thus, it is concluded that they are the same ions. According to the metastable ion (MI) mass spectra and the He collision induced dissociation (CID) of m/z 89 ions, it is suggested that four (4) structures exist. The proposed structures are as follows: the cyclopropaphenyl cation (from 2-bromocyclopropabenzene), $CH{\equiv}C\text{-}{}^{+}CH\text{-}CH{=}CH\text{-}C{\equiv}CH$ (from 1,6-heptadiyne), $CH{\equiv}C\text{-}CH{=}CH\text{-}C{\equiv}C\text{-}{}^{+}CH_2$ (from 1,5-decadiyne) and $CH{\equiv}C\text{-}CH{=}C(C{\equiv}CH)\text{-}{}^{+}CH_2$ (from benzyl alcohol, benzyl formate and benzyl acetate).

TABLE OF CONTENTS

FIGURES

TABLES

CHAPTER 1

INTRODUCTION

1.1 What is mass spectrometry?

The mass spectrometer, as its name implies, is an instrument used to measure the mass of an ionized compound. Actually, it measures a mass-to-charge ratio and gives no information on the structure of the ion. The structure of an ion is loosely defined as the arrangement of the atoms in the ion i.e. which atoms are bonded together, but without a detailed description of the ion's geometry. For small molecules, few possible structures exist for the ionized fragment and the neutral which is lost and identification of their structures is often easy. However, as the number of atoms increases, the task of assigning a structure to an ion becomes more difficult.

In earlier years, say up to about 1970, scientists tried to predict ion structures in the gas phase using analogies from the condensed phase, from gas phase photochemistry and thermal decomposition reactions. However, these were found often to be inadequate to describe the behaviour of ions in the gas phase. It is now known that complete classes of ions which have no stable neutral counterparts are stable species in the gas phase. Furthermore, trends and relationships in thermochemical data for organic neutral molecules (e.g. additivity) were found to be completely different for organic ions. The structures of larger ions have to be determined using indirect evidence such as thermochemical data, structure of the smaller fragments and

isotopic labelling. This approach will be discussed in Chapter 5 of this thesis.

The gas phase chemistry is not only useful to study gas phase ions but was also found to be very useful to perform novel studies such as the determination of the sequence of amino acids in peptides. Therefore, it is important to set a strong background for structure and thermochemistry of gas phase ion and neutrals.

Fortunately, advances in technology have allowed us to build more powerful instruments and obtain much greater sensitivity and resolution. The field of mass spectrometry is in a state of constant expansion and is nowadays used for much more than molecule identification and petroleum analysis. The coupling of a mass spectrometer with various instruments such as the gas chromatograph (GC), inductively coupled plasma (ICP) and high pressure liquid chromatography (HPLC) has seen this technique expand into the fields of environmental science, biochemistry and pharmacology.

1.2 What is in this thesis?

The work described in this thesis can be divided in two parts. The first concerns the elucidation of fragmentation mechanisms and the second is the generation and structure elucidation of some isomeric gas phase ion species. Both projects involved the use of ion and neutral thermochemistry and dissociative properties of ions.

Chapter 2 briefly describes the evolution of mass spectrometry and of the mass spectrometer in relation with the advancement of technology. A concise description of the VG-Analytical ZAB-2F mass spectrometer is made because it is the major instrument used in this work. A short description and reference to other instruments used in this work is also made. Finally, some basic concepts essential to understanding of mass spectra are explained.

In chapter 3, the thermochemistry associated with gas phase ion chemistry is discussed and the labelling technique is briefly described. There are also sections on the dissociative techniques: metastable ion (MI), collisional activation (CA), charge stripping (CS), and, more recently, collision induced dissociative ionization (CIDI) and neutralization-reionization (NR) mass spectrometry. Each section contains examples where the specific technique has been found extremely useful to solve either a structure assignment or fragmentation mechanism problem.

In chapter 4, definitions of unconventional ions: ylid and distonic ions, ion/radical, ion/molecule and proton-bridged complexes are given. Some basic kinetic rules and previously established general rules are explained. Since these ions can be difficult to identify experimentally, the use of theoretical calculation has proved an essential aid to their discovery. On the basis of the combination of theoretical and experimental results, it has been possible to establish some criteria for the existence of unconventional ions. Various examples where these ions are involved are described with more emphasis on ion/molecule and ion/radical complexes because they are the main topic of chapter 5.

Chapter 5 describes the "thinking" process used to determine the fragmentation mechanism of metastable ionized neopentyl alcohol. It describes the thermochemistry as well as the dissociative properties of various isomeric ions. In this study, the use of labelling was found an essential tool in the determination of the various intermediates participating in the metastable dissociation of the neopentyl alcohol molecular ion.

In the last chapter, $C_7H_5^+$ ions from various precursors were briefly studied. The possible structure of these ions was established mainly using their thermochemical data and dissociative properties. The use of metastable ion (MI) mass spectra was found to be a very useful tool in the attempt to clearly distinguishing the ions whereas the CA processes were helpful to assign a structure to each $C_7H_5^+$ ion.

CHAPTER 2

THE MASS SPECTROMETER: A CENTURY OF HISTORY.

2.1 The Pioneers.

There are many discoveries directly related to mass spectrometry. The scope of this section is not to discuss each of them but to identify the major turning points of mass spectrometry. A thorough description of these discoveries can be found in references 1 and 2.

The birth of mass spectrometry (MS) would not have occurred if E. Goldstein[3] had not discovered the existence of rays of positive particles in 1886. The confirmation of the existence of these positive particles was made by W. Wien[4], in 1898, when he noticed that he could deflect them in a magnetic field. J.J. Thomson, Nobel Laureate of 1906, deserves most of the credit for the birth of mass spectrometry. Also named "the Father of Mass Spectrometry", he designed the parabola mass spectrograph which is the direct precursor of today's mass spectrometer. In 1912, he made his major contribution to mass spectrometry, with the discovery of the two isotopes for Neon (m/z 20 and 22); although at that early date he thought that m/z 22 was NeH_2 and did not realize until a few years later that it was an isotope of Neon. F.W. Aston was Thomson's student and continued the great work by building a mass spectrograph remarkably

similar to today's apparatus and was the first person to use the term "mass spectrum". His greatest contribution to mass spectrometry was the observation that nucleic masses of atoms are not exact multiples of units being slightly different from their nominal mass number. Some of the other important contributors to mass spectrometry are: Dempster (1918) who discovered many other isotopes and their relative abundances, Conrad (1930) who performed the first chemical application of mass spectrometry to organic compounds, Nier and co-workers (1940) who were able to isolate and separate uranium-235 and 238 allowing the construction of nuclear power plants and Hipple and Stevenson (1943) who performed the first direct measurements of the ionization potentials of free radicals.

Nowadays, the list of important contributions to mass spectrometry is very long (by looking at the specialized journals appearing in the past 20 years: Organic Mass Spectrometry, International Journal of Mass Spectrometry and Ion Processes, Mass Spectrometry Reviews and more recently, Journal of the American Society for Mass Spectrometry) and many "sub-fields" to mass spectrometry have developed, each comprising very important contributions to general mass spectrometry.

2.2 The Evolution of the Instrument.

A description of the first instruments and their uses will be briefly made in this section. Again, reference 2 describes the complete history of the mass spectrometer's evolution. The following lines are only a summary of the most important instruments. Of course, Thomson's

parabola spectrograph is the forerunner of today's instruments. Its operation consisted of forming ions in a discharge tube and collimating them through an opening in a cathode. The ions then enter the analyzer and a photographic plate is used as the detecting device. The analyzer is composed of parallel and coterminous electric and magnetic fields which separate the ions according to their mass to charge ratio. The major disadvantage of this instrument was the great loss of sensitivity as the resolution was increased. The ions were separated according to their mass to charge (m/z) ratio by applying two magnetic fields simultaneously. Aston's instrument was very similar to Thomson's except that a single magnetic field was used and that ions were detected using velocity focusing i.e. focusing according to the momenta of the ions (see section 2.3.1.2 for the equations of motion for ions in a magnetic field). Aston's mass spectrograph had a better resolution than Thomson's by a factor of ≈10; for example it could separate an ion of mass 28 from an ion of mass 28.2 whereas Thomson's could not separate m/z 28 from 29. Dempster (1916) used a different approach to build his mass spectrometer: instead of using velocity focusing, he used direction focusing, meaning that an ion of a given mass and energy diverging from a slit will be focused through a 180° magnet deflection (Fig 1). This instrument was found to be very effective and was the basis for the prototype commercial mass spectrometer built by Consolidated Engineering Corporation (CEC) in 1942[5]. Note that the two earlier

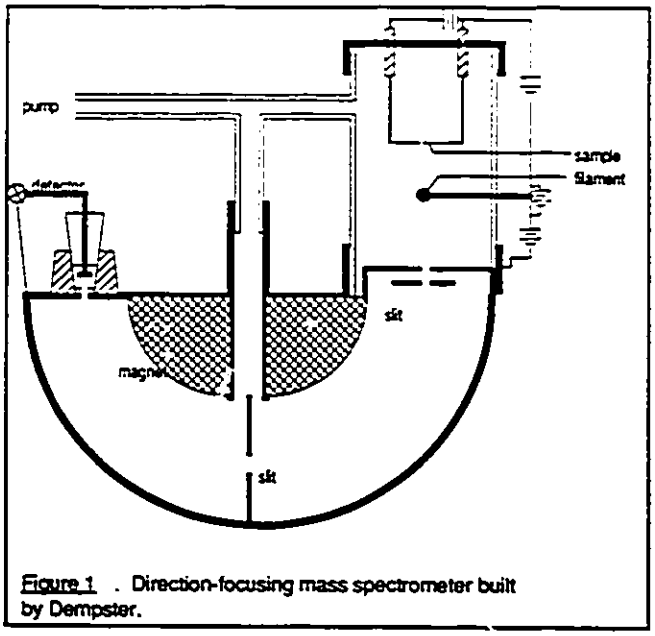

Figure 1 . Direction-focusing mass spectrometer built by Dempster.

instruments (Thomson and Aston) used high voltage discharge tubes to produce ions whereas Dempster's instrument produced ions by bombarding the samples with electrons emitted from a heated filament just as in almost all commercial instruments today.

Thus, by 1920, the mass spectrometer had the potential to determine masses, to measure relative abundances of ions and to perform electron impact studies. Not until 1940 did people realize the possibilities of this very versatile instrument. The period between 1920 and 1940 was spent on trying to improve the instrument's resolution and its precision. A very important new type of instrument was built by Nier in 1940, the magnetic sector analyzer having a 60° angle. It had many advantages, such as reducing the size of the instrument (smaller magnet) and improving resolution (important when determining isotopes).

The petroleum industry[5] revived the interest in mass spectrometers when it was realized that the instrument could be used to analyze complex hydrocarbon mixtures. It is around this period that the first commercial spectrometer was built (1942). During this decade, the mass spectrometer became a routine analysis instrument, particularly in the petroleum and related industries, accounting for approximately 80% of mass spectrometer users. Many variations of Dempster's and Nier's instruments were built, but the major improvement did not come from the instrument's design itself (although higher accelerating voltages became obtainable and better electromagnets were built), it arose from major advances in electronics (the transistor and computers) and the advent of ultrahigh vacuum technology. The change from vacuum tubes to transistors, allowed the recording of a complete normal mass spectrum to be improved in speed

from 15 minutes in the mid-1940s to three minutes in the mid-1950s to seconds in the 1980s. The high vacuum techniques allowed for much greater sensitivity and better mass resolution. Obtaining better resolution permitted the elucidation of molecular structures whereas the greater sensitivity allowed the analysis of trace amounts of compounds in samples. The 1960s saw the birth of new analytical techniques such as combination of mass spectrometers with gas chromatography (GC-MS) and the use of the heated direct insertion probe to analyze involatile solid samples. The large interest in mass spectrometry as an analytical tool in the past 30 years has resulted in the development of many techniques; e.g. high performance liquid chromatography (HPLC-MS), fast atom bombardment (FAB-MS), inductively coupled plasma (ICP-MS).

Finally, the unceasing evolution of electronic technology and computer science has reduced the instrument from a "three ton beast" to a bench top instrument and, from "wild guess" interpretations of mass spectra to few and limited choices when assigning a structure to a molecule from its mass spectrum. The main advantages gained from computers are speed of data analysis and the operation of the instrument itself.

There are many other types of mass spectrometers such as time-of-flight (TOF), quadrupole, ion cyclotron resonance (ICR) instruments etc, but the work performed in this thesis essentially involves sector instruments, so only the latter will be discussed here.

2.3 The Sector Instruments.

The work performed in this thesis involved the use of three different instruments: the VG ZAB-2F (Vacuum Generators), the GEC-AEI MS-902S (Associated Electrical Industries) and the electron energy selector mass spectrometer. However, the emphasis will be on the ZAB-2F because the majority of the work has been performed using that instrument. Generally, all mass spectrometers have the same three functions: *generate* and *accelerate* ions, *separate* these ions and *detect* them.

2.3.1 The ZAB-2F Mass Spectrometer.

The VG ZAB-2F is a double focusing, reversed geometry instrument. It is called reversed geometry because, as opposed to more traditional instruments, the electrostatic (energy) analyzer is located after the momentum analyzer (Fig 2). This configuration allows the isolation and study of the dissociation of mass selected ions taking place in the second field free region (2 FFR) of the instrument without interference of ions from other reactions. The following is a description of the modified ZAB-2F located at the University of Ottawa. For the description of the unmodified instrument, see reference 6.

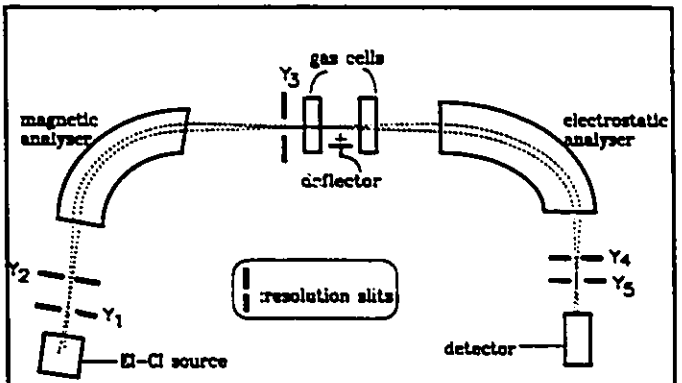

Figure 2. The VG Analytical ZAB-2F double focusing mass spectrometer of reversed geometry.

2.3.1.1 The Ion Source.

The samples may be introduced into the source of the instrument in three different manners (Fig 3). One of them is via a variable leak inlet (valve) and capillary which has the advantage of providing constant pressures throughout the experiments and works well with gases, liquids and volatile solids. When studying non-volatile compounds, the probe, on which a piece of glass capillary containing the sample is placed, is inserted into the source housing. Another method for introducing volatile liquid samples is a septum-injection inlet which allows vapours to diffuse slowly from the heated reservoir into the source through a capillary tube. However, this last method does not produce constant sample pressures as the sample in the reservoir is continuously depleted. An optimal observed sample pressure, which avoids ion-molecule reactions in the ion source is $\approx 10^{-6}$ torr.

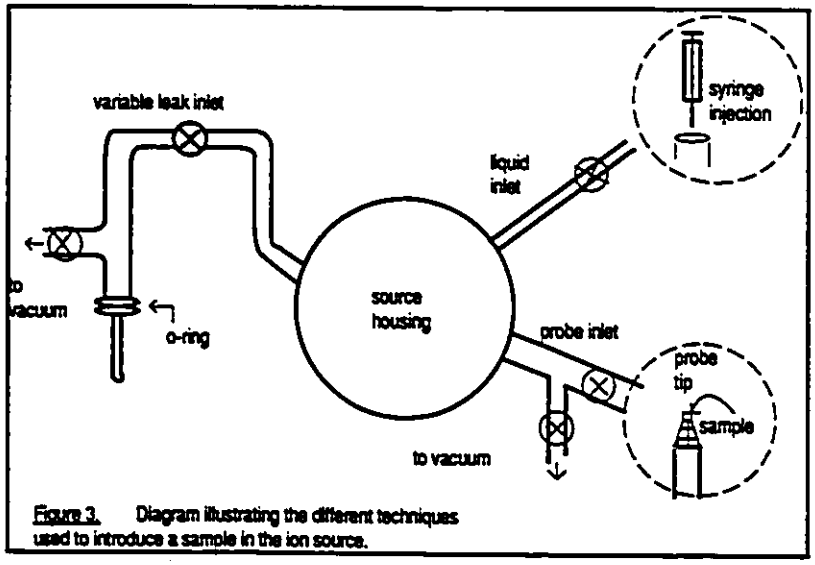

Figure 3. Diagram illustrating the different techniques used to introduce a sample in the ion source.

The ion source, as the name implies, is where the ions are generated. The samples are ionized upon collision with a beam of electrons emitted by a Tungsten filament. Generally, the energy of this beam is ca 70 eV. The process taking place is described by equation 1:

$$M + e \rightarrow M^{+\cdot} + 2e \qquad [1]$$

However, the ionization energy of typical organic molecules is approximately 10 eV, thus many of the molecular ions $M^{+\cdot}$ will contain excess energy, enough energy to decompose into fragments which may also decompose further

$$\begin{aligned} M^{+\cdot} &\rightarrow B^{+} + A^{\cdot} \\ &\rightarrow C^{+\cdot} + D \\ &\rightarrow C^{+\cdot} \rightarrow E^{+} + F^{\cdot} \text{ etc...} \end{aligned} \qquad [2]$$

A repeller (plate on which a excess positive voltage is applied) located in the source pushes the newly formed positive ions towards the source exit. The ions then fall into a large potential gradient and are accelerated towards the first field free region (1 FFR). The accelerating voltage (V_{acc}) is typically 8 kV. Therefore, all source generated ions with a mass m and a charge z will have the same kinetic energy as they leave the source

$$\tfrac{1}{2} mv^2 = z V_{acc} \qquad [3]$$

where z=ne, v is the velocity of the ion, n is the number of charges, and if n=1, z=e, the electron charge. This last equality is valid regardless of the mass of the ion. In this work, unless specified, singly charged ions are described i.e. n=1.

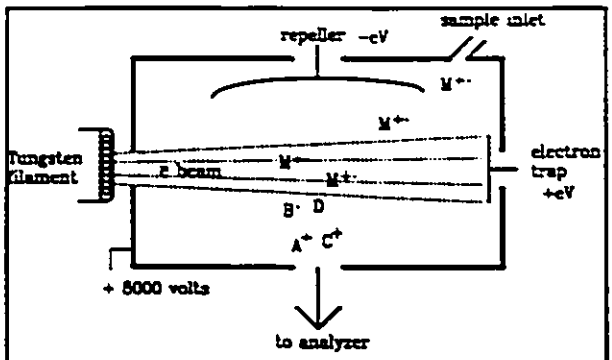

Figure 4. Diagram of an electron impact/chemical ionization source.

2.3.1.2 The Momentum Analyzer.

After being accelerated, the ions travel through the first field free region and pass into a variable magnetic field. The ions traversing this magnetic field, which is perpendicular to their motion, will follow a circular path of radius, r, and the equation of motion is

$$mv^2/r = Bzv \quad \text{or} \quad B=mv/zr \qquad [4]$$

The magnet is, therefore, a momentum analyzer. (However, it is usually referred to as a mass analyzer.) Equation [3] showed that the translational energy of source generated ions is zV_{acc} and, by substitution in [4], we obtain the following equation

$$m/z = (B^2 r^2)/2V_{acc} \quad [5]$$

Thus, by varying the strength of the magnetic field B, one can select ions of desired m/z since r and V_{acc} are kept constant. By scanning the magnet and detecting the ions right after they exit the magnetic field one can obtain the single focusing mass spectrum of the source generated ions. The resolution is defined as the ability to separate a pair of peaks. It can also be defined using $R=\Delta m/m$ where R is the resolution, m is the mass of interest and Δm is the difference between the mass of interest and the mass of the peak next to it (see section 3.3.1). The magnetic sector focuses the ion beam along the r_B radius in a direction perpendicular to the magnetic field. In figure 5, it is shown that if the ion enters and exits the magnetic field perpendicularly to the field boundaries, the point of origin of the ions, the apex of the field and the point of focus of the ions are collinear (long dashed lines). It should be noted that the dispersion of the ions is independent of the sector angle but the path length of the ions will increase as the angle becomes smaller (Fig 5). However, the resolution is quite low when using only one sector (generally less than 5000) and the use of an electrostatic analyzer placed after the magnet greatly improves this resolution. It also allows more experiments to be performed, as described below.

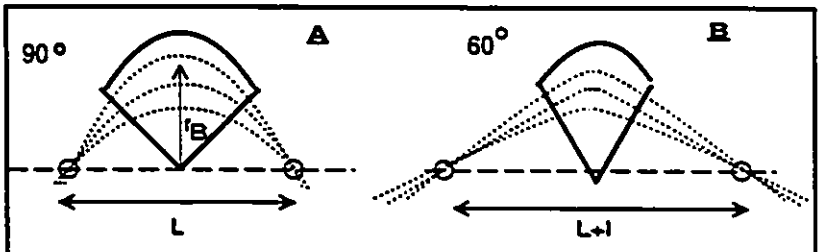

Figure 5- The distance travelled by the ions increases at the angle of the magnet increases.

2.3.1.3 The Second Field Free Region (2 FFR).

The second field free region is a very important part of the ZAB-2F. It contains two collision cells (Fig 6), (one of which was not present on the original instrument) cell 1 and cell 2. A deflector electrode was also added to the instrument[7] between cell 1 and cell 2, a full description of the modifications is included in reference 6. The two cells are 10 cm apart, collision cell 1 being 10 mm long and cell 2 being 20 mm long. Collision gases may be introduced independently in both cells, each having its own pressure gauge and diffusion pump nearby. The cells are electrically isolated and may support positive or negative potentials. As will be discussed in the following chapter, it is useful to apply a voltage to the cells because it allows one to separate processes taking place inside and outside the cell. The deflector electrode is a simple chargeable plate enclosed in a grounded metal box. When applying a voltage to this plate, ions are deflected away from the beam path and only neutral fragments may then enter cell 2. A newly built cell has been added to the ZAB-2F[6]; this metal vapour cell was designed to perform Neutralization-Reionization Mass Spectrometry (NRMS) experiments which allow the study of neutrals generated from positively charged ions by electron transfer (see section 3.6). The efficiency of this electron transfer is affected by the energy defect Q_N of the reaction. In general, the most efficient conditions are when $Q_N=(IE_{metal}-IE_{neutralization\ of\ compound})$ is close to zero. However, a $Q_N>0$ is also used to ensure that one does not generate the neutral with enough internal energy to fragment. Some metals have lower IE than Xe (Cd=9.0 eV, Hg=10.4 eV, Na=4.7 eV, Xe=12.1 eV[9]) and many organic ions have an IE of about 10 eV, therefore, they produce *exothermic* neutralizations instead of the endothermic reactions obtained with Xe. The

gas and metal vapour cells combined with the deflector electrode allowed many new experiments to be carried out on the ZAB; they will be discussed at length in the next chapter of this thesis.

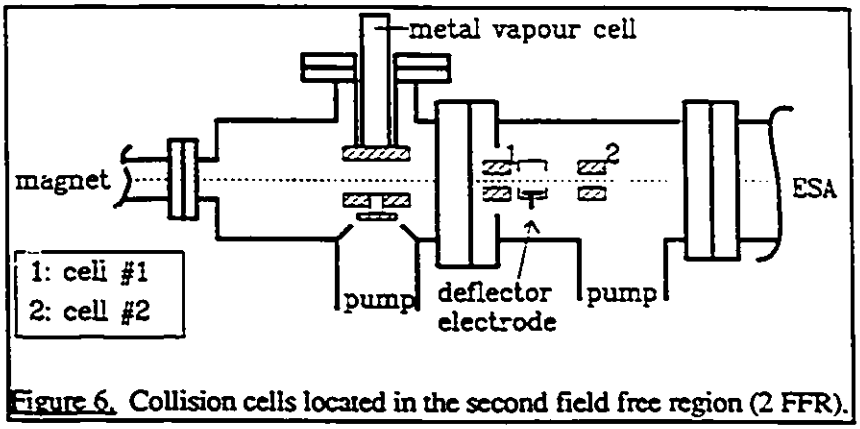

Figure 6. Collision cells located in the second field free region (2 FFR).

2.3.1.4 The Energy Analyzer.

The next part of the instrument is the electrostatic energy analyzer (ESA). It consists of two parallel curved plates of radius R across which a potential, E, is applied. The electric field produced, E, influences the trajectory of the ions. When the centrifugal force exerted on the ion is equal to the electric force (E), the ion is transferred through the ESA

$$mv^2/R = zE \qquad [6]$$

Therefore, ions may be separated according to their kinetic energy. By substituting equation 3 in equation 6, we obtain, for source generated ions:

$$E = 2V_{acc}z/R \qquad [7]$$

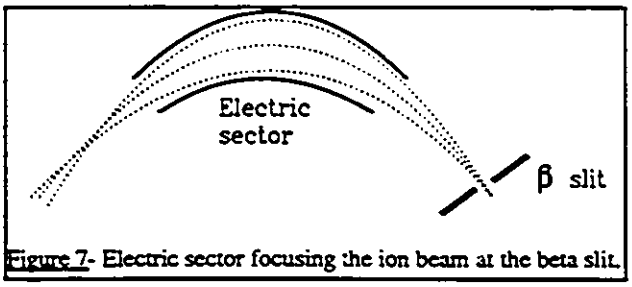

Figure 7- Electric sector focusing the ion beam at the beta slit.

By setting the E at the voltage given by equation 7, the detection of all mass selected, source generated ions is possible. The electric sector selects an ion beam according to the velocity of the ions. Upon applying a certain electric field to the plate, it is possible to select only those ions which have the required energy to travel along a curve of radius r_E. The ions are brought to focus at the ß-slit. When an ion detection device is located after the electric sector and the magnet is scanned, a double focusing mass spectrum of the sample is obtained. This supplementary focusing device allows a much greater mass resolution. Further mass and energy resolution may be obtained by narrowing the Y slits (see Figure 2) but this will lead to a loss of sensitivity.

2.3.1.5. The Detector.

The last part of the instrument is the ion detector, which consists of an off-axis electron multiplier. The term off-axis refers to the fact that the ion flux collides with a negatively charged conversion dynode which emits electrons, the latter are then accelerated and amplified by series of dynodes. Finally, all the electrons are collected on the anode and the current therefrom produces a signal which is electronically amplified. The sensitivity of the instrument is about 10^{-16} A of ion current.

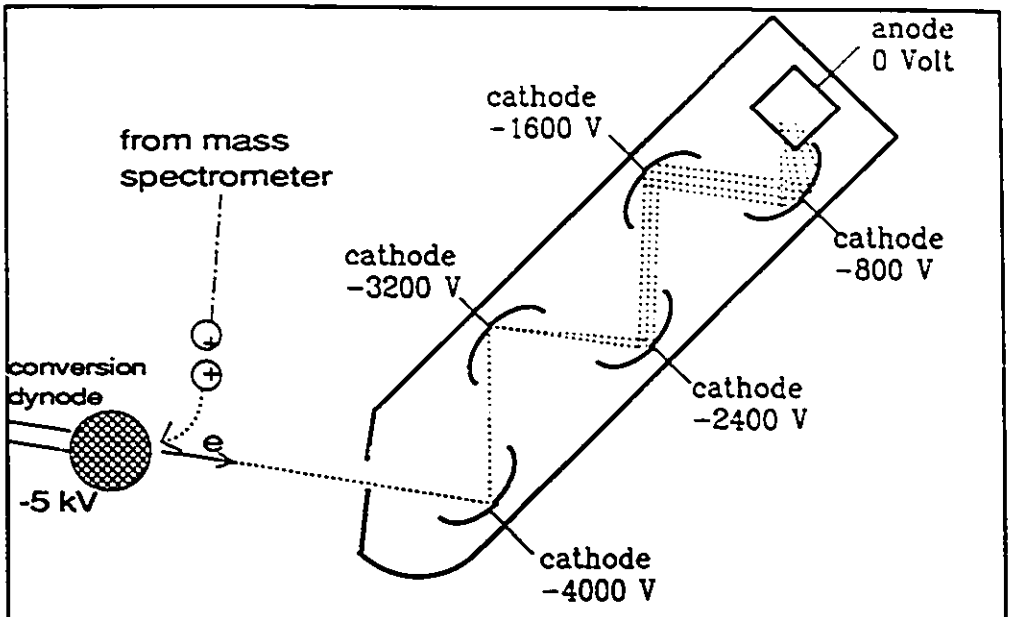

Figure 8- Diagram of an electron multiplier, the conversion dynode converts positively charged ions into a beam of electrons and the dynodes which have a difference of potential of 800 V permit the acceleration of the multiplied electrons.

2.3.2. The AEI-902S Mass Spectrometer.

The second instrument used in this work is the GEC-AEI-902S (Fig 9). It is a forward geometry mass spectrometer with the electric sector being before the magnetic sector (as opposed to the ZAB-2F)[10]. The sample introduction is similar to the ZAB but there is no septum inlet. This instrument is well suited to measure the appearance energy (AE) of ions produced by metastable dissociations in the first FFR. An important feature is a Daly detector which has the advantage that metastable ion signals may be increased relative to source generated ions. A complete description of the method used to obtain AE measurements for metastable ions is found in reference 11 and a short description will be given in the next chapter.

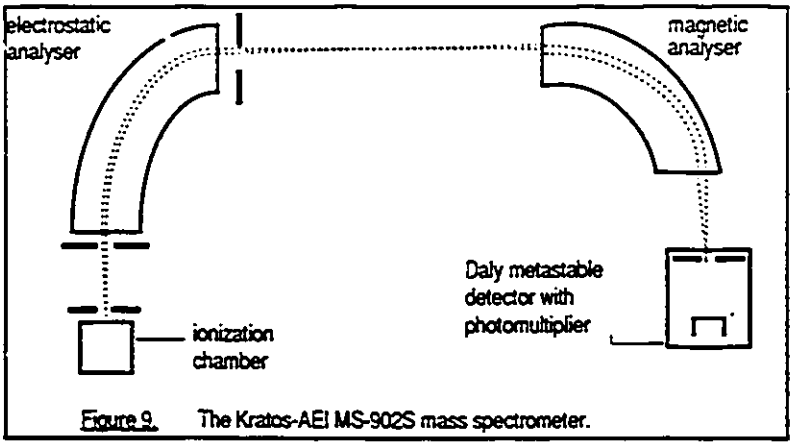

Figure 9. The Kratos-AEI MS-902S mass spectrometer.

2.3.3. The Electrostatic Electron Energy Selector and Quadrupole Mass Analyser.

The adiabatic ionization and appearance energy values (IE and AE) were measured with an electrostatic energy selector and quadrupole mass spectrometer. These values are accurate to ± 0.05 eV. For a complete description of the instrument and its operation refer to reference 12. This instrument has the major advantage of allowing the mass resolution of the quadrupole mass filter to be easily adjusted and its high sensitivity when resolution was not required.

2.4. The Behaviour of Ions.

Ions formed by 70 eV electron bombardment have wide ranges of internal energies and the electron impact mass spectra hardly change when electron energies are raised above 20 eV. So far, we have considered only ions formed in the source which contain insufficient energy for them to decompose before reaching the final detector. These are thus termed "stable ions".

However, there are other types of ions[13] which are unstable or metastable. The latter are ions sufficiently stable to leave the source but which decompose before arriving at the collector. These types of ions will be thoroughly discussed in chapter 3. Unstable ions are formed with so much internal energy that they decompose before leaving the ionization chamber. Thus, a very complex mixture of ions is formed in the source, forming the complete electron impact mass spectrum of the sample.

The rate constant, k, of an ion decomposition process rises rapidly with increasing internal energy to reach a constant value at highest energies[14] (Fig 10). This is logical because the shortest decomposition time is $\approx 10^{-13}$-10^{-15}s (Fig 11) (i.e. vibrational frequencies) and no matter how much internal energy the ion contains, the fastest decomposition is about 10^{-15}s. Metastable ions decompose in the field free regions and the rate constants associated to them is, 10^{5}-10^{7} s^{-1}. For example, an ion of m/z 50 with 8 kV energy will travel at a speed of 18 m/z according to equation [3]. However, it the same ion is given an accelerating energy of 6 kV, it will travel slower and thus, take more time to reach the second field free region. It might decompose outside the region of interest and will not be considered metastable anymore.

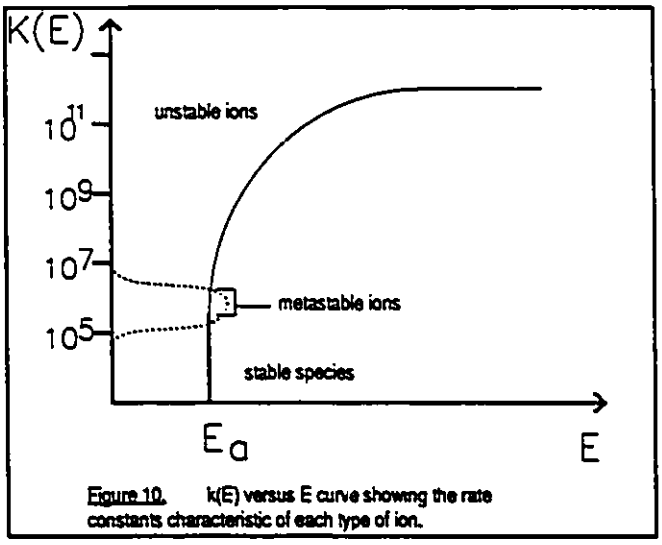

Figure 10. k(E) versus E curve showing the rate constants characteristic of each type of ion.

Stable ions, of course, have slower decomposition rates whereas unstable ions decompose faster. Figure 11 represents the time-scale of events applicable to the VG ZAB-2F instrument for a typical m/z=100 species at an accelerating voltage of 8000 volts.

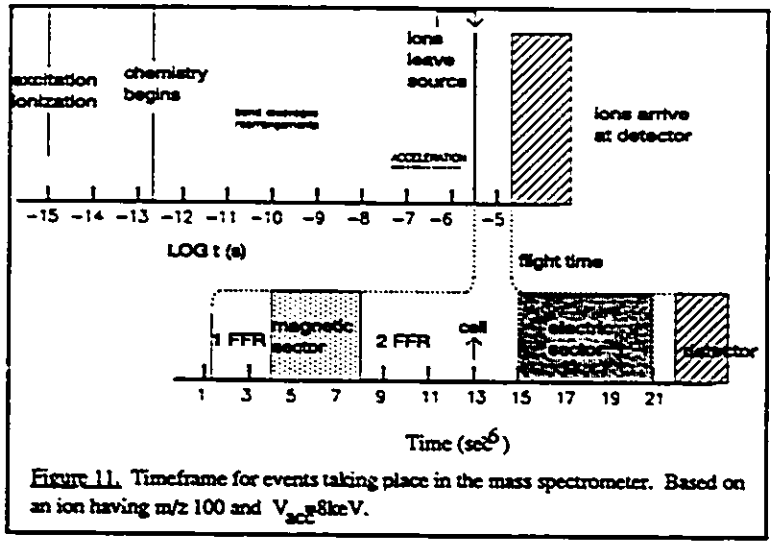

Figure 11. Timeframe for events taking place in the mass spectrometer. Based on an ion having m/z 100 and V_{acc}=8keV.

2.4.1. Isomerization.

Another important process that has not been considered yet is the problem of ion isomerization. Because a wide range of internal energies are contained in ions, it is possible for both molecular ions and fragment ions to isomerize into different structures. These isomerizations complicate the interpretation of mass spectra. The extent to which an ion A^+ rearranges into an isomer B^+ depends on the relative energy barriers for decomposition and isomerization (Fig 12). In case (i), the energy of isomerization is much bigger than the energy of all fragmentations. Therefore, the decompositions will occur much more readily than the isomerization. In case (ii), the isomerization energy is much smaller than the fragmentation

requirements of $A^{+\bullet}$ to its corresponding products. Thus, the interconversion between A and B will take place very easily giving rise to a possible mixture of products from both A and B. This type of fragmentation renders the structure elucidation of ions very difficult to perform. Case (iii) illustrates a combination of these two situations where $A^{+\bullet}$ must isomerize to B prior to fragmenting. Therefore, both ions $A^{+\bullet}$ and $B^{+\bullet}$ will give rise to identical mass spectra. A very good example of these various isomerization processes can be found in reference 15 where the fragmentations of five isomeric [H_3, C, N, O_2] ions were studied. It was found that $H_3CNO_2^{+\bullet}$, $H_2C{=}N(O)OH^{+\bullet}$ and $H_3CONO^{+\bullet}$ interconvert prior to fragmentation, but $HC(O)NHOH^{+\bullet}$ and $HC(OH){=}NOH^{+\bullet}$ can only isomerize to one another.

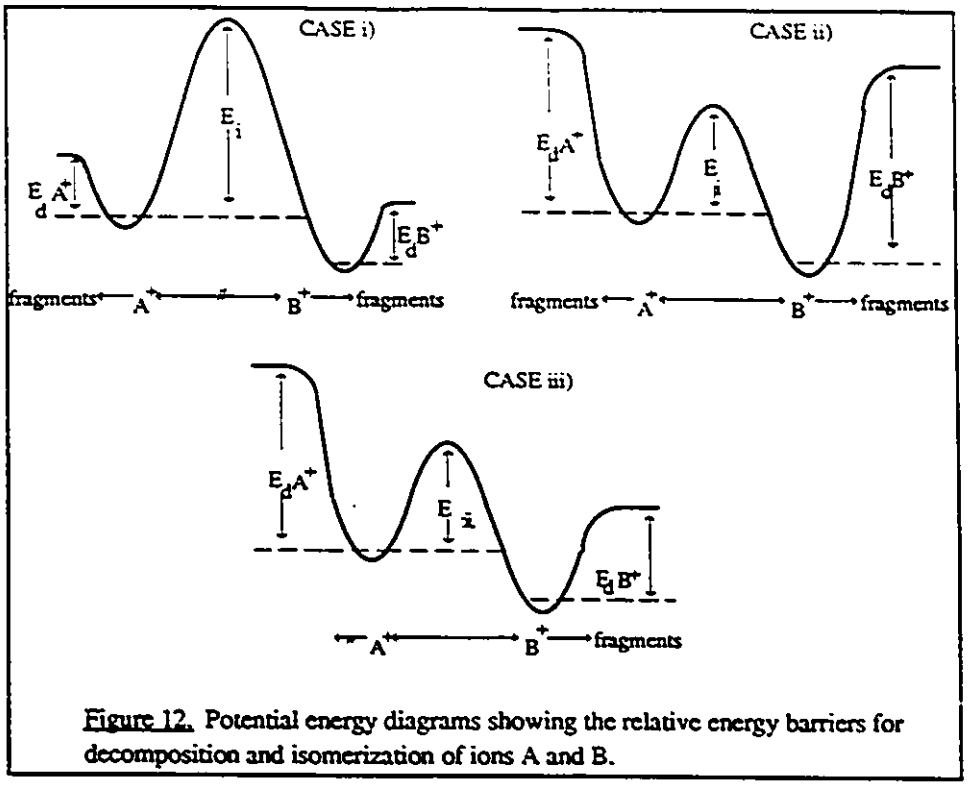

Figure 12. Potential energy diagrams showing the relative energy barriers for decomposition and isomerization of ions A and B.

2.4.2 Quasi Equilibrium Theory.

How can we understand the dissociation behaviour of ions in the gas phase? The Quasi-Equilibrium Theory (QET) developed by Rosenstock et al[16] depends upon the statistical distribution of internal energy in the ionized molecule. It is based on the following assumptions:

1) "The time required for dissociation of the initial molecular ion is long compared with the time of interaction leading to its formation and excitation." Meaning that the dissociation process takes long enough to occur that the molecular ion "forgets" how and where the ionization occurred i.e. the ionization mode is independent of the rate of decomposition. This also implies that the "rate of dissociation is slow relative to the rate of distribution of the initial excitation energy over all degrees of freedom of the molecular ion's ground state".

2) "The fragmentation products are formed by a series of competing and consecutive unimolecular reactions."

3) The ions generated represent isolated systems, therefore, the rate of a process is a function of the excitation energy only.

For a complete description of QET, see reference 16 and references therein.

Generally, two factors will govern the fragment ion abundances in the mass spectra:

1) The stability of the products, i.e. the lowest energy products ($\Delta H_f°$) will generally be favored.

2) The strength of the bonds cleaved.

It must be realized that the relationship between a mass spectrum and the neutral molecule from which it is generated may be very complex. The normal mass spectrum contains hidden information concerning the structures of the molecular ions which may change drastically before their dissociation takes place.

CHAPTER 3

USEFUL TOOLS FOR ION STRUCTURE ASSIGNMENT: TECHNIQUES AND APPLICATIONS.

3.0 Introduction

The use of high resolution electron impact mass spectrometry can be sufficient to confidently assign a structure to an ion from a knowledge of dissociative properties (fragments) and exact molecular mass. However, the very large number of isomeric ions discovered year after year (both conventional and unconventional) makes this task less certain. Fortunately, today's technology has produced very versatile new instruments. The approaches used for assigning structures to ions in the gas phase involve:

i) accurate measurements of ionic heats of formation.

ii) a wide variety of experiments on mass selected ions of known molecular formula; their metastable and collision induced dissociations.

iii) the time-honoured method of isotopic labelling.

Many techniques use "comparison" of the results obtained for an unknown ion *a* with all the available data for "known" ions of the same chemical composition *b*, *c*, *d*.... If ion *a* shows similar thermochemical and dissociative characteristics as, for example, ion *c*, it can be provisionally concluded that they have the same structure. When reference ions are not available, a combination of the various mass spectrometric techniques is used to allow one to infer a tentatively "correct" structure of a particular ion. In this chapter, the experimental techniques providing thermochemical information and dissociative characteristics of ions will be described. Applications of these techniques to elucidate ion structures and fragmentation mechanisms will also be discussed at the end of this chapter.

3.1 Thermochemistry

A knowledge of ion thermochemistry is essential to establish the structure of gas phase ions. The heats of formation, ΔH_f°, of ions are especially important because obtaining identical ΔH_f° values for two ions generally strongly implies that they have the same structure. The heat of formation of an ion under study is measured as accurately as possible and is compared with ΔH_f° values for ions of the same molecular formula from the literature (from previous experiments or from high level ab initio molecular orbital theory calculations). However, the ΔH_f° values are rarely exclusively used to identify an ion structure; dissociation characteristics are also studied.

3.1.1 Ionization and Appearance Energies.

The ΔH_f° values of molecular and fragment ions can be derived from ionization and appearance energies (IE and AE) and require a knowledge of heats of formation of neutral species. The first ionization energy of a molecule is defined[17] as the minimum energy required to remove an electron from the lowest molecular orbital. The heat of formation of a molecular ion $A^{+\cdot}$ is given by the equation below.

$$\Delta H_f^\circ(A^{+\cdot}) = IE\ (A) + \Delta H_f^\circ(A) \qquad [8]$$

Therefore, measuring the IE and knowing the ΔH_f° of the neutral (A) will allow the calculation of $\Delta H_f^\circ(A^{+\cdot})$ to be made. Many ΔH_f° values of neutrals can be found in the literature[9,18] but when this is not the case, they can be estimated via Benson's additivity scheme[19] including the use of new or provisional additivity terms[20].

The appearance energy (AE) of a fragment ion is the minimum energy required to obtain the specific fragment ion from a neutral precursor

$$A \rightarrow B^{+\cdot} + C + e \qquad [9]$$

The heat of formation of ion $B^{+\cdot}$ can then be obtained using the following equation:

$$\Delta H_f(B^{+\cdot}) = AE(B^{+\cdot}) - \Delta H_f(C) + \Delta H_f(A) \qquad [10]$$

Alternatively, using the same equation and if data for $\Delta H_f(B^{+\cdot})$ is available, ΔH_f of the neutral species (C) may be calculated. However, one has to be careful when assuming a value for $\Delta H_f(B^{+\cdot})$ when establishing ΔH_f for the neutral species C, because of the possibility that one may have incorrectly assigned a structure to $B^{+\cdot}$.

The ionization energy of molecule A and appearance energies of fragment ions $B^{+\cdot}$ are obtained by recording the intensity of the ion signal as a function of the energy of the ionizing electrons. The energy corresponding to the first observation of the ion of interest is obtained by extrapolation of the curve which results from plotting the ion current versus ionizing electron energy (Fig 13). Specialized instruments such as photoionization mass spectrometers[21] or a mass spectrometer having an energy-selected EI ion source[12] are used to measure IE and AE with good accuracy i.e. ±0.05 eV. Such measurements cannot be performed on the ZAB-2F because the electrons emitted by the filament are by no means monoenergetic and moreover, the ion source controls are unsuited to such work. A method to obtain the AE of a metastable peak using the MS-902S mass spectrometer is described in reference 11. Basically, it consists of measuring the

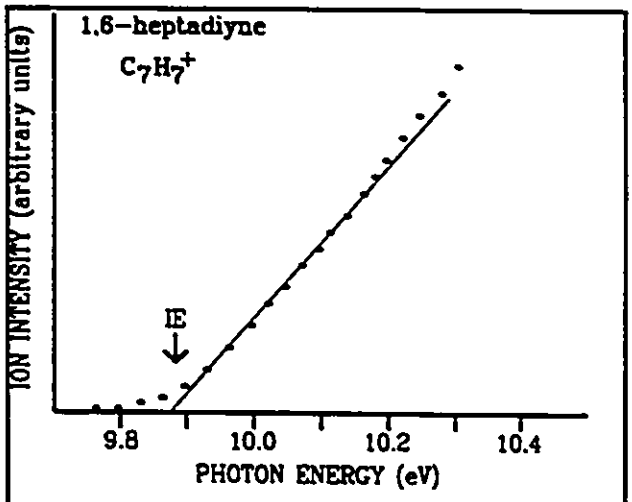

Figure 13- Photoionization efficiency curve for m/z 91 ion from 1,6-heptadiyne. Ionization Energy (IE) is at threshold, indicated by arrow.

intensity of the metastable peak of interest versus electron energy and one generated by a calibrant compound. The comparison of their threshold energy values will determine the unknown AE value. A good calibrant compound is diethyl ether which metastably loses a methyl group with an AE of 10.26 eV, i.e. $[CH_3CH_2OCH_2CH_3]^{+\cdot} \rightarrow CH_3CH_2^{+}OCH_2 + CH_3^{\cdot}$.

An example of the usefulness of AE values to investigate the heat of formation of a neutral compound is the determination of the heat of formation of vinyl iodide. The heats of formation of C_2H_3Br and C_2H_3Cl have been measured but there is no value for C_2H_3I. $\Delta H_f[C_2H_3I]$ may be estimated using the energy difference for ΔH_f RCl$\rightarrow \Delta H_f$ RI of a series of compounds e.g. the $\Delta(\Delta H_f)$ values in kJ/mol and are 96.6 for (CH_3X); 104.6 for (C_2H_5X); 101.6 for (1-C_3H_7X); 104.6 for (2-C_3H_7X); 110.2 for (t-C_4H_9X) and 112.9 for (C_6H_5X)[18] giving an average of 105 ± 8 kJ/mol with $\Delta H_f[C_2H_3Cl]$=37.3 kJ/mol then $\Delta H_f[C_2H_3I]$ is estimated to be 142 ± 9 kJ/mol. From AE $[C_2H_3^{+}]$ from C_2H_3I (=11.26 eV) and using $\Delta H_f[C_2H_3^{+}]$=1111kJ/mol and $\Delta H_f[I^{\cdot}]$=107 kJ/mol, the value of 133 kJ/mol was found for ΔH_f=$[C_2H_3I]$ which is at the lower limit for the estimated value of 142 ± 9 kJ/mol.

3.1.2 Adiabatic or vertical ionization?

Two types of ionization energy (IE) are frequently described, namely the adiabatic (IE_a) or vertical (IE_v). The former refers to the energy difference between the ground vibrational levels of the lowest electronic state of the ion and of the corresponding molecule (Fig 14) whereas the vertical ionization refers to the energy difference between the ground state of the molecule and

that of the ion having the same geometry. An adiabatic ionization energy can accurately be measured by electron impact using a double hemisphere electron energy selector such as that described in reference 12, when the difference between IE_a and IE_v is relatively small (say <0.3 eV). Indeed, in general, this difference is small for the majority of organic compounds but where the ion has a geometry significantly different from the neutral species it may be difficult to measure IE_a. An example is the case of ethyl fluoride for which there is a difference of 0.65 eV (adiabatic is lower) between the ionization energies[22]. This indicates a considerable geometry change between the neutral and ionized species and that the most probable result of electron impact ionization (vertical process) produces highly excited species. Adiabatic IE values should always be used when calculating ΔH_f. The National Bureau of Standards (NBS) has compiled IE and AE values from the literature up to 1988[9].

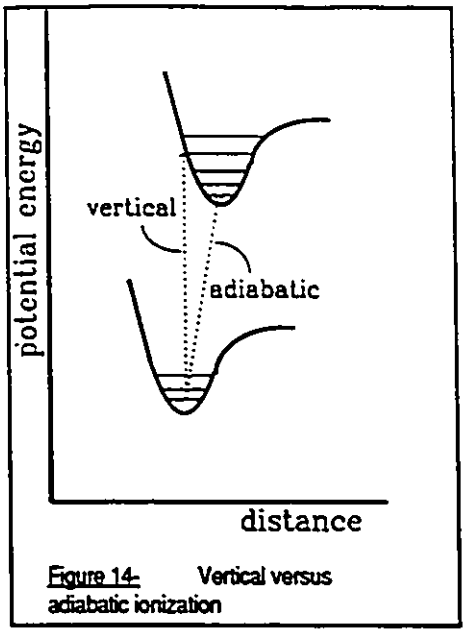

Figure 14- Vertical versus adiabatic ionization

3.1.3 Kinetic Shift and Reverse Activation Energy.

Two important factors which must be taken into account when evaluating AE values are the kinetic shift and reverse activation energy. The kinetic shift corresponds to the difference in AE for short and long observation times of the ions and is an essential factor which will ensure that a sufficient number of daughter ions are formed in the source (Fig 15). It depends

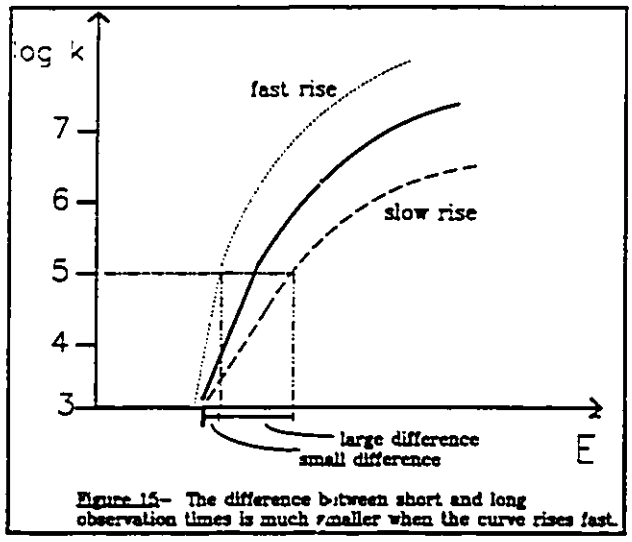

Figure 15- The difference between short and long observation times is much smaller when the curve rises fast.

on the residence time of the ions in the source and on the shape of the ln k(E) vs E curve. When we measure the AE of an ion A^+, we measure it on a given time-scale e.g. 1 μs, in the first field free region of the instrument. Therefore, the energy given to the precursor ion M^+ must be enough for the precursor to fragment to $A^+ + B^\cdot$ in ≤ 1 μs. This corresponds to a rate constant of $k_{M^+} \geq 10^6\ s^{-1}$ for the reaction $M^+ \rightarrow A^+ + B^\cdot$. To achieve this rate constant, it is often necessary to put significantly more than the minimum energy into the ion. If the rate constant k(E) rises only slowly with increase of internal energy E, the kinetic shift will be significant and the AE values will correspond to an upper limit of $\Delta H_f°$(ion). When the k(E) rises sharply with the increase of ion internal energy, there will not be a kinetic shift and the AE energy value can be used with confidence[23]. The effect of kinetic shift can be reduced by measuring metastably generated ions which are of lower excess energy. They give a value of $\Delta H_f°$ equal to or lower than the source generated ions (Fig 16). A problem, however, resides in the small number of precursors for a specific ion and in the very low intensity of some metastable peaks.

Furthermore, the absence of a metastable peak does not guarantee that the minimum value is obtained, there may be a contribution from the reverse activation energy (Fig 16). In general, simple bond cleavages have small or no reverse activation energy whereas rearrangement

reactions may well occur with a significant reverse energy[24]. Where the fragmentation is both metastable and involves large E_{rev}, the metastable peak will be broadened due to the kinetic energy release (see section 3.3.2). The various metastable peak shapes will be discussed in section 3.3.4.

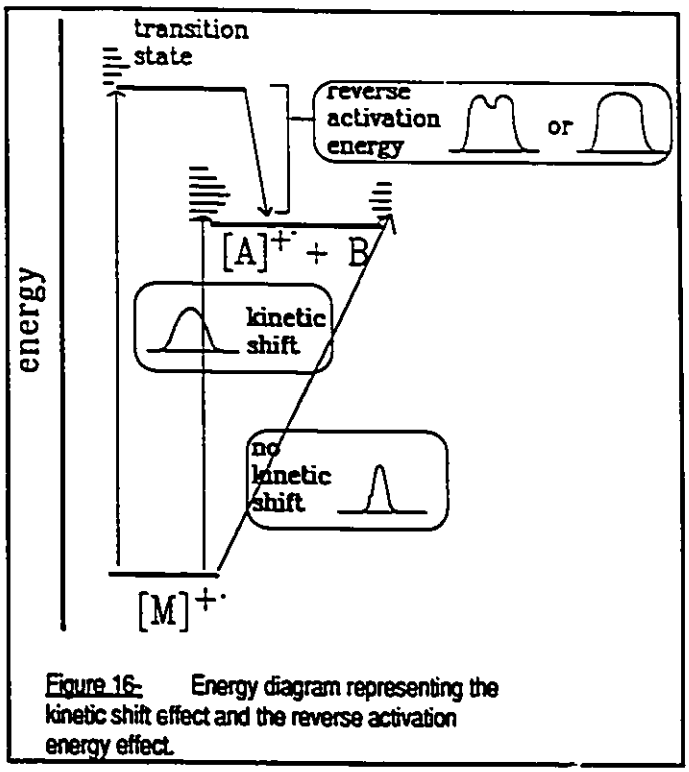

Figure 16: Energy diagram representing the kinetic shift effect and the reverse activation energy effect.

3.1.4 Effect of Rate Constant.

In general, the AE value derived from a metastable fragmentation is characteristic of a specific reaction channel, however if the rate constant k(E) versus E curves for two competing reaction channels intersect (Fig 17), it means that rearrangement and bond cleavage may compete. Therefore, the rise of k(E) may be very slow i.e. the AE value will be higher than the threshold

value. Finally, it is possible that a mixture of isomers is present at a given m/z value. Therefore, the AE value will correspond to the most stable isomer in the mixture. Thus, it is important that only a single species is monitored in the instrument.

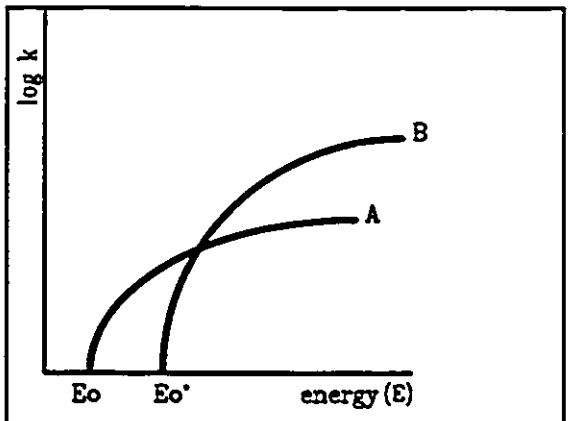

Figure 17- Log k versus energy (E) curves representing competing reactions A and B.

3.1.5 The Effect of Mixtures of Isomers on AE Measurements.

The AE of a fragment ion provides an upper limit for the heat of formation of that ion. Therefore care must be taken to ensure that the effects of kinetic shift and reverse energy are considered. If the energies required to produce an ion metastably and in the source are measured, the lower AE value should be used. Where a mixture of isomers is studied, the AE which is obtained corresponds to the most stable isomer. For example, ionized oxalic acid produces in the ion source $C(OH)_2^{+\bullet}$ and $HCOOH^{+\bullet}$[25]. However, only the former is obtained metastably and $\Delta H_f°[C(OH)_2]^{+\bullet}$ is determined by the AE measurement. It is also important to have a very pure sample since contaminants may strongly interfere by producing a more stable ion of the desired m/z value and so will give an incorrect, lower AE value.

3.1.6 Estimating $\Delta H_f°$(ions).

Once the $\Delta H_f°$ value of an ion is measured, it may be compared with reference ions from the literature or compared with estimated values of $\Delta H_f°$. One can estimate $\Delta H_f°$(ion) values by studying correlations within homologous series. The equation $\Delta H_f[ion]^{+\cdot} = A\text{-}Bn+C/n$ where A, B and C are constants[26] and n is the number of atoms in the molecule can give fairly acceptable values[27]. Many factors have to be considered when estimating ΔH_f(ions): location of the charge on the ion[28], nature of substituent[29], multiple substitution effects[30] and the relationship between stabilization energy and ion size[31]. Although the ΔH_f value of an ion is a very good criterion for its identification, it cannot be solely used. Isomers may have very similar ΔH_f values such as do $CH_3CH_2Cl^{+\cdot}$ (950 kJ/mol) and its ylid counterpart $CH_3CHClH^{+\cdot}$ (951 ± 4 kJ/mol)[32]. Sometimes the identity (and therefore ΔH_f) of the neutral fragment is not known. This is comparatively uncommon but an example is found in the fragmentation of ionized aniline[33] which produces $C_5H_6^{+\cdot}$ and [H,N,C] with an AE value 0.8 eV above the calculated threshold for $C_5H_6^{+\cdot}$ + HCN. It was proposed that the neutral is HNC, for which $\Delta H_f°$ is 0.6 eV higher than HCN. This proposition was confirmed by performing a CIDI (Collision Induced Dissociative Ionization) experiment (see section 3.5) on the neutral product[34] to establish its structure.

In the past few years[35,36], extensive work has been conducted by Holmes and Lossing to estimate heats of formation of ions of unconventional structure (ylid, distonic and H-bridged

ions; see Chapter 4) using bond strengths in even electron ions and the proton affinity of free radicals[37].

3.2 Labelling Techniques

3.2.1 Most Common Labels

A very useful tool to probe fragmentation mechanisms is isotopic labelling. The most common labels are D, ^{13}C and ^{18}O. These labels allow one to follow the behaviour of specific fragmentations of a selected ion. Chapter 5 of this thesis would have never been written if the labelling technique were unavailable. A review concerning the use of labelling as an aid to investigate the fragmentation of ions has been published[38], and so only a few examples will be given to emphasize the usefulness of this technique. "On paper", Figure 18 seems a plausible mechanism for the elimination of ketene from $C_6H_4(COOCH_3)_2$ followed by elimination of methanol. According to the position of the labels, CH_4O and CH_3DO should be lost in approximately equal amounts.

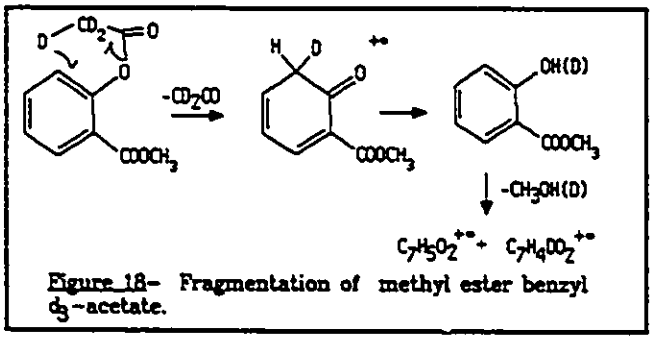

Figure 18- Fragmentation of methyl ester benzyl d_3-acetate.

However, the experiment showed that only CH_3DO is lost. Upon this result, a four-membered ring was proposed as an intermediate for the fragmentation.

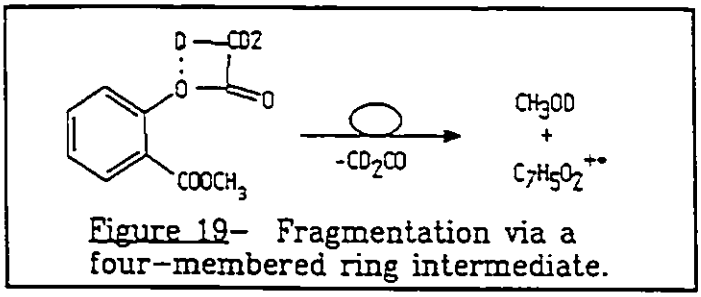

Figure 19– Fragmentation via a four–membered ring intermediate.

Another example of the usefulness of labelling is shown with nitrobenzene. Figure 20 shows the two possible pathways for successive losses of NO• and CO. Both mechanisms are plausible. However, ^{13}C labelling showed that only mechanism A occurs, the designated atom always being in the CO eliminated.

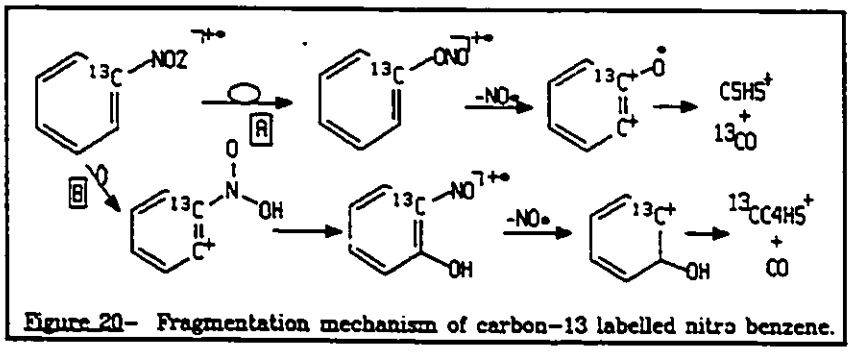

Figure 20– Fragmentation mechanism of carbon–13 labelled nitro benzene.

3.2.2 Isotope Effects

An important phenomenon which can sometimes occur upon labelling with deuterium is the *isotope effect*[14]. This effect sometimes takes place because the replacement of an H by a D may change the rate of the reaction. The difference in reaction rates arises from the fact that the activation energy for the D-labelled compound is higher than for the unlabelled compound (Fig

21) or it relates to the density of states for the reacting configurations. The magnitude of an isotope effect is usually calculated using the relative height of the appropriate peaks in a mass spectrum.

Only when the internal energy of the ion is appreciably higher than the dissociation limit will isotope effects tend to disappear. Note that an isotope effect is generally larger when it involves a simple bond cleavage than when a rearrangement is involved.

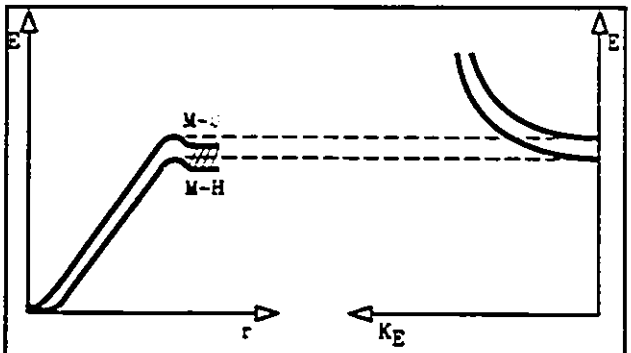

Figure 21- Variation of isotopic effect as a function of the excess energy.

3.3 Metastable Ions

A metastable ion is one which has enough energy to exit the ionization chamber but decomposes before reaching the detector[13]. Such ions have a small excess internal energy over the minimum for fragmentation and a typical lifetime of ca 1-10 μs. The first scientists to use the name "metastable ions" were Hipple and Condon[39] in 1945. Only the dissociations of the metastable ions occurring in the field free regions of the mass spectrometer (between the ion source and the first analyzer or between the two analyzers) will be detectable. When an ion dissociates metastably by a unimolecular process the excess energy of the original ion above the dissociation limit will be distributed amongst the degrees of freedom of the products. Considering $A^{+\cdot}$ -*→ $B^{+\cdot}$ + C, and assuming that the velocity of both fragments is essentially the

same, the kinetic energy of the products will be a fraction of the kinetic energy of the precursor ion:

$$1/2\ m_B v_B^2 = m_B/m_A \times zV_{acc} \qquad [11]$$

$$1/2\ m_C v_C^2 = m_C/m_A \times zV_{acc} \qquad [12]$$

Since the law of conservation of momentum has to be observed, Hipple and Condon[39] showed that the apparent mass m*, of the daughter ion $B^{+\cdot}$ is given by

$$m^* = m_B^2/m_A \qquad [13]$$

where m_B is the mass of the daughter ion and m_A is the mass of the metastable ion. The ions $B^{+\cdot}$ will be transmitted through the magnet with such an apparent mass because they only have a fraction m_B/m_A of the momentum of the precursor ion. If those same ions of apparent mass m* fragment between the two analysers ($B^{+\cdot} \rightarrow D^{+\cdot} + E$), the new ions $D^{+\cdot}$ will only have a fraction m_D/m_A of the momentum or of the energy of the precursor ion m_A. Therefore, it is possible independently to analyze the metastably generated ions in both sectors of the instrument (Fig 22).

In a normal EI mass spectrum we cannot, in general, identify the precursor(s) of any given fragment ion. The observation of a metastable peak allows us to link a fragment ion M_2

with all its precursors if, for example, metastable peaks were seen at nominal masses: M_2^2/M_1, M_2^2/M_1', M_2^2/M_1'', etc...[40]. By mass selecting an ion $B^{+\cdot}$ with the momentum analyser, it is possible to study all its metastable fragmentation characteristics by scanning the electric sector. Not only the metastable processes can give valuable information on an ion but the general shape and size of the peaks is also very informative. However, to be able to fully use metastable ion characteristics, it is important to record the data under controlled conditions (stable instrument, good resolution).

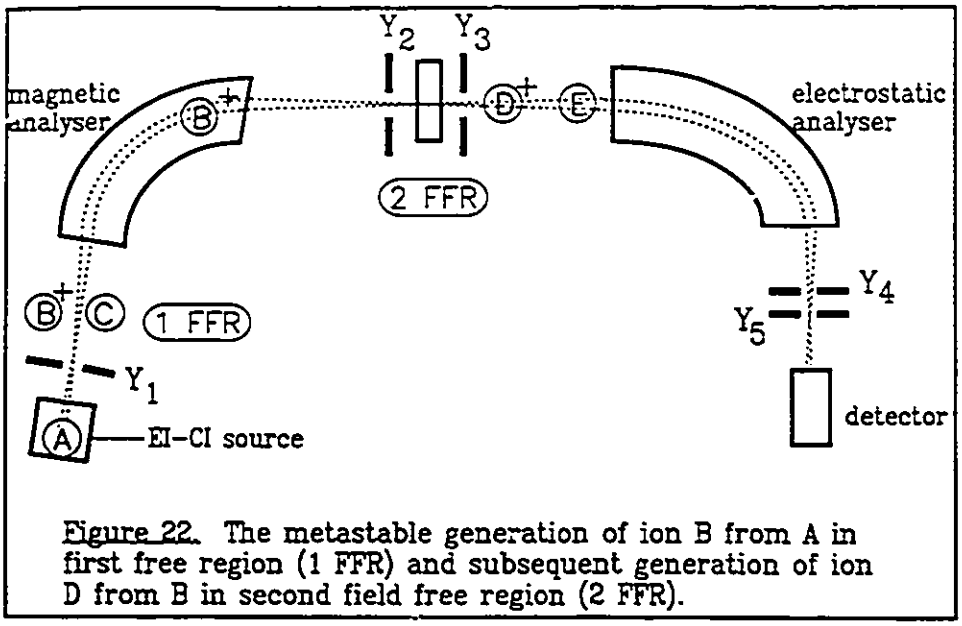

Figure 22. The metastable generation of ion B from A in first free region (1 FFR) and subsequent generation of ion D from B in second field free region (2 FFR).

3.3.1 Resolution

The resolution of the ZAB-2F can be given in terms of energy and mass. The mass resolution is given by the ability of the instrument to separate two masses M_1 and M_2 of mass difference δM, when $h/H \leq 0.1$ (Fig 23).

$$R = M_1^{+\cdot}/\delta M \qquad [14]$$

Using various beam defining slits (Y_1 to Y_5 in Fig 22), it is possible to achieve greater resolution and to separate ions which have the same nominal mass. For example, N_2 and CO which have molecular weights of 28.0174 and 27.9954 u respectively, can be separated if the instrument has a resolution of R=1300. Energy resolution can be quoted in a similar manner and is measured by the energy recorded at half height of the peak (Fig 23). The "real" voltage scanned by the electrostatic analyzer is 0-483 Volts but since an accelerating voltage of 8000 V is given to the ions, the sector voltage is scaled to 8000 V. Therefore, at 483 V, the ions are considered to have 8000 V. An energy resolution of less than 5 volts is considered acceptable.

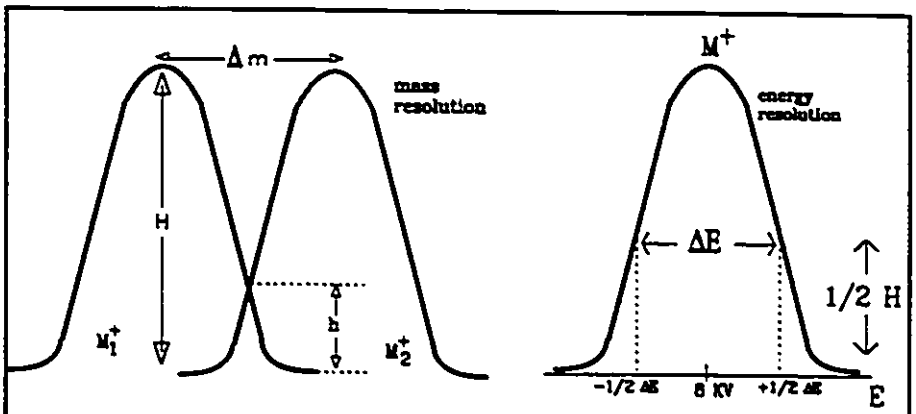

Figure 23- Criteria explaining how mass and energy resolution are obtained.

3.3.2 Kinetic Energy Release.

Ions fragmenting on mass spectrometric time scales (see Figure 11) have an excess of internal energy, some of which is released as kinetic energy given to the fragments. This magnitude and distribution of the energy released will have an influence on the shape of the

metastable peak as well as on the energy spread of that peak. It depends on the magnitude of the reverse activation energy as well as on the kinetic shift (see section 3.1.3). The process of partitioning the energy of the ion into the translational degrees of freedom of the products cannot at this time be predicted since no method exists to accurately calculate simultaneously the internal energy content and the kinetic energy release[41]. Therefore, kinetic energy release values ($T_{0.5}$ values) which are used to compare peaks, presently have no fundamental significance, but provide useful identifying features for decomposing ions.

3.3.3 $T_{0.5}$ values

The kinetic energy released upon a specific fragmentation can be measured as a $T_{0.5}$ value. It is obtained by the following experiment: the precursor ion of interest, M^+ is selected through the magnet and the electric sector is scanned slowly over a very small span of energy close to the fragment ion energy, under high energy resolution conditions i.e with the ß-slit narrowed (Fig 7). By considering the laws of conservation of energy and momentum, the equation 15 can be derived[13]. For a process $A^{+\cdot} \dashrightarrow B^{+\cdot} + C$, the $T_{0.5}$ value (kinetic energy released measured from the half-height of the peak) is given by:

$$T_{0.5}\ (meV) = (\Delta E_B)^2 \times (m_A)^2/(V_{acc} \times m_B \times m_C \times 16) \qquad [15]$$

where m_A, m_B and m_C are the masses of the ion and its fragments and ΔE_B is the width at half-height of the peak expressed in acceleration volts[13]. When the peak width ΔE_B is small relative

to the main beam width, it may be of significant importance to correct the peak for the main beam using the equation established by Ottinger[42]:

$$\Delta E_B \text{ (corr)} = \sqrt{[(\Delta E_B)^2-(\Delta E_A)^2]} \qquad [16]$$

The $T_{0.5}$ value is not the only way to express the kinetic energy release but it is the most common one. Other values may be obtained using peak widths at different heights of the peaks but these methods will not be discussed here. A review of the topic may be found in reference 41.

3.3.4 Metastable Peak Shapes

Another important criterion is the shape of a metastable peak. Equal shapes may indicate similar reacting configurations of two species whereas different shapes may indicate different reacting configurations (or possibly different experimental conditions). The term reacting configuration refers to an intermediate structure to which an ion isomerizes before fragmenting. Jones et al[43] proposed that fragmenting ions with the same reacting configuration should show the same $T_{0.5}$ values independent of the experimental conditions used to generate the ion. There are basically three different types of metastable peak shape (Fig 24): the Gaussian type, which are the most common, and are usually associated with small kinetic energy releases ($T_{0.5}$ values of up to about 50 meV) and dished and flat-topped peaks which are associated with larger kinetic energy releases arising from reverse activation energy. Note that the inverse is not true, not all

reactions with significant reverse activation energies reveal "dished" or flat-topped metastable peaks.

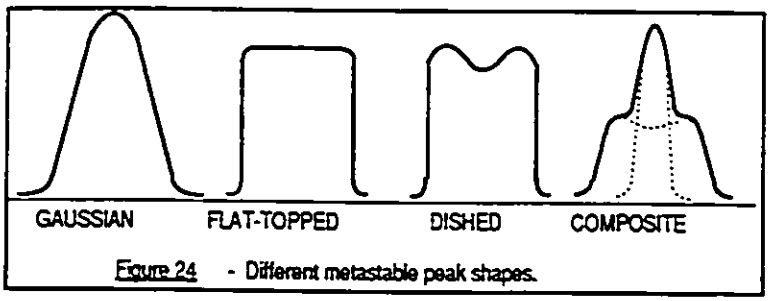

Figure 24 - Different metastable peak shapes.

The "dished" peak is caused by Z-axial discrimination in the instrument i.e. the fragment ions which contain large amounts of kinetic energy in the plane of the long axis of the energy resolving slit are not fully transmitted because the slit is of finite length (Fig 25). In order to examine peak shapes in detail it is essential that good energy resolution is obtained.

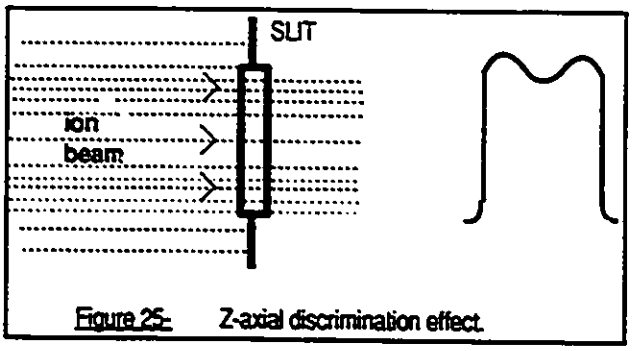

Figure 25- Z-axial discrimination effect.

A last type of peak is called composite. It may for example consist of the combination of a Gaussian peak atop a dished peak or, of a pair of superimposed dished peaks. They may arise from isomeric ions which lose a common neutral fragment to yield one or two daughter ion structures or, from a single ion giving rise to two isomeric daughter ions or, when a pair of isomers fragment to yield a common daughter ion via a different reacting configuration. A good

example is the hydrocarbons which have at least 3 carbon atoms for which the m/z 41 -*→ m/z 39 process takes place and shows a composite peak. There is a broad dished component corresponding to $CH_2^{\bullet}CHCH_2 \rightarrow$ [cyclopropenyl]$^{+}$ + H_2 and a less broad, also dished component corresponding to the formation of $HC{\equiv}CCH_2^{+}$ + H_2.

3.3.5 Metastable peak abundance ratio

The metastable peak abundance ratio test was proposed by Shannon and McLafferty[42] and studied by Rosenstock et al[44]. It consists of comparing the abundance ratio (peak height or area) of all competing metastably generated peaks of two ions under identical experimental conditions. If the ratios are similar for both ions, it can be concluded that they are of same structure. This test may be difficult to use because one has to decide what are the acceptable variations in ratios and also one has to decide whether the experimental conditions in different reports were similar (i.e. ion lifetimes and energy resolution conditions). In summary, identical metastable peak abundance ratios provide good evidence, but not proof, that ions having the same reacting configuration are being observed.

3.4 Collision Induced Dissociation of Ions.

The collisional induced dissociation (CID) of ions was first observed in 1924 by Smyth[45] but the interest in the phenomenon was revived by Jennings[46] and Haddon and McLafferty[47] in 1968. It was observed that the collision induced dissociation mass spectra had a large

similarity to the corresponding electron impact spectrum. This supported the view that collision-induced dissociations proceed via the generation of electronic excited states of the ion followed by its unimolecular fragmentation (the same as the process taking place in an electron impact ion source). When an ion collides with a neutral target, some of its translational energy may be converted into internal energy. This energy may also be sufficient to induce self-fragmentation of the ion

$$A^{+} + T \rightarrow A^{+} \text{-}^{*}\rightarrow B^{+} + N \qquad [17]$$

In their 1968 paper, Haddon and McLafferty[48] suggested that the structure of an ion may be characterized by the relative abundances of peaks in the CID mass spectrum of a mass selected ion and proposed that this technique may in future become a very useful tool to identify ion structures. They were never so right! Today, the collisionally induced dissociation behaviour of beams of fast charged or neutral species is a widely employed technique (refer to sections 3.5-3.7) for structural investigations.

The spectrum is formed by source generated, mass-selected ions, which do not have enough energy to fragment in the metastable timeframe, colliding with a gas located in one of the field free regions. With the ZAB-2F, only the second cell contained in the 2 FFR is used (Fig 26) for this purpose. The fragment ions are then analysed by scanning the ESA and detected.

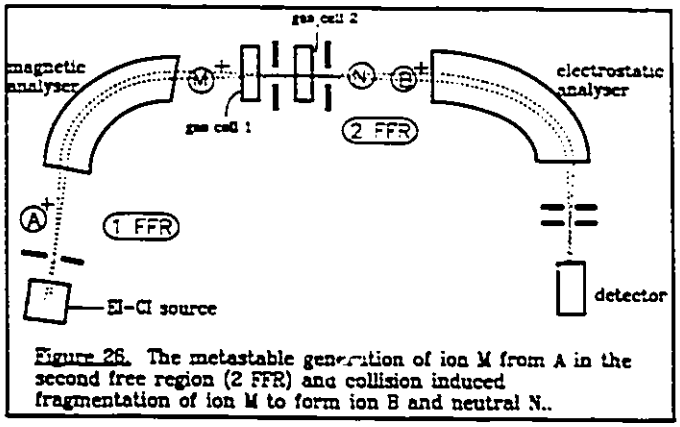

Figure 26. The metastable generation of ion M from A in the second free region (2 FFR) and collision induced fragmentation of ion M to form ion B and neutral N..

Amongst the factors which will affect the spectrum are the nature and pressure of the gas and the ion's internal and translational energies[23].

3.4.1 Nature of the gas.

The most commonly used gases for collisional activation (CA) are He and O_2, although N_2, H_2, Xe and other gases have also been used. They have been divided in two classes[48], "so called" soft targets (O_2, NO_2, Cl_2) which provide less fragmentation and hard targets (He, Xe, CH_4) whereas N_2 is considered an intermediate strength target. The choice of gas depends on the type of information needed[50]. For example, when looking for information related to structure, a large number of fragmentations is favourable and a "hard" target such as He should be used.

3.4.2 Pressure

Since the pressure of the collision gas is not directly measured in the cell, it is necessary

to use a constant reduction of the main beam's intensity in order to have reproducible results[23]. Thus the pressure measured at the top of the analyzer diffusion pump can be related to a certain percentage reduction of the main beam. As the beam reduction increases, multiple collisions become more important. However, one should not forget that collisions also lead to fragmenting, scattering, charge exchange ($A + B^+ \rightarrow A^+ + B$) and charge stripping (see section 3.7). Figure 27 shows that at a 10% beam reduction, 95% of the collisions are single encounters whereas at 60% beam reduction, only 75% of the collisions are considered single. Although maximum yields of fragments are obtained in a 40-80% beam reduction[49], the work described in this thesis was performed using collision gas pressures corresponding to 10% beam reduction to obtain essentially single collision conditions. In general, multiple collision induced dissociation leads to less useful information for ion structure evaluations because the amount of fragmentation is much greater.

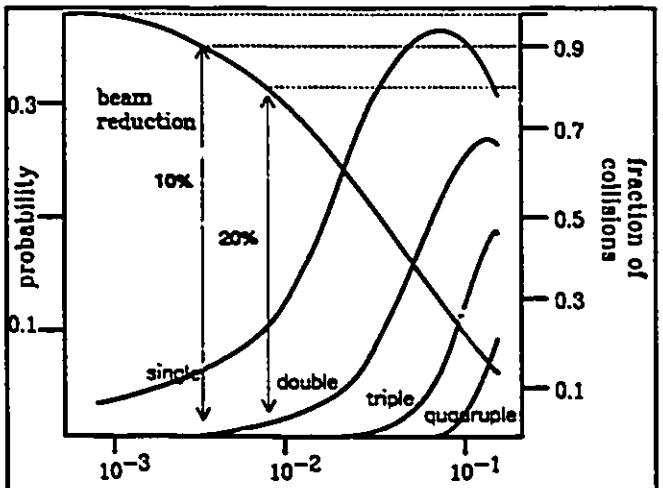

Figure 27- Total collision probability and fraction of single/multiple collision processes as a function of collision gas pressure.

Efficient differential pumping between the cell and its surroundings ensures that the

majority of the collisions occur within the cell itself. To separate the collision induced fragmentations which occur in the cell from those occuring outside the cell i.e the unimolecular metastable fragmentations, a technique consisting of applying a voltage on the cell is used.

3.4.2.1 Voltage on Cells

The cell being electrically isolated, it is possible to apply a voltage, typically 1000 volts. For a voltage -V applied on the cell, the ions $A^{+\cdot}$ entering the cell with an energy V_{acc} will acquire +V translational energy i.e. their kinetic energy will be raised to $V_{acc}+V$. The fragments B^+ produced from $A^{+\cdot}$ in the cell will then have a fraction of the energy $[B^+/A^{+\cdot} \times (V_{acc}+V)]-V$ as they exit the cell. The fragments produced before and after the cell will have an energy of $B^+/A^{+\cdot} \times V_{acc}$ being unaffected by the voltage. This technique thus separates the MI contribution from a CA process (Fig 28).

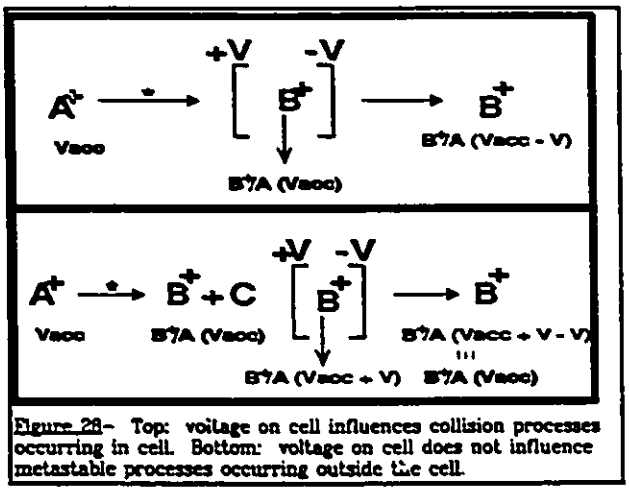

Figure 28- Top: voltage on cell influences collision processes occurring in cell. Bottom: voltage on cell does not influence metastable processes occurring outside the cell.

3.4.3 Energy in CA Processes

In 1973, two papers by McLafferty and co-workers appeared[50,51], pointing out that a CA mass spectrum was a helpful tool to characterize ion structures. In general, the relative abundances of the peaks in the CA mass spectra are dependent on the precursor ion's internal energy and on its structure. Since the CA mass spectrum is composed of ions formed via fast processes (bond cleavages rather than rearrangements) it bears a lot of similarity with the electron impact mass spectrum. Therefore, although the MI mass spectrum is specific to a structure, the CA mass spectrum is often more characteristic because it represents dissociation pathways which are "fragment characteristic". It is thus possible to identify a fragment ion by comparison of its CA mass spectrum with available data for species of the same molecular formula.

3.4.4 Applications of CA Experiments

Here are a few examples showing that CA mass spectra can be used to characterize various isomers. Investigation of $C_3H_8O^{+\bullet}$ ions, m/z 60, has shown the existence of a new isomer[52] of [propan-1-ol]$^{+\bullet}$ of structure $^{\bullet}CH_2CH_2CH_2OH_2^+$. The precursor to this distonic ion is $HOCH_2CH_2CH_2CH_2OH$ losing CH_2O. Their heats of formation being different by only 7 kJ/mol, one may suggest, allowing for experimental error, that they are the same isomer, but it is not the case. The MI mass spectra of both ions show metastable peaks at m/z 42 corresponding to loss of water. However, the CA mass spectrum of [propan-1-ol]$^{+\bullet}$ shows major peaks at m/z 59, 42 and 31 whereas [$^{\bullet}CH_2CH_2CH_2OH_2^+$] is dominated by a cluster of peaks between m/z 42-37. The CA information is characteristic of the structure of each isomer. Why are the MI spectra so similar? The explanation is that the MI decomposition is characteristic of [$^{\bullet}CH_2CH_2CH_2OH_2^+$]

and that propan-1-ol ions isomerize to this distonic ion before fragmenting. However, the fast CA processes do not allow this rearrangement (Fig 29). A third isomer [$CH_3^{\cdot}CHCH_2OH_2^{+}$] is also known, it can be generated by $HOCH_2CH(CH_3)CH_2OH$. The MI mass spectrum shows only m/z 42 whereas in the CA, there is m/z 42 as base peak with fairly intense peaks at m/z 41 ($C_3H_5^{+}$), m/z 27 ($C_2H_3^{+}$) and m/z 19 (H_3O^{+}). The CA information was argued to be indicative of a proton bound water molecule and allyl radical structure (the proton bound type ions will be discussed in more depth in the next chapter), a suggestion which resulted from the study of deuterium labelled analogues.

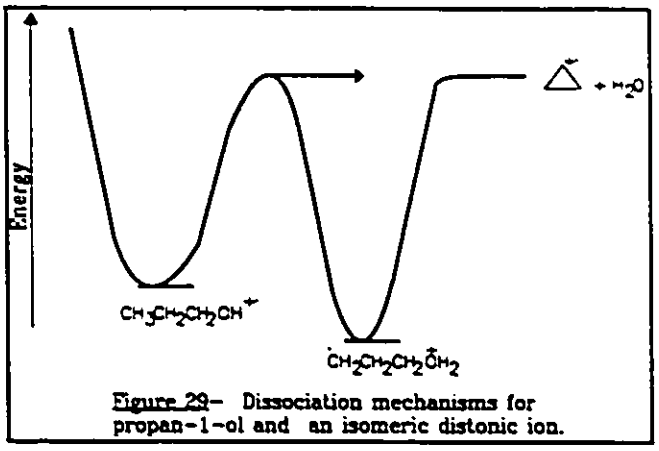

Figure 29- Dissociation mechanisms for propan-1-ol and an isomeric distonic ion.

The second example uses a combination of metastable and collision activation mass spectra, kinetic energy release and labelling experiments to probe the structures of various C_2H_6O ions[53,54]. The $C_2H_6O^{+\cdot}$ ion is generated from 1,3-propanediol[55], ($HOCH_2CH_2CH_2OH \rightarrow {}^{\cdot}CH_2CH_2{}^{+}OH_2 + CH_2O$), and its major dissociation process gives rise to m/z 28 ($C_2H_4^{+\cdot}$) in both the MI and the CA mass spectra. The CA results are markedly different from those obtained with ionized ethyl alcohol (m/z 29, 31) and dimethyl ether (m/z 29,30) (see table I). A complex formed by a water molecule and an ethylene ion was proposed as the structure for $[C_2H_6O]^{+\cdot}$ from 1,3-propanediol. This proposal was made on the basis of two important observations. First, the very small kinetic energy release (0.2 meV) for loss of water and large intensity of m/z 28 in the

CA points to a facile loss of water i.e. bond cleavage $^{\cdot}CH_2CH_2OH_2^{+} \rightarrow CH_2{=}CH_2^{+\cdot} + H_2O$. Second, the labelled compound ($DOCH_2CH_2CH_2OD$) produced only $C_2H_4D_2O^{+\cdot}$ and this ion showed a specific loss of D_2O in both MI (20:1 versus HDO) and CA (60:1 versus HDO) mass spectra. This is in keeping with a structure in which both D atoms are attached strongly to oxygen. In the second publication[56], more $[C_2H_6O]^{+\cdot}$ isomers were studied: $CH_3O(H)CH_2^{+\cdot}$, $CH_3CHOH_2^{+\cdot}$ and possibly $CH_2{=}CH^{\cdot\cdot}H^{+\cdot\cdot}H_2O$. Table I compares the CA results obtained for all $[C_2H_6O]^{+\cdot}$ isomers. It clearly indicates that each isomer has a distinct structure, the CA peaks being very characteristic in each case.

TABLE I Relative intensity of CA fragments for six C_2H_6O isomers.

ION	45	31	30	29	28	27	19	18	16	15	14	13
$CH_3CH_2OH^{+\cdot}$	550	100	6	15	3.5	<1	1.5	-	-	2.5	1	0.5
$CH_3OCH_3^{+\cdot}$	1200	8	15	100	6.5	1	-	-	2	37	5	1
$^{\cdot}CH_2CH_2{}^{+}OH_2$	1.5	1.3	0.4	1.3	100	12	2	0.7	-	0.3	0.5	0.1
$CH_3{}^{\cdot}CH^{+}OH_2$	-	7	-	10	100	33	2	-	-	0.8	0.3	-
$CH_3O^{+}(H)^{\cdot}CH_2$	-	100	5	20	-	-	-	-	0.4	1.5	1	0.5
$CH_2{=}CH^{\cdot\cdot}H^{+\cdot\cdot}H_2O$	-	27	10	12	100	25	1.3	0.2	0.3	1.4	0.8	0.3

3.5 Collision Induced Dissociative Ionization Mass Spectra

The technique of Collision Induced Dissociative Ionization (CIDI) mass spectrometry provides a way to study neutral fragments produced from metastable ions. Only recently (1983)[33] did the interest in this new technique begin. Although it is generally easy to identify the neutral fragment from a dissociation, some complicated cases may occur when the neutral can exist in more than one form i.e. $^{\cdot}CH_2OH$ and $CH_3O^{\cdot}$[55]. CIDI is used to study the neutral fragments from the following process:

$$A^{+\cdot} \text{ -*}\rightarrow B^{+\cdot} + C$$

$$C \text{ --}^{He}\rightarrow C^{+\cdot} \rightarrow D^{+\cdot} + E + \text{etc...} \qquad [18]$$

The mass selected ions $A^{+\cdot}$ metastably fragment in the second FFR where a positively charged electrode repels all ions to let only the neutral fragments through to the gas cell. The neutral C will collide with the gas (typically He or O_2, chosen on the same basis as for a CA gas) and will be ionized. The resulting CIDI mass spectrum will be obtained by analysis of the new ions using the electrostatic analyzer. Note that the ions derived from the ionized neutral, $C^{+\cdot}$ (and fragments), will have only a fraction (m_C/m_A x zV_{acc}) of the initial translational energy of the ion $A^{+\cdot}$.

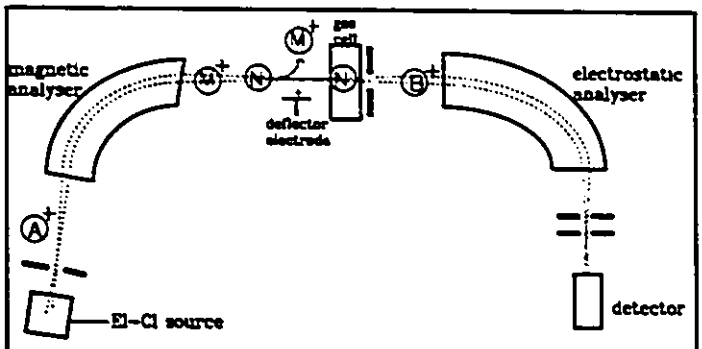

Figure 30. The ion M and its corresponding neutral N are metastably generated in the second field free region, the ions are deflected by means of a positive electrode and only the neutrals N are ionized in the gas cell to give new products which give rise to the CIDI mass spectrum.

As seen in section 3.1.6, the knowledge of heats of formation of neutrals is essential to assign their structures. To establish the heat of formation of a specific neutral, it is necessary to confirm the structures when more than one isomer is possible. Work by Burgers et al[56] showed that CIDI mass spectra can be used as an efficient technique to differentiate isomers. The CIDI mass spectra of neutral HCN and HNC were obtained and easily characterized the two isomers: HCN generated from pyridine shows two intense peaks at m/z 12 and 13 (ratio 2:3) and a weaker peak at m/z 15 whereas HNC from aniline shows only a very intense peak at m/z 12 and a weaker peak at m/z 15.

Since the neutrals generated from metastable ions usually have little excess internal energy they are unlikely to undergo rearrangement. However, it was suggested that an increase in collision gas pressure could convey energy to the neutrals allowing them to isomerize before collision induced ionization[34]. Information on the structure of many neutral fragments has been obtained via CIDI[57] mass spectra and has helped to solve various mechanistic problems. The usefulness of this technique will be shown in chapter 5 where it provides information concerning hydrogen/deuterium exchange mechanisms and, indirectly, on the details of the fragmentation mechanism of the ion of interest.

3.6. Neutralization Reionization Mass Spectrometry

The Neutralization Reionization Mass Spectrometry (NRMS) technique is, similarly to CIDI, a technique used to study neutrals in the gas phase. In 1977, Lieder and Brauman[58]

described a "technique applicable to the identification of neutral products derived from ion-molecule reactions". It involved generating a continuous flow of fragments followed by removal of the ions and analysis of the neutrals via mass spectrometric techniques. However, the term NRMS did not appear until 1983[59] when Danis et al showed that this technique could provide valuable information on the structure and chemistry of neutrals, ions and molecules. Since then, the subject has been reviewed several times[60,61,62].

The technique is simple: the mass selected ions enter cell 1 where the target gas induces collisional charge exchange to produce a neutral species. Then, as in CIDI experiments, all remaining ions are deflected out of the ion beam path (deflector voltage typically 500 V) and only the neutrals enter cell 2 where they are reionized by collision with a second target gas. The resulting mass spectrum is obtained by scanning the energy analyzer in the usual way.

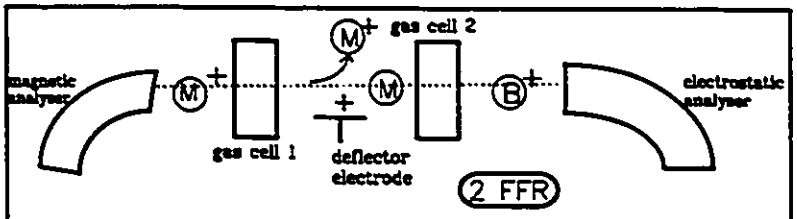

Figure 31– The ion M+ is neutralized in cell 1 and the deflector ensures that only neutrals M enter cell 2 to form products B+ which give rise to the NR mass spectrum.

The neutrals entering cell 2 may, however, be generated in more than one way[62]. There is, of course, the neutral corresponding to the mass generated by electron transfer

$$ABC^{+} + G \rightarrow ABC + G^{+} \rightarrow AB + C^{+} \qquad [19]$$

but also, the neutrals resulting from metastable dissociations of the ion ABC^+, collision induced dissociations and further dissociation of the resulting fragments e.g.

$$ABC^+ + G \rightarrow AB + C^+ + G \text{ -*}\rightarrow A + B^+ \quad [20]$$

$$ABC^+ \text{ -*}\rightarrow AB + C^+ \text{ -*}\rightarrow A + B^+ \quad [21]$$

The neutrals generated unimolecularly (equation 21) before the first cell may be identified by applying a voltage on the cell in a similar fashion to the technique used in the CA technique (see section 3.4.2.1). The importance of the neutrals produced by the mass selected CA fragmentation (equation [21]) depends on the target and their contribution to the overall mass spectrum cannot be subtracted. However, choosing the right target will allow neutralization to be favored over fragmentation[63]. He which was the preferred gas for CA because of its low probability of charge exchange, is very inefficient as a neutralization target because of its high ionization energy (24.6 eV). Alkali metal vapors were found to be very effective for neutralization[62] and Xe (more convenient to use since it is a gas) was found to produce an excellent yield of neutrals without major CA contributions[64]. Neutral fragmentation is favored with targets of lower IE[62,65] producing exothermic reactions, (K=4.34 eV, Na=5.14 eV, Zn=9.39 eV, Hg=10.4 eV, Xe=12.13 eV, etc...) but in general, the ideal target should have an IE near or above (resonant) that of the neutral to obtain a beam of neutrals with low internal energy.

The pressure at which the neutralization is typically performed corresponds to approximately 30% beam reduction, corresponding to mostly single collisions (see Fig 27). The

choice of reionization gas is performed similarly to the choice of CA gas (section 3.4.1) with 90% transmission as the ideal gas pressure. However, O_2, considered a "soft-target", is better to obtain "molecular information" because when studying the structure of a neutral fragment, less fragmentation of the new ions is required.

An important factor when performing NRMS experiments is optimizing the sensitivity. Since the neutralisation and reionization processes reduce the flux in the instrument, the final mass spectra may be 3-5 orders of magnitude less intense than in the normal mass spectrum[62]. Therefore, in some cases, it may be necessary to use a mini-computer system to record a series of scans and obtain a signal averaged spectrum.

Often, the NRMS of molecular ions from stable neutral molecules is similar to the corresponding EI and CA mass spectra indicating that the species do not undergo major rearrangements during the neutralization and reionization processes. When stable neutral fragments corresponding to M or M-1 or M-2 are not present in the NRMS, it indicates the rapid decomposition of the unstable neutral. Alternatively, when there is a recovery signal for the molecular ion (peak located at m/z of the molecular ion) but the NRMS differs from the CA mass spectrum, this can indicate that the neutral M_B rearranges rapidly into a more stable neutral M_C (fig 32). Again, as for the CA mass spectra, the NRMS is not only useful by comparison with previous data but may provide structural information. During the reionization process, the electron transfer will be considered as a vertical Franck-Condon process. In general, if the geometries of the ion and the neutral are similar, a stable neutral will be produced (M_A) in the

charge transfer process whereas if the geometry is different, the neutral will have a very short lifetime before decomposing via low-energy channels[63] (Fig 32).

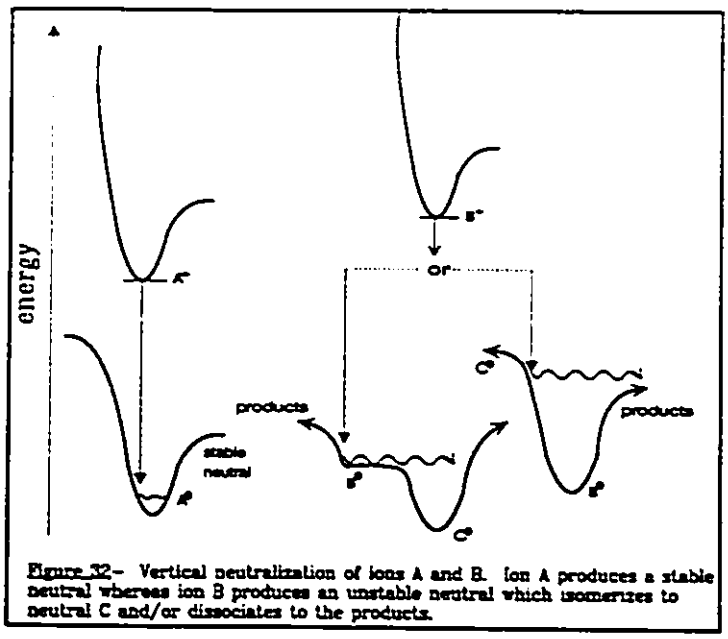

Figure 32- Vertical neutralization of ions A and B. Ion A produces a stable neutral whereas ion B produces an unstable neutral which isomerizes to neutral C and/or dissociates to the products.

3.6.1 Species Obtained via NRMS

There are two major types[63] of ion for which NRMS has been particularly useful: distonic and ylid ions and protonated ions. There has been much controversy concerning the proof of the possible existence of the following hypervalent species using NRMS: $CH_5^{\bullet}$, $CD_5^{\bullet}$, $H_3^{\bullet}$, $H_3O^{\bullet}$, $D_3O^{\bullet}$, $NH_4^{\bullet}$, $ND_4^{\bullet}$, protonated hydrogen halides and protonated methanol. The results for $H_3^{\bullet}$ radical, ammonium radicals and protonated hydrogen halides are now generally agreed upon and their existence established, whereas there remains controversy over the other hypervalent radicals. Work performed very recently in this laboratory has clearly shown that protonated dimethyl ether, protonated methyl ethyl ether and their deuteronated analogues are stable hypervalent species[65].

Unconventional ions such as ylid, distonic and proton-bridged ions, which were predicted by theory to be stable, have had their existence confirmed by there being a recovery signal in the

NRMS spectrum. Examples of stable ylids are $CH_3{}^{\cdot}CHCl^{-}H$ and $^{\cdot}CH_2{}^{-}NH_3$[66]. The existence of proton bridged ions is proven, not by a recovery signal, but by the production of a signal corresponding to the formal components of the ion (for example, $^{\cdot}CH_2O^{-}H^{+}{}^{-}NH_3$ produces $^{\cdot}CH_2OH$ and NH_3 in the NRMS spectrum).

3.7 Charge Stripping

Charge Stripping reactions were first described by Cooks, Beynon and Ast in 1972[67]. They arise from collision of a high energy ion with a target to produce the doubly charged ion

$$M^{+\cdot} + G \rightarrow M^{2+\cdot} + G + e \qquad [22]$$

This process is characterized by very sharp peaks in a CA mass spectrum which appear at half the ESA voltage required to transmit the precursor ion. It should also be mentioned that these processes are much less intense than CA processes involving singly charged ions and may sometimes be difficult to observe. The low intensity of these peaks is due to the large energy required to generate them. In some cases, singly charged ions in the CA mass spectra may not yield enough information to differentiate two isomers. Such is the case of ionized propene and cyclopropane, $C_3H_6^{+\cdot}$,[68] which give very closely similar CA spectra but produce distinctive charge stripping mass spectra. Similar experiments have shown that charge stripping mass spectra were more effective than CA mass spectra to identify and assign a structure to $C_5H_{10}^{+\cdot}$ isomers[69].

Therefore, it may be concluded that generally, if the charge stripping mass spectra for two ions are identical, then so are their structures.

3.8 Combination of Techniques to Assign Structures to Ions

In this section, t.. examples where the combination of various techniques is used to answer questions concerning ion structures and fragmentation mechanisms, will be described.

3.8.1 Methyl Acetate and its Isomers

Both methyl acetate, $CH_3COOCH_3^{+\cdot}$, molecular ion and its enol, $[CH_2C(OH)OCH_3]^{+\cdot}$, show metastable peaks corresponding to $[C, H_3, O]^{\cdot}$ loss with a $T_{0.5}$ of 14 meV[70]. These results suggest the same structure for both ions. Source generated methyl-d_3 acetate ions give a predominance of $[C, D_3, O]^{\cdot}$ fragments whereas at longer lifetime, the H/D mixing between the two methyl groups increases to nearly random statistical. For the enol ion, labelling shows that the original methoxy group is not lost as $[C, H_3, O]^{\cdot}$ but that the enol hydrogen is lost to a large extent with two of the methoxy hydrogens. This seems to imply that the keto ion is involved in the fragmentation via two 1,4-shifts from the enol ion. However, the CA mass spectra show different results for both acetate and enol, consistent with the fact that low energy ions do not interconvert easily.

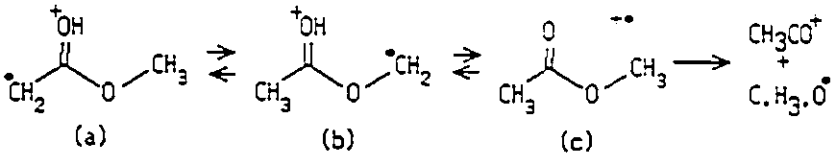

Figure 33 - Hydrogen mixing in methyl acetate occurs via two 1,4-H shifts.

In 1985, the problem was studied by Wesdemiotis et al[71] and Terlouw et al[72]. The former studied two new $C_3H_6O_2$ isomers: $CH_3C(OH)OCH_2^{+\bullet}$ and CH_3COCH_2OH and concluded that they were not related to any of the above species. They also stated (using D-labelling) that the isomerization a<->b was easier than b<->c (lower energy barrier). But that both barriers were comparable to c $\rightarrow$ CH_3CO^+ + $CH_3O^{\bullet}$. The work performed by Terlouw et al consisted of performing the CIDI of the neutral products obtained for a, b and c. The results showed that apparently $^{\bullet}CH_2OH$ was mainly produced. From results of isotopic labelling and ion energetics, a fourth structure was proposed, $CH_3COO^+(H)CH_2^{\bullet}$, which is lower in energy than a, and could be the reacting configuration for the fragmentation yielding $^{\bullet}CH_2OH$. The structure would arise from the 1,4-shift taking place in (b) to yield a four-centered intermediate producing the ylid ion. A simple bond cleavage yields the products.

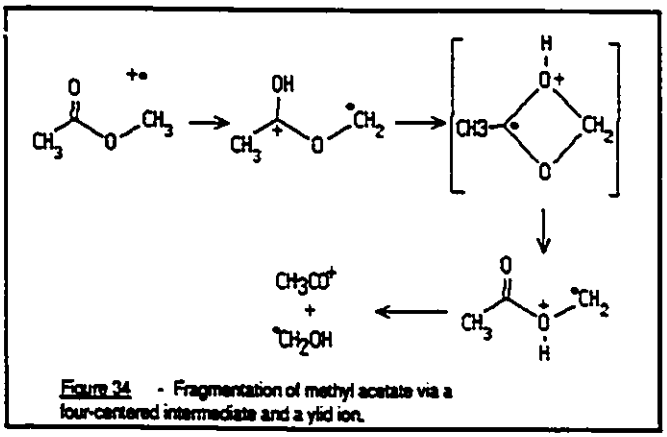

Figure 34 - Fragmentation of methyl acetate via a four-centered intermediate and a ylid ion.

There is no doubt that both $CH_3O^{\cdot}$ and $CH_2OH^{\cdot}$ are produced, and a quantitative analysis has shown that they are generated in a 4:1 ratio. However the $CH_2OH^{\cdot}$ radicals do not originate from isomerization of $CH_3O^{\cdot}$ but from rearranged methyl acetate molecular ions[73]. This is supported by an ab initio molecular orbital theory study[74] which showed that the minimum energy pathway for dissociation of ionized methyl acetate is via the H^+-bridged ion $[CH_3{}^{\cdot}CO\text{-}H^+\text{-}OCH_2{}^{\cdot}]$ which yields CH_3CO^+ and $CH_2OH^{\cdot}$. This mechanism was found to be lower by 10 kJ/mol than the direct dissociation $CH_3COOCH_3{}^{+\cdot} \rightarrow CH_3CO^+ + CH_3O^{\cdot}$. However, at higher energies, the formation of $CH_3O^{\cdot}$ is certainly favored.

3.8.2 1,2-propanediol

It has been shown that ethylene glycol loses $HCO^{\cdot}$ via proton-bridged species: $[HOCH_2CH_2CH^{+\cdot}] \rightarrow [CH_2{=}O\text{-}H^+\text{-}O(H)^{\cdot}CH_2] \rightarrow [H\text{-}^{\cdot}C{=}O\text{-}H^+\text{-}O(H)CH_3] \rightarrow [CH_3{}^+OH_2] + HCO^{\cdot}$. The homologue 1,2-propanediol was then studied with the suspicion that it may behave similarly to ethylene glycol[75]. The EI and CA mass spectra are significantly different indicating that a rearrangement has taken place for the molecular ion. The MI processes taking place are loss of $CH_3^{\cdot}$, H_2O, CH_4O, $CH_3^{\cdot} + H_2O$, $CH_4 + H_2O$ and $C_2H_3O^{\cdot}$. Note that it is very uncommon for an ion of this size to undergo six competing metastable dissociations. The measured appearance energy of these processes showed that they are all indeed competitive (all in the range 10.06-10.14 eV) and very probably take place via rearranged stable isomers of the molecular ions. The CA and MI mass spectra of 1,2-propanediol and of the isomeric H-bridged species $[CH_2{=}CHO\text{-}H\text{-}O(H)CH_3]^{+\cdot}$ (produced from 4-methoxybutanol) showed similar characteristics,

indicating a probable isomerization of 1,2-propanediol in the H-bridged species. The proposed mechanism is illustrated below. The ΔH_f values support this mechanism.

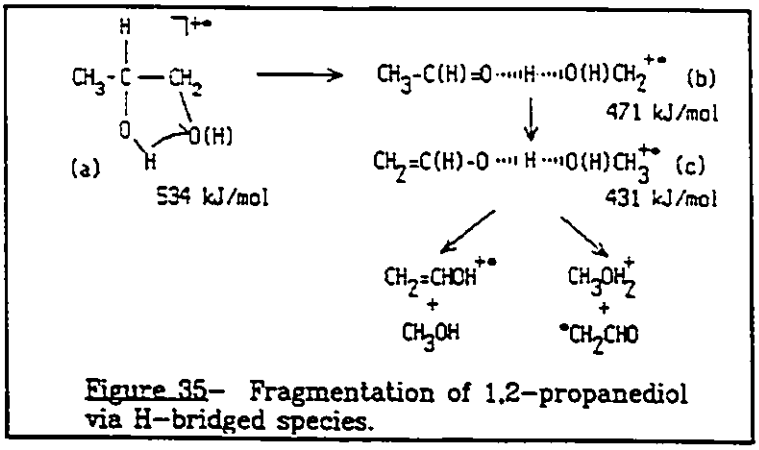

Figure 35– Fragmentation of 1,2-propanediol via H-bridged species.

To study the structure of the neutrals, a CIDI experiment was performed. The results showed that $CH_3^{\bullet}$, CH_4, H_2O, CH_3OH and $CH_3CO^{\bullet}$ were the only neutrals present during the fragmentation of 1,2-propanediol. However, the species in the above mechanism do not rationalize the formation of $CH_3CO^{\bullet}$ ($CH_2CHO^{\bullet}$ would be expected to be generated). A second H-bridged structure, $CH_3C{=}O^{-}H^{+\bullet}{-}O(H)CH_3$, (d), was then added in the fragmentation mechanism, ΔH_f=478 kJ/mol. Its existence was established by a NRMS experiment. The comparison of the NRMS obtained with 1,2-propanediol with the NRMS of both H-bridged species show many common characteristics, allowing one to interpret the neutralization of the diol via the two species (c) and (d). From the results, it was concluded that (c) is the intermediate producing vinyl alcohol ion whereas (d) produces protonated methanol and acetyl cations. The results of D-labelling posed new questions as to the amount of internal energy in the molecule. Some of the H/D exchanges were very specific whereas others were randomized. Another possible intermediate which can rationalize losses of H_2O and CH_4 is (e), $CH_3CO(H)^{-}H^{-}O(H)CH_2^{+\bullet}$, which

can rearrange into (f), a water molecule electrostatically bonded to propen-2-ol ion, $CH_3C(OH)=CH_2^{\cdot+} \cdots H_2O$, to form an ion-molecule complex. Labelling experiments confirm this structure.

The combination of the various techniques allowed one to probe into the various fragmentation routes for 1,2-propanediol. It was shown that the involvement of H-bridged species and ion-neutral complex was essential to explain the various H/D label exchanges.

CHAPTER 4

UNCONVENTIONAL ION STRUCTURES, WHEN ARE THEY NECESSARY TO EXPLAIN FRAGMENTATION MECHANISMS ?

4.1 Introduction.

In 1989, Burgers and Terlouw published a review entitled "Structures and Reactions of Gas Phase Organic Ions"[76] which described new techniques, the existence of new classes of ions and dissociation mechanisms. Since the techniques have been fully discussed in the previous chapter, the emphasis of this chapter will be placed upon describing the unconventional ions and the way they may be involved in various fragmentation mechanisms. Finally, the section on ion/molecule and ion/radical complexes will be discussed in more detail because it is the basis for the study performed in chapter 5.

4.1.2 Some Definitions.

Unconventional ions have been divided into various classes such as distonic ions, ylid ions, ion/neutral and ion/radical complexes, proton-bridged complexes and destabilized carbenium

ions. Figure 36 gives an example of each type of ion.

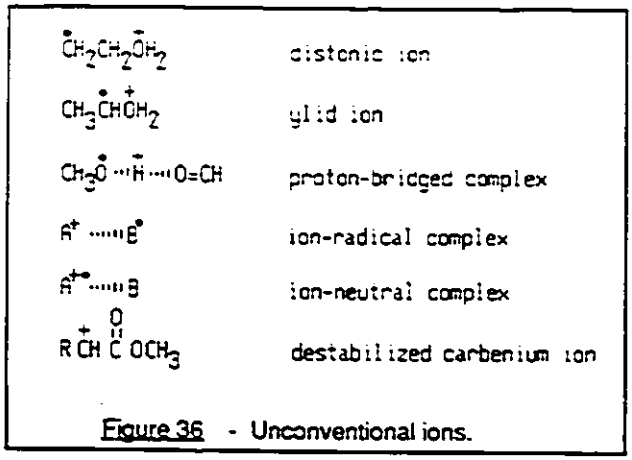

Figure 36 - Unconventional ions.

The destabilized carbenium ions will not be discussed here because they are not closely related to the projects included in this thesis. However, more information on such ions can be found in reference 77.

Distonic and ylid ions are radical cations which have the charge and the radical located on different atoms in the molecule. The difference between ylid and distonic ions is that the charge and radical are located on adjacent atoms in an ylid ion but are further apart in a distonic ion. Ion/molecule or ion/radical complexes are best described as ions composed of two entities (ion and neutral molecule or ion and free-radical) held together by means of electrostatic bonding. Finally, proton-bridged complexes are ion-radical or ion-neutral pairs held together by an H^+ ion forming a bridge between the two parts.

4.2 Energetic Aspects of these Unconventional Ions.

In chapter 3, it was shown that it is possible to estimate the heats of formation of ions using empirical equations (section 3.1.6) as well as to obtain them by experiment. No special experimental technique is required to measure ΔH_f° for these unconventional ions. However, a new set of criteria are required for estimating their heats of formation.

For ion/radical and ion/neutral complexes, it is difficult to estimate any ΔH_f values because the binding energy for the electrostatic bond is generally not known. All that is likely to be known is the energy of the products relative to ground state structures of the ion other than the above complexes.

The use of ab-initio molecular orbital theory calculations solves a lot of questions when it comes to estimating the heat of formation of H-bridged and distonic and ylid ions. However, as the size of the ion increases, so does the cost (i.e. computer time) of such calculations. It was found[78] that the use of proton affinities (PA) and hydrogen bond strengths (D-[AH$^+$-B]) to calculate ΔH_f of proton bridged odd-electron species reproduced the theoretical calculations and the experimental data. The proton affinity (PA) of a neutral or an ion is defined as the energy binding it with a proton. Larson and McMahon[79] have shown that the value of the H bond strength in a proton bound pair is related to the proton affinities of the partners according to the following equation

$$D[AH^{+}\text{-}B] = 0.46\ [PA(B)\text{-}PA(A)] + (30.8 \pm 2\ kcal/mol) \qquad [23]$$

The heat of formation of the ion is then given by

$$\Delta H_f[I^{+}] = \Delta H_f[AH^{+}] + \Delta H_f[B] - D[AH^{+}\text{-}B] \qquad [24]$$

Mautner[80] has also derived an expression for proton-bound pairs which was to be applied to other types of complexes, e.g. which contain N and S as heteroatoms.

$$D[AH^{+}\text{-}B] = 0.26\ [PA(B)\text{-}PA(A)] + (30 \pm 2\ kcal/mol) \qquad [25]$$

The equations were derived for molecular species A and B but the equations can also be used for a molecule A and a free radical B$^{\cdot}$.

Here is an example[78], $CH_3CO^{\cdot}\text{--}H^{+}\text{--}OCH_2$ to which the following values are associated: $PA[CH_3CO^{\cdot}]$=158 kcal/mol, $PA[OCH_2]$=171.7 kcal/mol, $\Delta H_f[CH_3OH^{+}]$=203 kcal/mol and $\Delta H_f[CH_2O]$=-26 kcal/mol. Considering that the ion is in the form $A^{\cdot}\text{--}H^{+}\text{--}B$, where A=$CH_3CO^{\cdot}$ and B=CH_2O and using the above equations, we obtain $\Delta H_f[I^{+}]$=140 ± 5 which compares extremely well with the theoretical ab initio calculation value of 138 kcal/mol.

The heats of formation of distonic and ylid ions are estimated in a different manner. Originally, they were thought to be accessible using one of the following two assumptions[38]:

(1) That the strength of a given bond in an even electron ion is the same as that in the analogous neutral molecule.

e.g. $D[H\text{-}^{\cdot}CH_2CH_2] \equiv D[H\text{-}CH_2CH_3]$

(2) That the proton affinity of a free radical (not at the radical site) is the same as that of the analogous molecule.

e.g. $PA[CH_3O^{\cdot}CH_2]$ at the oxygen site is the same as $PA[CH_3OCH_3]$

The hydrogen affinity (HA) of an ion is the enthalpy change associated with the liberation of an H radical from a protonated molecule (and is an alternative way of expressing item (1) above)

$$RXH^{+} \rightarrow RX^{+\cdot} + H^{\cdot} \qquad [26]$$

and the HA of an ion is given by

$$HA[RX^{+\cdot}] = IE[RX] + PA[RX] - IE[H^{\cdot}] \qquad [27]$$

where IE are ionization energies and PA is the proton affinity.

In a recent publication, Holmes and Lossing established some rules related to the hydrogen affinities (HA)[37] of various classes of molecules. For hydrocarbons, it was shown that the strength of a bond depends on the nature of the adjacent charge-bearing carbon atom, e.g. if the charge site is tertiary, the HA is smaller than for secondary and primary sites e.g. tertiary (H), $((CH_3)_2\underline{C}H^+CHCH_3$=66 kJ/mol and, primary (H), $(C\underline{H}_3)_2{}^+C(CH_2CH_3)$=95 kJ/mol). The effect of attachment to a π-system on the bond strength is not very great. For oxygen-containing species, the presence of an OH group at the charge bearing site does not reduce the strength of an adjacent secondary or tertiary bond as much as for the corresponding alkyl ion e.g. HA values for ($CH_3C\underline{H}_2{}^+CHOH$=80 kJ/mol and $CH_3C\underline{H}_2{}^+CHCH_3$=76 kJ/mol). In the case of hydroxylic ions, a size effect is observed i.e. HA falls slightly with increase in ion size. For nitrogen-containing ions, the HA values correspond quite well to the bond strength in NH_3 for protonated primary amines, to the bond strength of primary amines for protonated secondary amines and bond strength of secondary amines for protonated tertiary amines. From these and related results, it can be concluded that the HA values (in ions) are seldom the same as the homolytic bond strength values for neutral counterparts and so assumption (1) is clearly false. For distonic ions, some data are available and it can be observed that for oxygen containing ions, the CH_2-H bond is significantly stronger than for any neutral counterpart. This also contradicts assumption (1) above.

For the proton affinities of free radicals, the PA increases with size in approximately the same way as for neutrals. The available PA values for a variety of free radicals[37] indicate that the assumption (2), saying that the PA of free radicals equals that of the analogous molecule, is

also probably incorrect.

How then can the ΔH_f values of distonic and ylid ions be calculated? The use of a thermochemical cycle, bond strengths and PA values allows one to make a fair estimate (Figure 37).

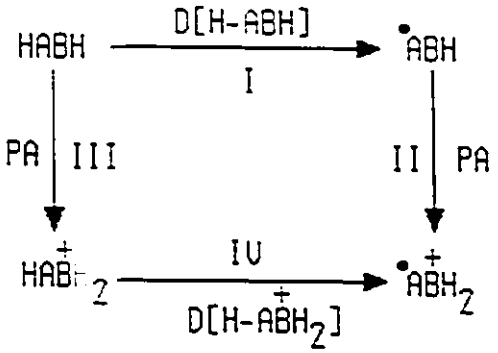

Figure 37 - Thermochemical cycle for calculating heats of formation of distonic and ylid ions.

The ΔH_f of the desired distonic or ylid ion $^{\bullet}AB^{+}H_2$ can be determined following route I and II, or III and IV whose net enthalpy changes must be the same values i.e.

$$\Delta H_f(I, II) = D[H\text{-}ABH] - PA[AB^{\bullet}H] \qquad [28]$$

$$\Delta H_f(III, IV) = D[H\text{-}A^{+}BH_2] - PA[HABH] \qquad [29]$$

Using the data established for proton affinities and hydrogen affinities, one can obtain a fairly reliable estimate for the heats of formation of H-bridged, distonic and ylid species.

In the next three sections, the dissociative properties of unconventional ions will be discussed with emphasis on ion-dipole complexes. The last section of this chapter describes a few cases where the involvement of these unconventional ions was not justified.

4.3 Proton-bridged complexes.

The existence of H^+-bridged complexes has been established for a number of systems by ab-initio calculations[81,82]. However, it is quite difficult unequivocally to prove their existence by experiment because their predictable dissociation pathways may be indistinguishable from those for other isomeric forms. That is why calculations are particularly useful; they can evaluate the height of the energy barriers between isomers, thus showing whether isomer interconversion can precede fragmentation. For example, theoretical calculations[81] had shown that complexes between ionized vinyl alcohol and water, $[CH_2CHOH\text{-}OH_2]^{+\cdot}$, and ionized vinyl alcohol and methanol, $[CH_2CHOH\text{-}OHCH_3]^{+\cdot}$, are stable in the gas phase, but no direct experimental confirmation was available. Observations from dissociation experiments only provide information which may be common to two different isomers. That is why the combination of both theory and experiment is useful. In a paper published by Burgers et al in 1987[82], a number of $C_2H_6O_2^{+\cdot}$ ions were studied by both experiment and theoretical calculations. Three thermodynamically stable isomers were studied in terms of their relative stability using ab-initio calculations: ionized ethylene glycol, $CH_2OHCH_2OH^{+\cdot}$ (1), and the three H-bridged ions, $[CH_2\text{-}O(H)^{-}H^{-}O{=}CH_2]^{+\cdot}$ (2), $[CH_3O^{-}H^{-}O{=}CH_2]^{+\cdot}$ (3) and $[CH_3OH^{-}H^{-}O{=}CH]^{+\cdot}$ (4). The dissociative characteristics of two ions was also studied: (1) was made from direct ionization of the neutral molecule, (3) was produced by CO loss from ionized methyl glycolate.

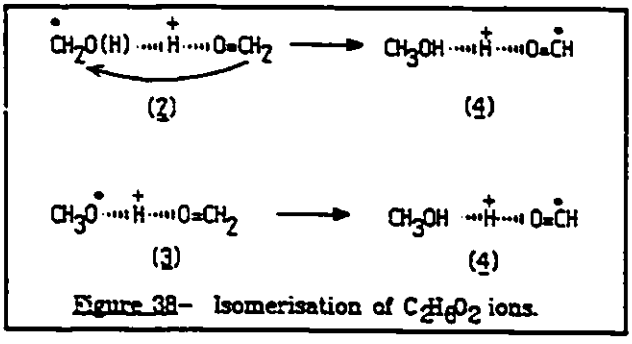

Figure 38– Isomerisation of $C_2H_6O_2$ ions.

Ion (1) produces $HCO^{\cdot}$ and $CH_3OH_2^{+}$ in its metastable fragmentation. The ionization energy of ethylene glycol was measured and the activation energy for this metastable process was determined as 0.49 ± 0.15 eV. This activation energy is too small to allow the molecular ion to be metastable. Therefore, ionized ethylene glycol must, before fragmenting, isomerize to an intermediate having a lower heat of formation. A possible structure is ion (2) which is 13 kcal/mol lower in energy. A 1,5-H transfer in (2) would produce ion (4) which, by direct bond cleavage, forms the products (Fig 39). The metastable characteristics of ion (3) are very similar to those of ion (1) but the kinetic energy release value is different ($T_{0.5}$ = 27 meV versus $T_{0.5}$ = 13 meV for (1)). Furthermore, the CA mass spectra of the $CH_4O^{+\cdot}$ ions collisionally generated from ethylene glycol and from ion (3) show different characteristics supporting the hypothesis that they fragment via distinct intermediates. Therefore, it is proposed that ions (3) may isomerize directly to structure (4), without interconverting to (1) or (2), and produce $CH_3OH_2^{+}$ + $HCO^{\cdot}$ via direct bond cleavage. Ab-initio calculations were found very useful to estimate the heights of the barriers (Figure 38).

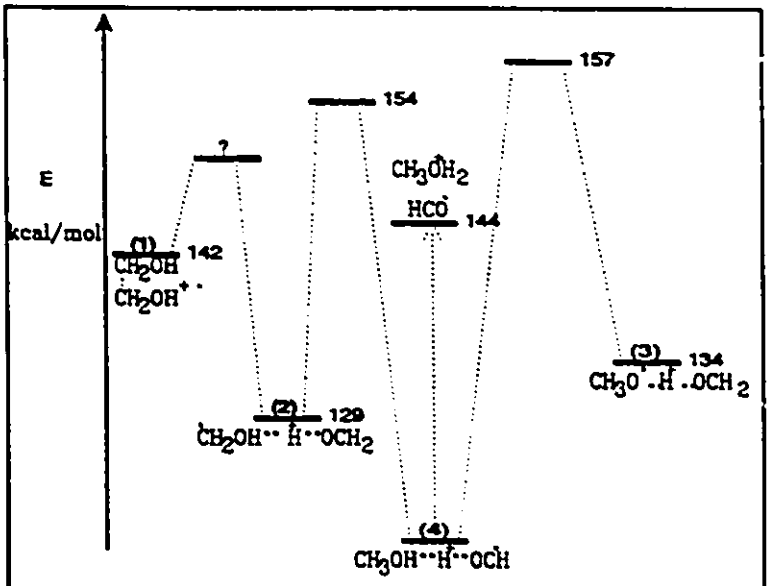

Figure 38- Energy diagram for dissociation of $C_2H_6O_2$ isomers.

4.4 Distonic and Ylid Ions.

Returning to the problem of methyl acetate (from section 3.8.1), it was proposed that, prior to dissociation, CH_3COOCH_3 rearranges to the ylid ions $CH_3CO^+O(H)^-CH_2$ and $^-CH_2{}^+C(OH)OCH_3$. More recent work[83] shows that the distonic ion may also be involved, because under collision conditions $CH_3{}^+C(OH)O^-CH_2$ can be forced to lose a methene fragment. Collision experiments suggested that the methene is lost from the distonic ion $CH_3{}^+C(OH)OCH_2{}^\cdot$. There was no direct evidence for the existence of the ylid ion and ab-initio calculations for molecules of this size are very difficult. Nevertheless, some calculations were performed on parts of the energy surface by Heinrich and coworkers[74]. They suggest a multistep reaction scheme. First, $CH_3COOCH_3{}^{+\cdot}$ isomerizes to the distonic ion $CH_3C(OH)OCH_2{}^{+\cdot}$ which then rearranges to a hydrogen-bridged complex $CH_3CO^\cdot{\cdots}H^+{\cdots}OCH_2$. This ion would then dissociate to give the experimentally observed products, $CH_3CO^+ + {}^\cdot CH_2OH$.

4.5 Ion-dipole Complexes.

The intermediacy of ion-radical and ion-neutral complexes has become very popular in terms of a rationale for many fragmentation mechanisms. The complexes are best described as ion-radical, $[R_1{}^{+\cdot}{\cdots}X^\cdot]$, or ion-molecule, $[R_1H^+{\cdots}(X\text{-}H)]$, pairs bound together by electrostatic forces. The existence of such complexes has been inferred from observations[76] which indicate:

i) isomerization of the cation portion, R_1^+ into R_2^+

ii) specific H transfers between the two formal components of the complexes

Hammerum[84] has outlined some criteria which permit these complexes to exist: one of them is that the complex must be non-dissociative long enough to allow for physical reorganization and chemical reactions to take place between the components. Another criterion is that the two entities are separated (without dissociation) far enough from each other to allow for their independent rearrangement to take place.

In a recent review, McAdoo[85] also proposed a set of criteria which indicate the existence of a complex. The list is as follows:

1. Complete dissociation of the ion will be observed and will increase in importance relative to the electrostatically bound complex as the energy of the system increases.

2. Complex-mediated processes will be among the lowest energy reactions of a given ion.

3. Reactions within and between partners may occur below the threshold for simple dissociation.

4. Alternative mechanisms to complexes would require higher energy transition states,

transition states of impossible geometries, or transition states in which multiple bond-breaking and making would necessarily occur simultaneously.

5. Unusually large isotope effects may be observed.

6. Translational energy releases in corresponding metastable decompositions may be small.

However, none of these criteria are exclusive to ion-dipole complexes nor will they all be exhibited by the complexes. Therefore, the use of this list may not be enough to characterize complex-mediated reactions. Conclusions must then be drawn by comparing the overall behaviour of the ion with predictions obtained by studying the potential surface of the system, obtained either by extensive experiments or by high level ab-initio molecular orbital theory calculations.

Figure 40 represents the reaction coordinate for both complex-mediated and simple dissociation reactions[85]. The complex is formed when a bond is broken sufficiently that the fragments begin to rotate freely relative to each other (-1-).

The dotted line represents a direct dissociation whereas region (-2-) represents the potential well in which the complex is stable. When the electrostatic pair is further apart, the potential energy increases to reach point (-3-). The energy rises again at the centrifugal barrier

(to conserve angular momentum) and, to overcome the electrostatic attraction, decreases as both species are separated into $HA^+ + B$. The lower energy pathway $A^+ + BH$ represents a possible activation energy for H transfer. A complex formally exists only if the lifetime between bond breaking and overcoming electrostatic attractions is long enough to allow a chemical reaction other than dissociation to occur. Therefore, time is an important constraint, because otherwise all fragmentations can be considered to take place via complexes.

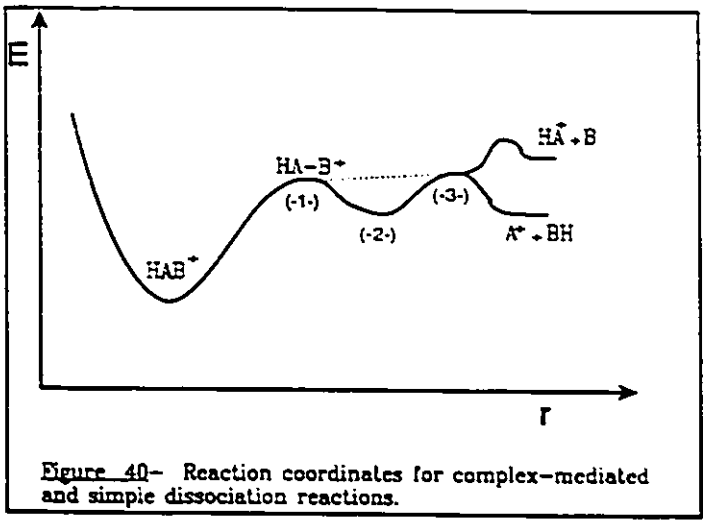

Figure 40- Reaction coordinates for complex-mediated and simple dissociation reactions.

4.5.1 Examples.

A large variety of ionized molecules have been proposed to dissociate via ion-dipole complexes. Amongst these are protonated alcohols, ionized ethers, acids and alkanes. However, no specific rules seem to apply to each class of compound. Therefore, until such rules are formulated, each class of ionized molecule has to be studied separately. As work continues on ion-dipole complexes, it is expected that in the reasonably near future, some strict ground rules may be established. This section contains some examples where the participation of ion-molecule and/or ion-radical complexes was essential to explain the fragmentation behaviour.

4.5.1.1 Protonated Alcohols.

The unimolecular dissociation of protonated iso- and n-propanol and protonated tert- and iso-butanol was studied by Schwarz and Stahl in 1980[86]. It was concluded, from kinetic energy release measurements, that protonated iso- and n-propanol lose water via $(CH_3)_2{}^+CH{-}OH_2$ and $CH_3CH_2{}^+CH_2{-}OH_2$ complexes which can rearrange into each other. However, for loss of water from isobutanol, a kinetic energy release value larger than for tert-butanol is observed. The rearrangement iso-$C_4H_9^+ \rightarrow$ tert-$C_4H_9^+$ requires 32 kcal/mol which is larger than the stabilization energy, therefore, an excess of energy is expected to be observed (Figure 41). It is concluded that the fragmentation of isobutanol ions takes place via a complex between a tert-butyl ion and a water molecule.

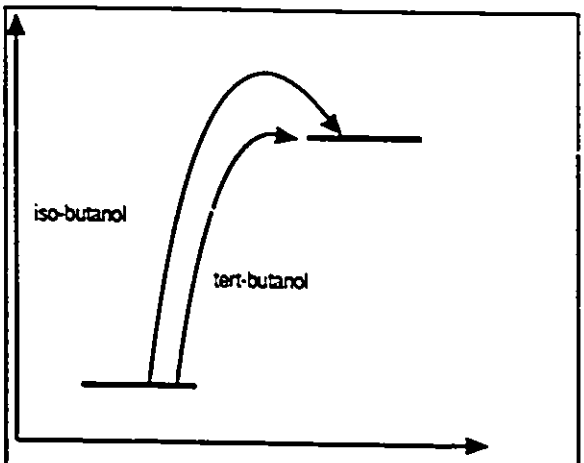

Figure 41- The dissociation of tert-butanol takes place at threshold energy whereas there is excess energy for iso-butanol.

At low energies, ionized isobutyl alcohol itself, $[(CH_3)_2CHCH_2OH]^{+\cdot}$ fragments to produce $CH_3OH_2^+ + C_3H_5^{\cdot}$ rather than the more simple products of direct bond cleavage[87], i.e. $(CH_3)_2CH^{\cdot} + [CH_2OH]^+$. The former pair of products is lower in energy i.e. more stable than the latter. To explain the formation of protonated methanol and $C_3H_5^{\cdot}$, an ion dipole complex between ionized propene and methanol followed by an H transfer was proposed. Figure 42 represents the possible

mechanism where route I (α-cleavage) is more energy demanding than route II (H transfer).

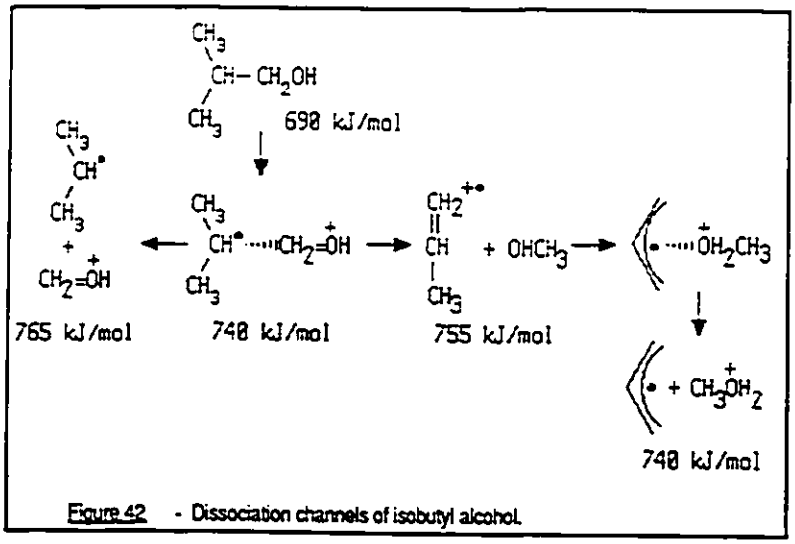

Figure 42 - Dissociation channels of isobutyl alcohol.

4.5.1.2 Ethers.

The decomposition of ionized isopropyl methyl ether was studied by McAdoo and coworkers[88]. They observed two metastable processes: loss of methane and a methyl radical. Both processes, i.e. bond cleavage and bond cleavage directly followed by H transfer, were found to be close in energy and were proposed to be complex mediated, $CH_3O^+=CHCH_3\cdots CH_3$. However, at higher energy, the simple bond cleavage is favored. A fact in favor of the existence of an ion-molecule complex between the methyl radical and the oxonium ion for the ionized methyl ether is the large isotope effect. Therefore, the decomposition may well be complex-mediated, but only over a narrow range of energies above threshold. In accordance with these results[88], Traeger et al concluded that for ethers in general, at the threshold for alkyl loss, there is a rapid shift from alkane elimination to alkyl loss and that alkane eliminations occur

predominantly below the threshold for alkyl loss.

4.5.1.3 Alkanes.

The unimolecular dissociation of alkanes containing 4 or more carbons takes place via the loss of atoms from internal positions of the molecules[86]. This "strange" behaviour has given rise to a lot of interest. Holmes et al[89] studied pentane and methylbutane using ^{13}C and H labelling. They concluded that the H atoms do not lose their positional identities upon fragmentation and that ionized pentane isomerizes to energy rich methylbutane ion before elimination of $CH_3^{\bullet}$, CH_4 and $C_2H_5^{\bullet}$. These fragmentations can be rationalized with the participation of $[CH_3CH_2CH_2^{-}CH_2CH_3]^{+\bullet}$ and $CH_3CH_2CH_2CH_2^{-}CH_3^{+\bullet}$ complexes similarly to the suggested mechanisms for butane and isobutane ions[86].

4.5.2 Are ion-dipole complexes always justified?

This section describes a few cases where the involvement of ion/dipole complexes was first thought to be essential but was later considered to be unnecessary to explain various mechanisms. The low energy isobutylamine and neopentylamine ions were studied by Hammerum and Derrick[90]. The ions produced respectively $CH_2NH_2^+$ by direct bond cleavage and $CH_3NH_3^+$ by double hydrogen migration. They argued that the competition between bond cleavage and rearrangement is not governed by accessibility to ion-molecule complexes but by the kinetics of these reactions. Both ions having the same energies, the only way to explain the

difference in their reactions is by proposing that crossing of the ln k versus E curves for rearrangement and direct bond cleavage occurs at lower energies for isobutylamine than for neopentylamine (Figure 43).

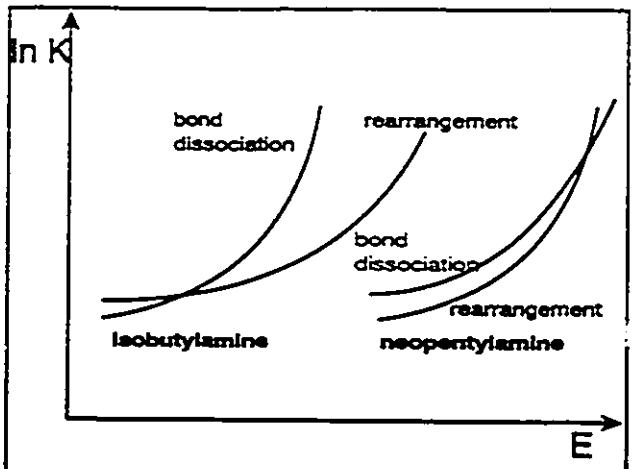

Figure 43- Crossing of the ln k vs E curves for rearrangement and dissociation of neopentylamine and isobutylamine.

A case where ion-neutral complexes are necessary to explain fragmentation is for ionized alkyl phenyl ethers[91]. Their principal fragmentation is the loss of an olefin accompanied by the phenol ion. In light of labelling experiments, kinetic energy release measurements, MI, CA and CIDI mass spectra, some general conclusions were drawn. The fragmentation behaviour of these ethers is governed by two factors, one being the strength of the bond between the phenoxy radical and the ionized alkyl group and the other is the possibility that as the distance between the phenoxy radical and the alkyl ion increases, the alkyl ion may isomerize to give a more weakly bound pair. This was demonstrated for n-propyl and n-butyl ethers for which isomerization to energy rich sec-alkyl ions via a complex, takes place at lower energy than secondary ß-H transfer. The resulting ions then transfer primary and/or secondary ß-H and fragment. For the isobutyl ether, the tertiary ß-H transfer occurs. However, for sec- and tert-amyl ethers, ß-H^+-transfer from the secondary position is dominant and thus, no extensive rearrangement is involved (Figure 44).

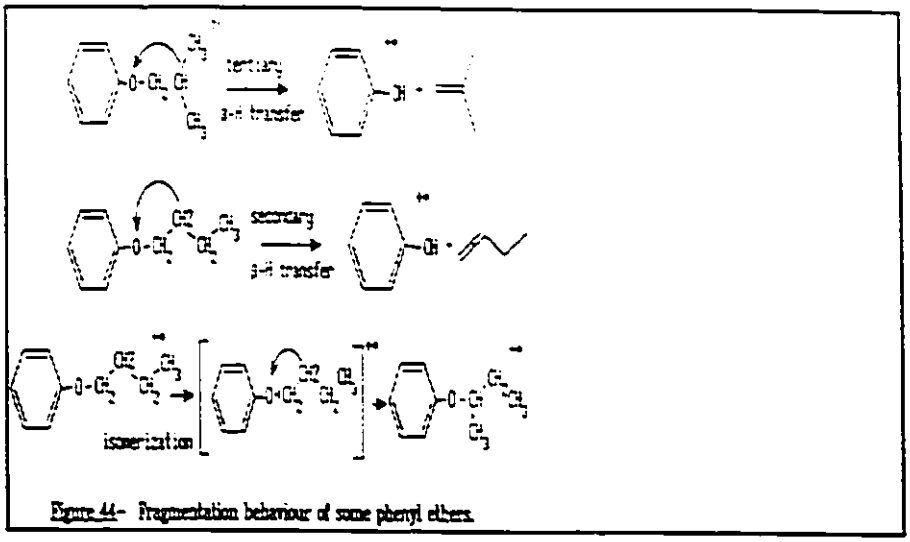

Figure 44- Fragmentation behaviour of some phenyl ethers.

Returning to the case of the ethers studied by Traeger et al[88] in section 4.5.2.1, there seems to be some controversy. Weiske et al studied ionized methyl isopropyl ether[92] and came to a different conclusion. They claim that the fragmentation mechanism can be explained using kinetic arguments rather than ion/molecule complexes. If the ion-neutral complex participated in this mechanism, one may have expected a small kinetic energy release values on the grounds that electrostatically bound complexes do not equilibrate internal energy on dissociation and little of the excess energy appears as translational energy. For the formation of CH_4, a value of 15.5 meV is observed and this implies an appreciable amount of excess energy. It points to a transition structure lying energetically above the products. Thus, there is some disagreement as to when the ion/molecule has to intervene. However, the hypothesis of Weiske et al. for metastable loss of CH_4 from methyl isopropyl ether seems the most plausible to explain the energetics.

In conclusion to this chapter, one can say that it is a very delicate and complicated task to assign ion structures to fragmentation intermediates when unconventional ions are involved. The main reason is the difficulty in performing experiments which unequivocally identify the intermediate species and in the expense of theoretical calculations for larger molecules i.e. with more than 3 carbon atoms. Chapter 5 is an excellent example where the involvement of ion/neutral and ion/radical complexes was unavoidable. The structure assignment are strongly supported by experimental data but, due to the size of the molecule, no theoretical ab-initio calculations were available.

CHAPTER 5

THE FRAGMENTATION OF NEOPENTANOL INVESTIGATED BY EXPERIMENT

5.1 Introduction

Part of the subject treated in this chapter has been published in the literature. The story appeared in two parts: "The Experimental Investigation of $C_5H_{12}O^{+\cdot}$ Ion Structures related to Neopentyl Alcohol and its Methyl Ether", International Journal of Mass Spectrometry and Ion Processes, **101**, 309-324, (1990) and "Ion/radical and Ion/Molecule Complexes: Experimental Demonstration of their Participation in the Fragmentation of Ionized Neopentanol", Organic Mass Spectrometry, **90**, 689, (1990).

As discussed in the previous chapter, unconventional ions are often found to be the solution to explain the fragmentation mechanisms of various ions. Very recently, T.H. Morton published a paper where he described these species as "non-covalently bonded aggregates of an ion with one or more neutral molecules in which at least one of the partners rotates freely (or nearly so) in all directions"[93]. The existence of these ion-neutral complexes has been clearly established for various compounds such as alkanes, ketones, alcohols, ethers, etc... In 1988, a pair of communications by Hammerum[84] and Hammerum and Audier[94] introduced some generalizations concerning ion/molecule and ion/radical complexes. The fragmentation

behaviours of 3-methylbutan-2-ol and 2,2-dimethyl propanol (neopentyl alcohol or neopentanol) were briefly described. The former is characterized by loss of a propane molecule to form $CH_2CHOH^{+\cdot}$ and the latter by loss of methanol to form the methyl propene ion. Both ions were proposed to dissociate via complexes between the fragments (Fig 45).

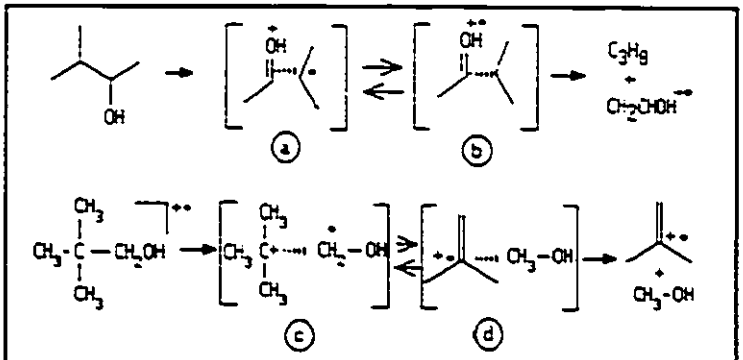

Figure 45- Fragmentation behaviour of methylbutan-2-ol and 2,2-dimethyl propanol.

It was proposed that ionized 3-methylbutan-2-ol undergoes a simple bond cleavage to form complex *a* which, by a H transfer, is in equilibrium with complex *b*. For neopentanol, a similar situation arises, the bond cleavage in the molecular ion produces a complex between a hydroxymethyl radical and the tert-butyl ion *c* which is in equilibrium with complex *d*, methyl propene ion/methanol. The authors also suggested that neopentyl methyl ether behaves in a similar manner. Finally, they made the prediction that ionized methyl-t-butyl ether should display a similar hydrogen exchange and fragmentation mechanism as for neopentanol, i.e. by transferring an H of the methoxy group onto the oxygen in the t-butyl methyl ether, an ion with an inverted C-O bonding, in comparison to neopentanol. The possible structures are illustrated in Figure 46.

With molecular ions of this size, it is quite difficult to perform high level ab initio molecular orbital theory calculations. The work described in this chapter was undertaken to

probe more deeply in the behaviour of ionized neopentyl alcohol, its isomers and possible analogues. The next section describes all the ions which were studied and the analysis of the various results.

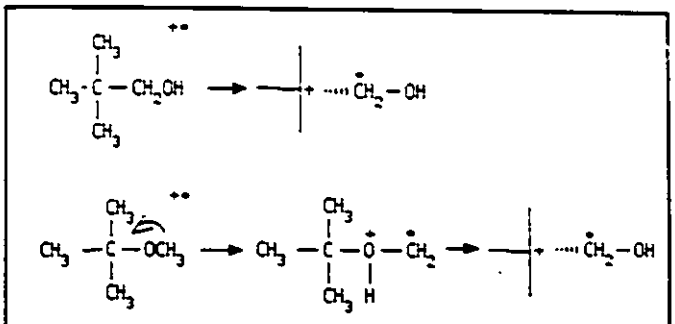

Figure 46- Possible intermediates for neopentanol and t-butyl methyl ether.

5.2 Results and Discussion.

The results obtained for neopentanol will be described first, followed by the description of each isomer/analogue. In section 5.3, comparisons between the ions involved in the fragmentation mechanism of neopentanol will be made and a general reaction scheme supported by energetics will be proposed. All experimental conditions and synthetic methods are described in section 5.5.

5.2.1 Neopentyl Alcohol.

The electron impact (EI) mass spectrum of neopentanol is dominated by a base peak at m/z 57 corresponding to $C_4H_9^+$. There is a very weak molecular ion of ≈2% of the base peak. The combination of $\Delta H_f[(CH_3)_3CCH_2OH]$=-318 kJ/mol (from Benson's additivity scheme[19], Figure

47) and the measured ionization energy of 9.72 ± 0.05 eV gives ΔH_f(molecular ion)=620 kJ/mol. This value is 48 kJ/mol below the energy of the products of the simple bond cleavage ($\Delta H_f[(CH_3)_3C^+]$=694 kJ/mol and $\Delta H_f[^{\cdot}CH_2OH]$=-26 kJ/mol). All the energies given are from reference 9, unless otherwise stated.

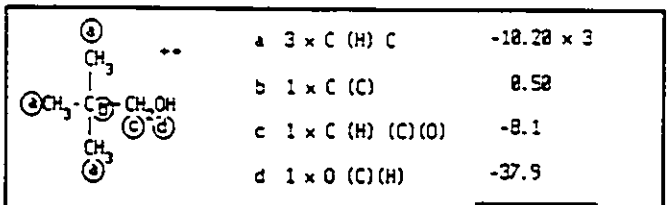

Figure 47– Calculation of the heat of formation of neopentanol using Benson's additivity scheme.

The metastable ion (MI) mass spectrum contains only two peaks: loss of CH_3OH which produces m/z 56 (abundance 100%) and apparently, the loss of water to give m/z 70 (abundance 5%). However, it was found that m/z 70 wholly arises from the ^{13}C contribution of the very intense m/z 87→m/z 69 process, $^{13}CC_4H_{11}O^+ \rightarrow {}^{13}CC_4H_9^+ + H_2O$. Therefore, the only metastable process is loss of methanol. The kinetic energy release derived from the half height width of this peak ($T_{0.5}$) was measured as 1.4 ± 0.1 meV, in agreement with the results stated in reference 100.

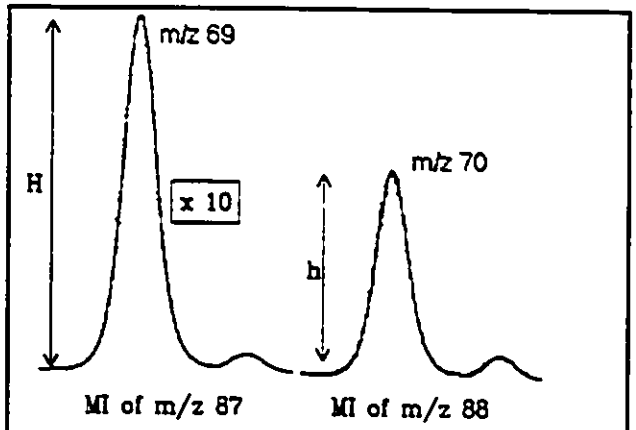

Figure 48– The natural isotopic abundance contribution to m/z 70 is calculated by multiplying the height of m/z 69 by 5.5% (5 carbons in the original molecule). In the present case, h=5.5% x H.

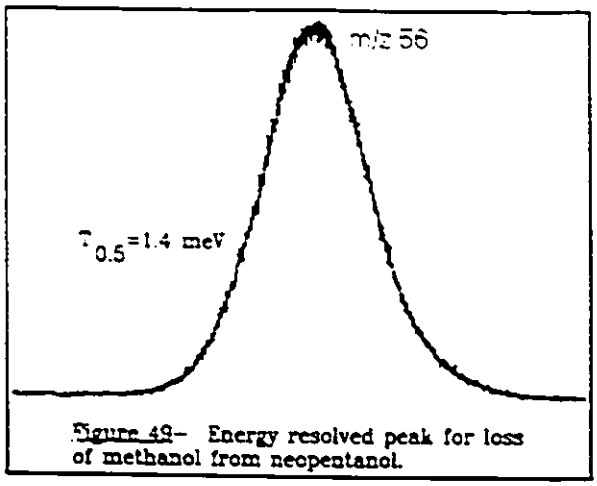

Figure 49- Energy resolved peak for loss of methanol from neopentanol.

The appearance energy (AE) of this peak was also measured by the method described in Chapter 3 (10.2 ± 0.1 eV) and was found to correlate very well with the value calculated (see below) from the products and reactants: 10.26 eV.

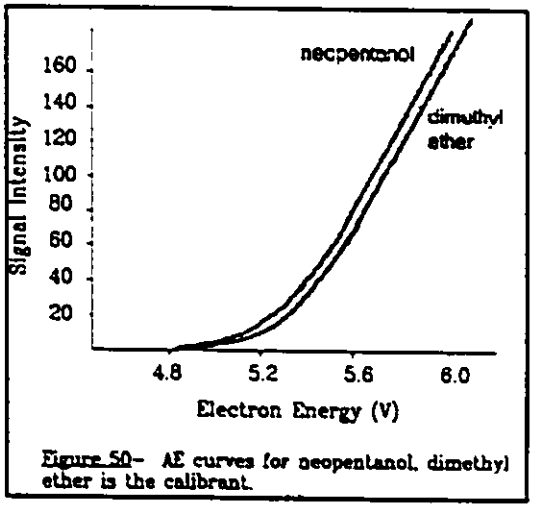

Figure 50- AE curves for neopentanol, dimethyl ether is the calibrant.

$$AE = \Delta H_f(prod) - \Delta H_f(react) \quad [30]$$

$$AE = \Delta H_f[(CH_3)_2CCH_2^{+\cdot}] + \Delta H_f[CH_3OH] - \Delta H_f[(CH_3)_3CCH_2OH^{+\cdot}] \quad [31]$$

$$AE = 874 \text{ kJ/mol} + (-202 \text{ kJ/mol}) + 620 \text{ kJ/mol} \equiv 10.26 \text{ eV} \quad [32]$$

It may be concluded that both losses of $^{\cdot}CH_2OH$ and CH_3OH take place at very similar energies ($\Delta H_f[C_4H_9^+]$=694 kJ/mol, $\Delta H_f[^{\cdot}CH_2OH]$=-26 kJ/mol and $\Delta H_f[C_4H_8^{+\cdot}]$=874 kJ/mol,

$\Delta H_f[CH_3OH]$=-202 kJ/mol, the sum of the product energies being 668 and 672 kJ/mol, respectively, see Figure 51) with only the latter process being metastable.

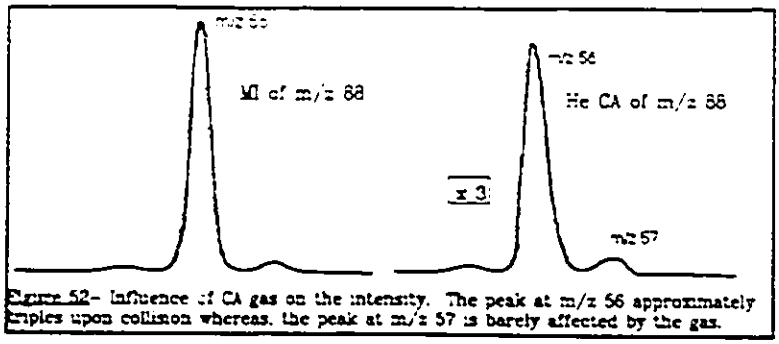

Figure 52- Influence of CA gas on the intensity. The peak at m/z 56 approximately triples upon collision whereas, the peak at m/z 57 is barely affected by the gas.

Therefore, the molecular ions must rearrange into another structure which does not favor C-C bond cleavage. This is supported by the Helium Collisional Activation (CA) mass spectrum of the molecular ion which displays only a small peak at m/z 57 (4%) and a very intense peak at m/z 56 which increased sharply upon introduction of collision gas (Figure 52). From these results, one may conclude that very few ions have retained the original neopentyl structure otherwise, the features of the EI mass spectrum would have been reproduced, i.e. showing an intense peak at m/z 57. This result is therefore not in favor of a complex between t-butyl ion and hydroxymethyl radical being a major fragmentation intermediate, although it does not rule out its involvement.

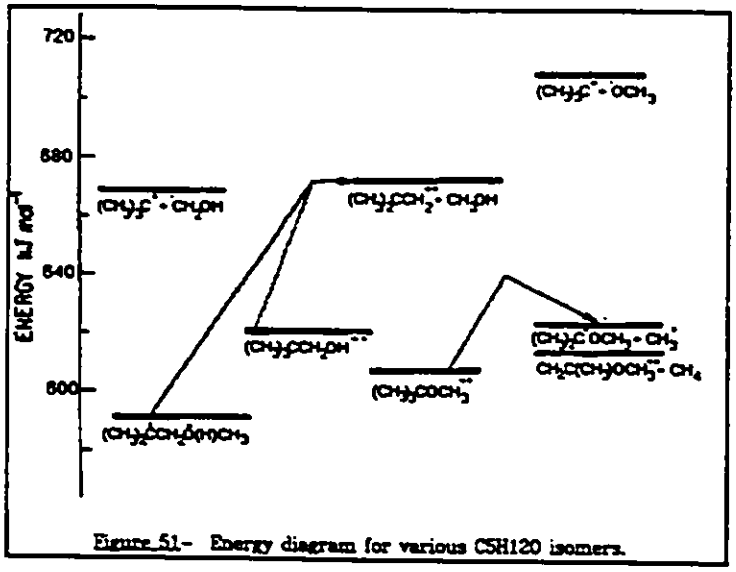

Figure 51- Energy diagram for various C5H12O isomers.

Several labelled molecules were studied. The $(CH_3)_3C^{13}CH_2OH$ molecular ion, m/z 89, produced only m/z 56 ions showing that there is no skeletal rearrangement before fragmentation. Table II shows the results of the MI spectra of the labelled OD, α-CD_2, α-CD_2OD, CH_2D and (CH_2D + α-CD_2) compounds. The kinetic energy releases (relative peak heights) for losses of labelled methanol, $T_{0.5}$, were all close to 1.4 meV with sharp Gaussian peak shapes. Note that the ratios for compounds containing the same number of label atoms are the same no matter where the label is located. However, by comparing these with the statistical ratio, there is a preference for label retention in the methanol fragment.

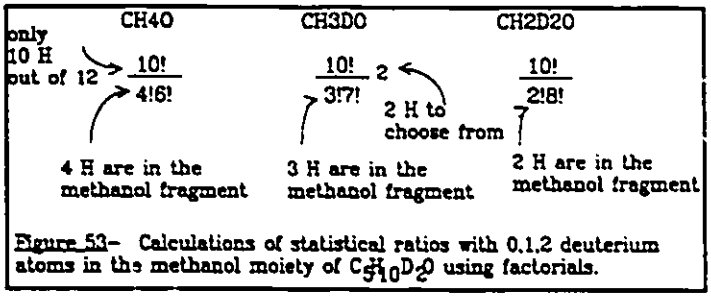

Figure 53- Calculations of statistical ratios with 0,1,2 deuterium atoms in the methanol moiety of $C_5H_{10}D_2O$ using factorials.

Table II H/D distribution (%) among $[C_4H_8]^{+\cdot}$ ions produced from metastable D-labelled neopentyl alcohol ions. Numbers in parentheses are the random statistical ratios.

ION	LABEL POSITION	C_4H_8	C_4H_7D	$C_4H_6D_2$	$C_4H_5D_3$
$(CH_3)_3CCH_2OH^{+\cdot}$	-OD	56(*33*)	44(*67*)		
	$-CD_2OH$	28(*9*)	56(*48*)	16(*43*)	
	$-CH_2D$	55	45		
	$-CD_2OD$	12(*2*)	43(*22*)	37(*51*)	8(*25*)
$(CH_3)_2C(CH_2D)CD_2OH^{+\cdot}$		16	42	34	8

It should be noted that all the EI mass spectra of the D-labelled ions show specific

retention and loss i.e. no mixing between methyl hydrogens and CH_2OH. For example, the m/z 73 and 74 are cleanly shifted to m/z 75 and 76 in $(CH_3)_3CCD_2OH$. Since it was found that the label atoms were largely retained in the methanol neutral fragment from the metastable molecular ions, collision induced dissociative ionization (CIDI) experiments were performed to analyze the various neutrals. Both OH and OD molecular ions were studied; the observations are shown in Figure 54. These measurements were essential to allow determination of the D atom(s) position in the neutral.

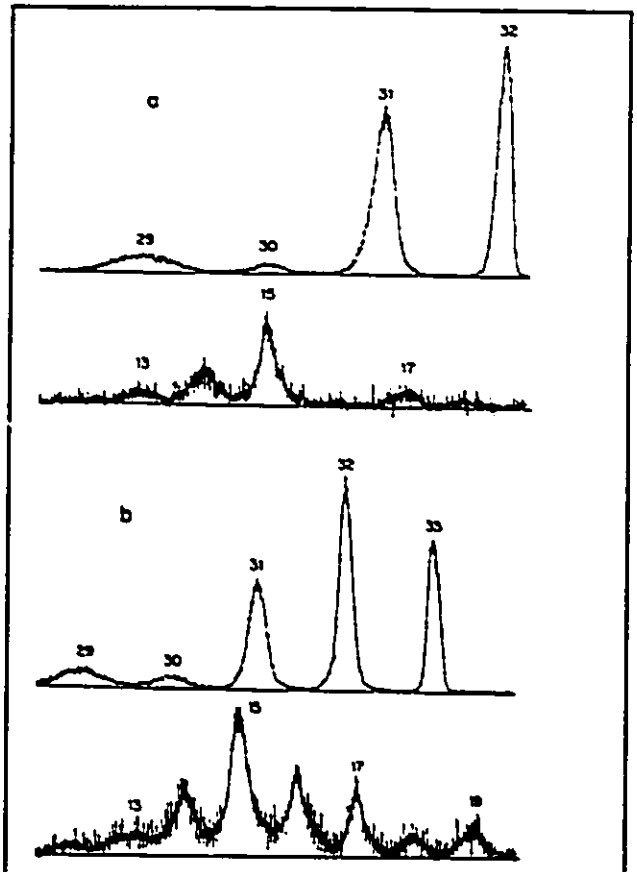

Figure 54– CIDI mass spectra for CH4O (a) and CH3DO (b) produced from neopentanol and neopentanol–OD respectively.

To obtain the location of the label in the methanol molecule one has to suppose that if the label stays only on the oxygen, the ratio of 74:100 for the m/z 31/32 ions from unlabelled neopentanol should become the same for m/z 32/33 in the OD analogue. This is not the case because there is a peak at m/z 31. This means that there is also loss of CH_2DOH from the OD compound. The predicted ratios for 31/32/33 if only CH_2DOH was produced are 24.7:49.3:100 (from 31/32=74:100, if there is one chance out of three to lose D from the methyls, 1/3 x 74= 24.7) but 48:100:76 is obtained. This indicates a mixture of CH_2DOH and CH_3OD in the CIDI

spectrum of the OD compound. Using the ratio of m/z 56/57 (1:1.25) in the MI mass spectrum, it is possible to set equations to find out where the label is located and in what amount. These equations are valid if there are no isotope effects nor collision cross-section effects involved for the various labelled compounds (Figure 55).

From these numbers, it can be concluded that both CH_2DOH and CH_3OD are formed, in a 2:3 ratio. Randomization of label would lead to a 3:1 ratio. We can assume that there is a preference for label retention at the oxygen position. The CIDI of the OD compound also confirms the presence of CH_2DOH by showing an intense peak at m/z 16, characteristic of CH_2D. For the α-CD_2 compound, a similar method is used supposing the following ratios: for CH_3OH m/z 31/32 is 76:100, for CH_3OD m/z 32/33 is 76:100, for CH_2DOH m/z 31/32/33 is 25.3: 50.6: 100, for CH_2DOD m/z 32/33/34 is 25: 50: 100 and for CHD_2OH m/z 32/33/34 is 50: 25: 100. The experimental observed ratio for m/z 31/32/33/34 is 30: 78: 100: 48 and the ratio for m/z 56/57/58 is 28: 56: 16. The observed ratio for $CH_3OH/CH_3OD/CH_2DOH/CH_2DOD/CHD_2OH$ is 1.5: 2: 4: 2: 1. The random calculated value for CH_3OD/CH_2DOH is 1:3 versus 1:2 and the calculated value for CH_2DOD/CHD_2OH is 1:1 versus 2:1. Again, these numbers show a marked preference for retention of the label at the

posing x + y = 1.25 where x=CH3OD y= CH2DOH

CH3OH	31/32	74:100
CH3OD	32/33	74.100
CH2DOH	31/32/33	24.7:43.3:100

-the results obtained are 31/32/33 ⟶ 48:100:76

For peak 31 0.48 = 74 + y(24.7)

For peak 32 1.00 = 100 + x(74) + y(49.3)

For peak 33 0.76 + x(100) + y(100)

SOLVE FOR x AND y

x = 0.75
y = 0.50

Figure 55- Calculation of the ratio of CH_3OD and CH2DOH from fragmentation of monolabelled neopentanol.

oxygen site.

The Xe/O_2 neutralization-reionization mass spectrum (NRMS) of neopentyl alcohol was also measured to investigate the stability of the product from the neutralized ions. It showed an intense peak at m/z 56 (100%) and weaker peaks at m/z 57 (15%), m/z 41 (60%) and m/z 39 (65%). There was no recovery signal for the molecular ion. This indicates that the neutral $C_5H_{12}O$ generated by electron transfer is not a stable species. If it were stable, we would expect the same major peaks as in the EI mass spectrum: the base peak at m/z 57, m/z 73 (25%), m/z 56 (50%), m/z 41 (38%) and m/z 39 (9%). The peak at m/z 56 is characteristic of a large amount of methyl propene ion whereas the weaker m/z 57 indicates a smaller amount of $C_4H_9^+$.

5.2.2 Methyl-t-butyl ether.

This species was proposed to fragment via the same intermediates as neopentyl alcohol[94]. This section clearly shows that methyl-t-butyl ether does not have any dissociation channel in common with neopentanol.

The mass spectrum of the ether is dominated by a base peak at m/z 73 (loss $CH_3^{\bullet}$). The molecular ion (m/z 88) is very weak, 0.4% and the intensities for m/z 56 and m/z 57 are respectively 5% and 23% (quite different from neopentanol). The MI mass spectrum of $(CH_3)_3COCH_3$ contains four peaks m/z 73 (31%), m/z 72 (100%), m/z 56 and m/z 55. The latter pair (4:1 ratio) arises from the very intense m/z 87 → m/z 55 process. The ^{13}C natural abundance

from m/z 87 forms $^{13}CC_4H_{11}O^+$ which loses $^{13}CH_4O$ and CH_4O in a 1:4 statistical ratio. Thus the only metastable processes for the molecular ion are loss of methane (m/z 72), $T_{0.5}$=17 meV, and methyl radical (m/z 73), $T_{0.5}$=7 meV. A labelling experiment, using $(CH_3)_3COCD_3$, showed that there is no label mixing since the MI processes at m/z 72 and 73 are cleanly shifted to m/z 75 and 76. This behaviour is also different from metastable neopentanol ions which mix extensively and therefore, negates the initial hypothesis that ionized $(CH_3)_3COCH_3$ and neopentanol may fragment via a common intermediate.

A few comments on the above metastable processes deserve mention. Their calculated AE values 9.30 eV (CH_4 loss) and 9.40 eV ($CH_3^\cdot$ loss) (from $\Delta H_f[(CH_3)_3COCH_3]$=-284 kJ/mol, $\Delta H_f[(CH_3)_2COCH_3$=477 kJ/mol, $\Delta H_f[CH_2=C(CH_3)OCH_3]$=688 kJ/mol, $\Delta H_f[CH_3^\cdot]$=146 kJ/mol and $\Delta H_f[CH_4]$=-75 kJ/mol) are close to the measured value of 9.52 ± 0.05 eV for both reactions and lie so close to the ionization energy (IE[$(CH_3)_2COCH_3^{+\cdot}$]=9.24 eV) as to exclude the possibility of these reactions being metastable. However, it is possible to have a $C_5H_{12}O^{+\cdot}$ structure lying in a deep potential well, easily accessible to the molecular ion which would give rise to the products without requiring isomerization.

Recently, Parker[95] described ab initio molecular orbital theory calculations on the t-butanol molecular ion. The principle is that the vertical ionization of the ground state produces an ion in which the charge is formally at the O-atom, following the removal of a lone-pair electron. However, the optimum geometries of the ground states of the ion and of the neutral are significantly different, the geometry of the ion being best described as a complex between

a methyl radical and protonated acetone, which may fragment rapidly by loss of $CH_3^{\cdot}$. The situation is proposed to be similar here, the ionized ether having a ground state consisting of a methyl radical-$(CH_3)_2{}^{+}COCH_3$ species whose geometry is significantly different from that of the neutral molecule. Vertical ionization of the latter leads to an energy rich ground state ion (Figure 56).

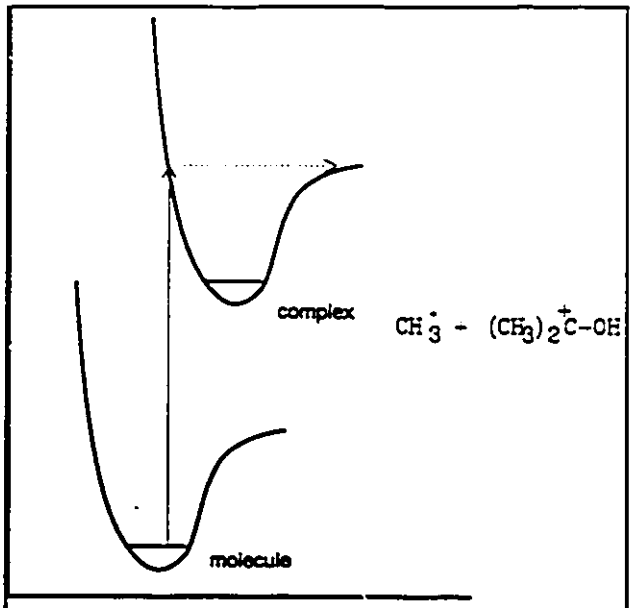

Figure 56- Dissociation of the t-butanol molecule.

The CA mass spectrum of $(CH_3)_3COCH_3^{+\cdot}$ was studied and it showed an increase in intensity for m/z 73 upon introduction of a collision gas whereas m/z 72 was unaffected. This feature reproduces quite well the EI spectrum of the ether and it can then be concluded that, unlike neopentanol, the $(CH_3)_3COCH_3^{+\cdot}$ ions have undergone no major rearrangement.

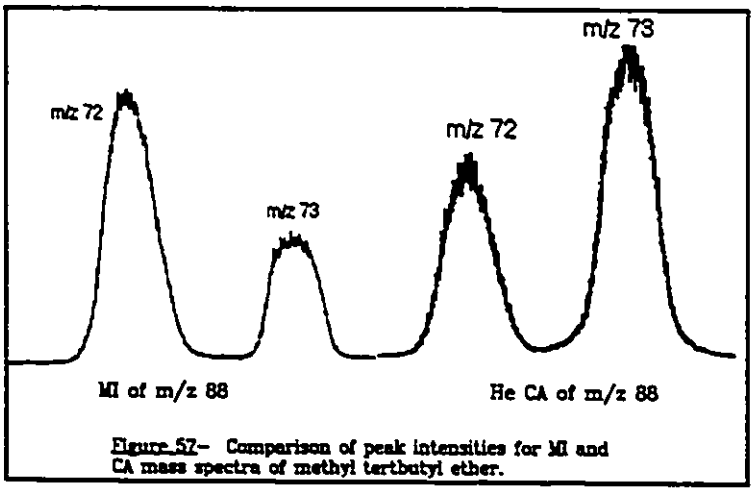

Figure 57- Comparison of peak intensities for MI and CA mass spectra of methyl tertbutyl ether.

The next six sections (5.2.3 to 5.3.8) briefly describe the behaviour of isomers which, according to their structure and their energetics (Figure 51), might behave like neopentanol to produce m/z 56 ($T_{0.5}$=1.4 meV) in their MI mass spectrum, but which showed no such fragmentation.

5.2.3 Methyl-n-butyl ether.

The EI mass spectrum of this ion displays a base peak at m/z 45 (loss of $C_3H_7^{\cdot}$), a peak at m/z 56 (21%) and a weak molecular ion, 4% relative intensity. Its MI mass spectrum shows a very intense signal at m/z 59 (100%), loss of $C_2H_5^{\cdot}$ with $T_{0.5}$=11.4 meV and a weaker signal at m/z 73 (9%), loss of $CH_3^{\cdot}$, with $T_{0.5}$=11.0 meV. These processes are almost unaffected by introduction of Helium in the collision cell, but peaks at m/z 56 and m/z 45 developed in the CA mass spectrum, thus reproducing the properties of the EI spectrum. This compound clearly does not behave in a manner similar to neopentyl alcohol.

5.2.4 2-Methoxybutane

The base peak in the EI mass spectrum of this ion is m/z 59 (loss of $C_2H_5^{\cdot}$) with a weaker m/z 73 (13.5%), loss of $CH_3^{\cdot}$, and a molecular ion, m/z 88, of 6% relative intensity. The MI mass spectrum shows a very intense process at m/z 58 (loss C_2H_6) a weak peak at m/z 56 and a weaker peak at m/z 55. However, the latter two signals wholly arise from loss of CH_4O and $^{13}CH_4O$ from the $^{13}CC_4H_{11}O$ isotope of m/z 87. The metastable loss of C_2H_6 takes place with a

kinetic energy release, $T_{0.5}$=8.9 meV. The He CA mass spectrum shows a weak increase in intensity for m/z 58 (≈25%) whereas an intense m/z 59 and a weaker m/z 73, respectively 53% and 7% relative intensity to the base peak, appear. Thus, the features of the EI mass spectrum are again reproduced and indicate that no major rearrangement has taken place. Again this compound shows no behaviour in common with neopentyl alcohol.

5.2.5 3-Methylbutan-2-ol

The base peak in the EI mass spectrum of this ion is m/z 45 (loss of $C_3H_7^{\bullet}$), a weaker m/z 55 (13%), loss of [$CH_3^{\bullet}$, H_2O], and m/z 73 (10%), loss of $CH_3^{\bullet}$. There is also a weak molecular ion of ca 2% intensity. The MI spectrum contains two intense peaks m/z 72(100%), loss CH_4, and m/z 44 (37%), loss C_3H_8. Of these two processes, only the CH_2CHOH ion (m/z 44) is considerably affected by collision-induced dissociation. The CA mass spectrum also shows a large peak at m/z 45 which reproduces the EI spectrum and suggests that a stable $C_2H_5O^+$ fragment ion is produced. This ion, as mentioned before, was studied by Hammerum and Audier[94] and only the MI process giving rise to m/z 45 was described. The proposed mechanism via ion-dipole complexes is shown in figure 45. George and Holmes[96] have studied this ion in depth and performed labelling studies using deuterium and ^{13}C and, on the basis of these results, proposed that the low energy $(CH_3)_2CHCH(OH)CH_3^{+\bullet}$ ions can form a proton-bridged molecule-radical complex $HOCHCH_2^{-}H^{+\bullet}{}^{\bullet}CH(CH_3)_2$. This intermediate can explain the label exchange occurring upon propane loss and may also be the key to explaining why the loss of CH_4 becomes a less important process upon introduction of a collision gas. The kinetic energy release values

($T_{0.5}$) are 25.6 meV for methane loss and 1.4 meV for propane loss. This is in agreement with the statement made in reference 100, that the metastable peaks for loss of alkanes from ether and alcohol are narrow when they involve a thermoneutral hydrogen transfer whereas when the alkanes arise by an exothermic hydrogen transfer (as for CH_4), they release 10-25 meV.

5.2.6 Methyl isobutyl ether.

The base peak in the EI mass spectrum of this ion is at m/z 45. There is a clearly visible molecular ion (13%) and much weaker peaks at m/z 73 (1%), loss $CH_3^{\bullet}$, and m/z 56 (4%), loss of CH_3OH. The MI mass spectrum displays three metastable processes: loss of $CH_3^{\bullet}$, m/z 73 (7%), loss of $C_2H_5^{\bullet}$, m/z 59 (100%) and loss of CH_3OH, m/z 56 (46%), after correcting for ^{13}C contribution to m/z 56. The O_2 CIDI spectrum confirms that both $C_2H_5^{\bullet}$ and CH_3OH were the neutrals produced by showing respectively, clusters of peaks at m/z 26/27/28/29 in a 9: 21: 28: 100 ratio[97] and a pair of peaks at m/z 31/32 with a 85:100 ratio. Since the formation of $C_4H_8^{+\bullet}$ was metastable, it was of interest to obtain the characteristics of that process. The kinetic energy release values ($T_{0.5}$) for m/z 59 and m/z 56 were, respectively 10.2 meV and 7.2 meV. Although it is a very small value, it is still five times larger than for the m/z 88 → m/z 56 process of neopentanol (which has $T_{0.5}$=1.4 meV). The CA mass spectrum shows that m/z 72, 59 and 56 are unaffected by the collision gas whereas m/z 45 increases. On the basis of all these results, one can conclude that methyl isobutyl ether does not rearrange extensively before fragmentation (CA reproduces EI features) and since the $T_{0.5}$ is 5 times larger than neopentanol, it very probably does not share any common intermediate with the latter.

5.2.7 Halogen substituted 2,2-Dimethyl-propan-1-ol

A series of three halides was studied in attempt to obtain the distonic ion A (illustrated in Figure 58) by protonation of the molecule (using water) followed by loss of the halogen atom. It was not possible to protonate the chloro and bromo substituted ions but, the protonated iodo ion was obtained. However, it showed a preference for loss of HI rather than the loss of the halogen only and produced an ion of m/z 87. Not being able to produce ion A of Figure 58 does not prove that it does not exist and therefore, its participation in the fragmentation mechanism of neopentanol cannot be ruled out. Furthermore, its estimated ΔH_f° value of 620 kJ/mol is much lower than the dissociation energy to produce CH_3OH and $C_4H_8^{\cdot+}$ (672 kJ/mol) and its distonic structure provides a simple rationale for the positional mixing of H and D. The possible participation of this ion will be discussed in greater detail in section 5.3.

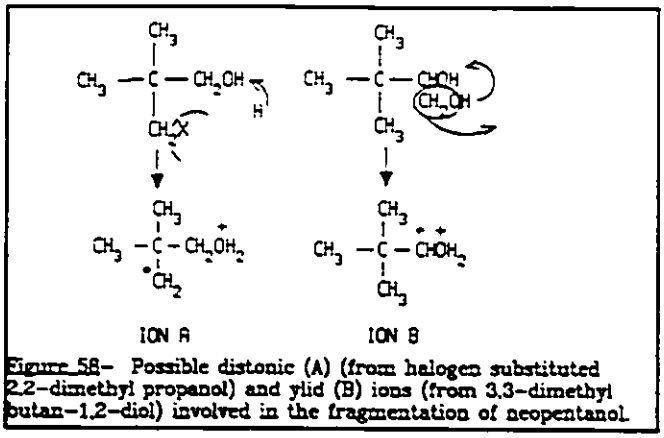

Figure 58- Possible distonic (A) (from halogen substituted 2,2-dimethyl propanol) and ylid (B) ions (from 3,3-dimethyl butan-1,2-diol) involved in the fragmentation of neopentanol.

5.2.8 3,3-Dimethyl butan-1,2-diol

This molecule was studied hoping that a hydrogen transfer followed by loss of a formaldehyde molecule would occur to produce the wanted m/z 88 distonic ion (Figure 58, structure B), with ΔH_f=605 kJ/mol. Unfortunately, the ion prefers to lose a CH_2OH fragment.

Again the involvement of ion B in Figure 58 in the dissociation of neopentanol may be considered as the solution to allow for H/D exchange between the α-CH_2 and OH groups (only if the structure A of Figure 58 is involved to allow for exchange between the OH and the CH_3 groups).

5.2.9 3-Methoxy-2,2-dimethyl propanol

This ether shows a fairly intense peak at m/z 88 (8%) in it EI mass spectrum. It arises from the loss of CH_2O from the molecular ion m/z 118 (Figure 59) possibly to form the distonic ion (ion C).

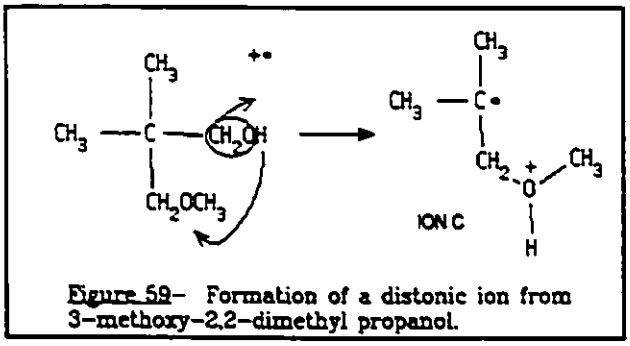

Figure 59– Formation of a distonic ion from 3-methoxy-2,2-dimethyl propanol.

The base peak in its normal mass spectrum is m/z 56, loss of $C_4H_8^{+\bullet}$, and a weak fragment at m/z 100 (4%), loss of H_2O, is also observed. The only metastable processes of the weak molecular ion, m/z 118 (<1%), are loss of CH_2O, H_2O and CH_3OH. The MI mass spectrum of m/z 88 shows several signals at m/z 45, 46, 55, 56, 69 and 70. However there is a very intense peak in the normal mass spectrum at m/z 87 which in turn in its MI mass spectrum fragments to produce m/z 45 and m/z 55. The natural isotope abundance of m/z 87 is $^{13}CC_4H_{11}O^+$ (m/z 88)

and wholly accounts for the presence of m/z 45 and m/z 46 in a 3:2 ratio by producing both $^{13}CC_2H_6$ and C_3H_6. In a similar manner, the $^{13}CC_4H_{11}O^+$ ion also accounts for m/z 70 and m/z 55 in the MI mass spectrum of $C_5H_{12}O^{+\cdot}$. However, this ^{13}C ion does not account completely for the presence of the peak at m/z 56. Only 60% of m/z 56 comes from the natural isotopic abundance of the peak at m/z 87, $C_5H_{11}O^+$. Upon high energy resolution, the peak at m/z 56 shows two components: a very narrow one, and a broader one which has the same shape as that for m/z 55 generated from metastable m/z 87 ions. The $T_{0.5}$ value of the narrow peak is 1.4 meV, and it is identical in shape to the metastable peak for neopentyl alcohol. The collision induced characteristics of m/z 88 (ion C) are very similar to neopentanol, the peak at m/z 56 increasing sharply upon introduction of gas into the cell, whereas m/z 57 is almost unaffected (0.8%). The CA mass spectrum of ion C thus shows similar behaviour to that from ionized neopentanol and so provides more evidence that the two ions are interrelated.

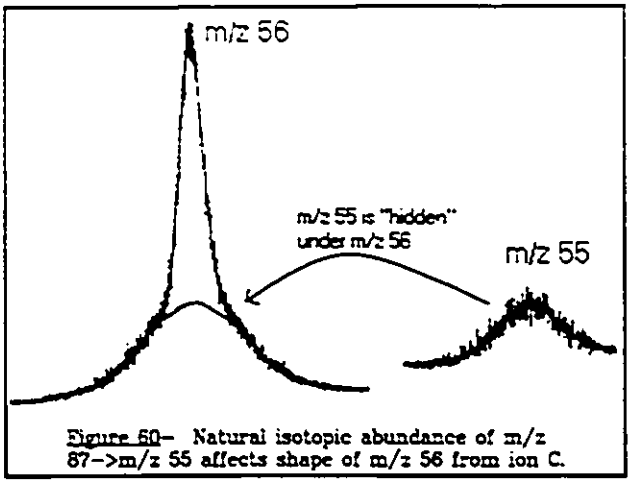

Figure 60– Natural isotopic abundance of m/z 87->m/z 55 affects shape of m/z 56 from ion C.

More information which can be obtained from the CA mass spectrum of ion C is that the features of the EI mass spectrum are reproduced, unlike the behaviour of neopentanol. This suggests that the distonic ion, $(CH_3)_2{}^{\cdot}CCH_2{}^{+}O(H)CH_3$ does not rearrange to ionized neopentanol before fragmenting, but that neopentyl alcohol ions rearrange to the distonic ion instead. The O_2 CIDI mass spectrum was also recorded and the presence of CH_3OH was confirmed by observing

peaks at m/z 31 and m/z 32 having the correct ratio of 76:100. The Xe/O_2 NRMS of the distonic ion revealed two peaks, one at m/z 56 and another at m/z 39, but no peak m/z 57. There were also peaks at m/z 43 (45%), m/z 42 (30%) and m/z 41 (75%). The peak at m/z 56, which is also a characteristic of the EI mass spectrum, indicates that the neutral has not undergone major rearrangement whereas the absence of m/z 57 clearly indicates that the ion does not rearrange into a structure containing the $C_4H_9^+$ group. Therefore, these characteristics indicate that the distonic ion is a lower energy species than neopentanol. The appearance energy of ion C was measured, AE=9.66 ± 0.05 eV and, using ΔH_f[3-methoxy-2,2-dimethyl propanol]=-449 kJ/mol and $\Delta H_f[CH_2O]$=-109 kJ/mol, the ΔH_f calculated for $(CH_3)_2{}^{\cdot}CCH_2{}^{\cdot}O(H)CH_3$ is 592 kJ/mol. This is in keeping with the prediction made (see Figure 51).

The approximate estimation of ΔH_f can be made using the method described by Holmes and Lossing in reference 38. The thermochemical cycle is shown in figure 61. Two routes can be used to estimate the ΔH_f value of the distonic ion, one via the homolytic bond strength in the molecule and the proton affinity of the radical and the other route involves protonation of the ether followed by homolysis of the resulting ion.

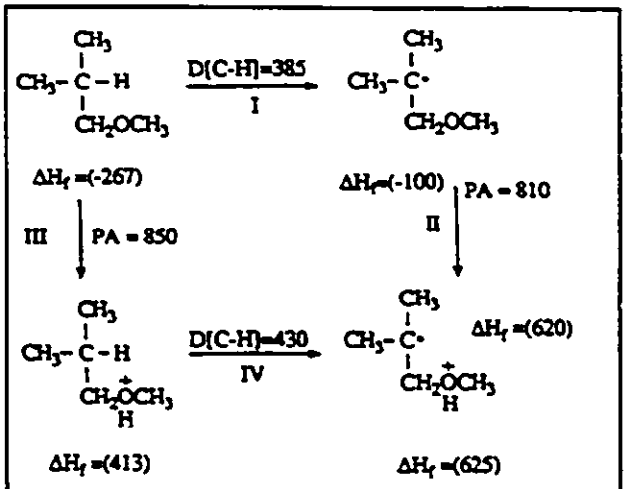

Figure 61.- Calculation of heats of formation (in kJ/mol) using a thermochemical cycle.

Routes I and III can be estimated with confidence whereas routes II and IV are a more difficult task[37]. The bond strength for step I can be reasonably placed at 8 kJ below the corresponding value in methyl propene (393 kJ/mol) and the PA of step III is estimated at 850 kJ/mol, which is typical for ethers[1]. PA values are reduced by adjacent or nearby radical sites in carbonyl and OH containing radicals[37] but no values are available for radicals containing an ether linkage. Typically, the bond strengths in protonated molecules are greater than those in analogous neutral molecules[37]. These effects make the ΔH_f values higher by ca 30 kJ/mol than if the unmodified (values for molecules, rather than for radicals) proton affinities and bond strengths had been used. Thus, the estimated ΔH_f values are higher than the experimental results. A good estimate for $(CH_3)_2\dot{C}CH_2\dot{O}(H)CH_3$ is 590 kJ/mol.

Table III shows the results obtained for deuterium labelled 3-methoxy-2,2-dimethylpropanol. The fragmentation of $(CH_3)_2C(CH_2OD)CH_2OCH_3$ produced an ion at m/z 89 (no loss of D with CH_2O) which dissociates metastably in the same manner as neopentanol OD. The 3-trideuteromethoxy-2,2-dimethyl propanol was investigated and it produced a peak at m/z 91 in the EI mass spectrum. The peak at m/z 57 was not displaced to m/z 60 indicating no label mixing before forming the distonic ion. The kinetic energy release, $T_{0.5}$=1.4 meV for m/z 88 → m/z 56 was indistinguishable from the energy resolved peak for neopentanol ions. The d_3 compound showed

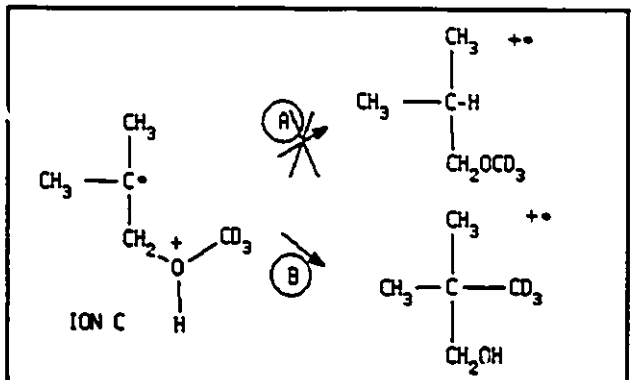

Figure 62– Proposed intermediates for dissociation of d_3-labelled ion C.

considerable mixing taking place with greater retention of label in methanol than predicted. This is in keeping with results obtained for labelled neopentyl alcohol. Two intermediates may be proposed for fragmentation of the d_3 ion (Figure 62).

Table III H/D distribution (%) among $C_4H_8^{+\cdot}$ ions produced from D-labelled $C_5H_{12}O^{+\cdot}$ from 3-methoxy-2,2-dimethyl propanol.

ION	LABEL	C_4H_8	C_4H_7D	$C_4H_6D_2$	$C_4H_5D_3$
$(CH_3)_2{}^{\cdot}CCH_2{}^{+}O(H)CH_3$	-OD	58	42		
	$-OCD_3$	14	43	37	6

Channel A is, however, not possible according to the results obtained for the methyl isobutyl ether (section 5.2.6). Moreover, on the basis of the previous results for $(CH_3)_2{}^{\cdot}CCH_2{}^{+}O(H)CH_3$ and its labelled analogues, the interconversion to neopentanol via a methyl transfer to the radical site is not a favoured pathway.

To confirm this hypothesis, ^{13}C-methoxy-2,2-dimethyl propanol was studied. It yields $^{13}CC_4H_{12}O^{+\cdot}$ ions at m/z 89 and its molecular ion m/z 119 only produces m/z 101 (loss of H_2O) and m/z 86 (loss of $^{13}CH_3OH$). The MI mass spectrum of m/z 89 shows only one peak at m/z 56 indicating that <u>only</u> $^{13}CH_3OH$ is lost. If channel B of Figure 62 had been right, one would have expected to observe a single peak with label retention in the alkane at m/z 57, since $(CH_3)_3C^{13}CH_2OH$ produced only $^{13}CH_3OH$ (Figure 63).

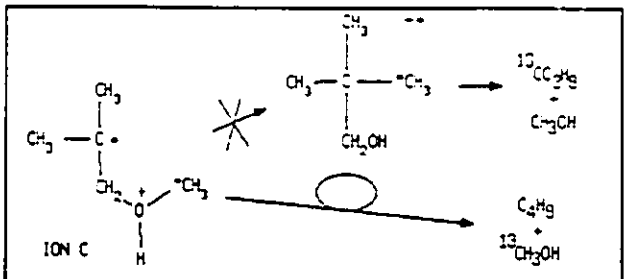

Figure 63- Proposed and actual label distribution upon fragmentation of *C-ion C.

The presence of $^{13}CH_3OH$ is also confirmed by O_2 CIDI experiments which shows peaks shifted to m/z 32 and m/z 33. On the basis of these results, it is proposed that $(CH_3)_2{}^{\bullet}CH_2{}^{+}O(H)CH_3$ from 3-methoxy-2,2-dimethyl propanol and ionized neopentanol fragment via a common reacting configuration but that the former does not rearrange into the latter ion.

5.2.10 2-tert-butoxyethanol.

The base peak in the EI mass spectrum of this compound is m/z 57 ($C_4H_9^+$). It also contains peaks at m/z 103, loss $CH_3^{\bullet}$ (19%), m/z 88, loss of CH_2O (2%) and m/z 87, loss of CH_3O (8%). The mass spectra of the labelled molecules $(CH_3)_3COCD_2CD_2OH$ and $(CH_3)_3COCH_2CH_2OD$ display a shift of the m/z 87 and m/z 88 peaks to m/z 89, 90 and m/z 87, 89. The structure for m/z 88 (ion D) is proposed to be $(CH_3)_3C^{+}O(H)^{\bullet}CH_2$ according to Fig 64.

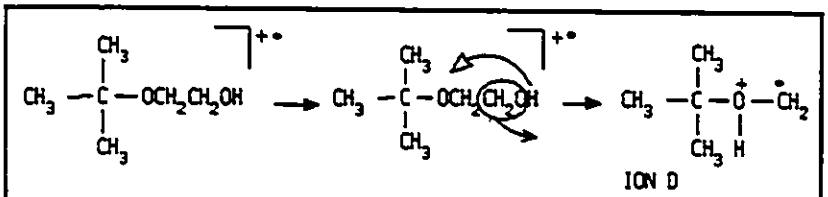

Figure 64- Proposed mechanism for the formation of an ylid ion (ion D) from 2-tert-butoxyethanol.

The deuterium labelled compound, $(CH_3)_3COCH_2CD_2OH$, was also studied and, according to Figure 64, it is expected to produce only a peak at m/z 88. It does so indeed, but there is also a small peak at m/z 90, approximately five times weaker than m/z 88. It may arise from loss of formaldehyde in a different manner (Figure 65).

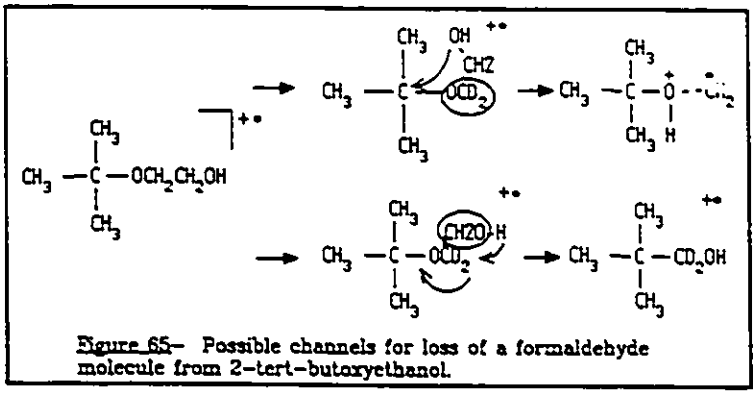

Figure 65– Possible channels for loss of a formaldehyde molecule from 2-tert-butoxyethanol.

The characteristics of the m/z 90 ion from the d_4 compound were studied to avoid interferences from m/z 88 in the $(CH_3)_3COCH_2CD_2OH$ ion.

The MI mass spectrum of this ylid ion (ion D) displays three peaks at m/z 56, 57 and 58 in a 100:5:20 ratio. The latter two arise from losses of $^{13}CH_2O$ and CH_2O respectively from $^{13}CC_4H_{11}O^{+\bullet}$ (natural isotopic abundance of the very intense m/z 87, $C_5H_{11}O^+$). Note that the metastable m/z 87 ion from neopentanol only produces m/z 69, there is no trace of m/z 57. Therefore, the two ions have different structures and the path at the bottom of Figure 65 is not possible. High energy resolution of metastably generated m/z 56 shows a $T_{0.5}$ of 1.5 ± 0.1 meV which is in good agreement with the value of 1.4 meV obtained for neopentanol. The α-CD_2 and OD labelled compounds also show the same label retention as di- and mono-deuterated neopentyl

alcohol (Table IV) suggesting that they share a common fragmentation route. The He CA mass spectrum of $(CH_3)_3C^+O(H)^{\cdot}CH_2$ shows a sharp increase in intensity for m/z 56 and a very weak collisionally induced m/z 57. This again reproduces the behaviour of neopentyl alcohol.

Table IV H/D distribution (%) among $C_4H_8^{+\cdot}$ ions produced from D-labelled metastable $[C_5H_{12}O]^{+\cdot}$ ions from 2-tert butoxyethanol.

ION	LABEL	C_4H_8	C_4H_7D	$C_4H_6D_2$
$(CH_3)_3C^+O(H)^{\cdot}CH_2$	-OD	56	44	
	$-OCD_2$	29	53	18

The Xe/O_2 NRMS of ion D shows the same peaks as neopentanol but in different ratio: m/z 57 (18%), m/z 56 (89%), m/z 41 (77%) and m/z 39 (100%). This may indicate that the same entities are present in both ions but in a different arrangement i.e. both ions contain C_4H_9 and CH_2OH groups but attached together via a different atom (Figure 66).

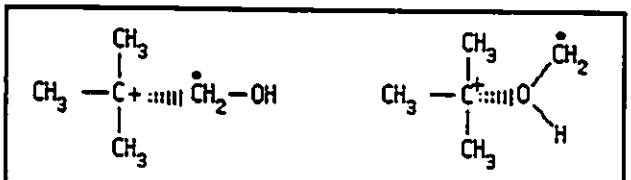

Figure 66- The hydroxymethyl radical may be bonded to the t-butyl cation in two different manners.

The AE of ion D was not measurable because the m/z 88 ion is too weak a peak. Therefore its heat of formation was estimated using $\Delta H_f[(CH_3)_3C^+O(H)C\underline{H}_3]$=402 kJ/mol[9] and $D[C\underline{H}_2\text{-}H]$=444 kJ/mol[37]. The value of 444 kJ/mol is perhaps uncertain to ±15 kJ/mol but C-H

bond strengths in protonated ether ions are stronger than those in the unprotonated species[37]. The ΔH_f value for $(CH_3)_3C^+O(H)^+CH_2$ was estimated to be 628 kJ/mol.

5.3 Possible Mechanism for Fragmentation of Ionized Neopentyl Alcohol.

In light of the results obtained in the previous section, it is clear that neopentanol, the distonic ion from 3-methoxy-2,2-dimethylpropanol and the ylid ion from 2-tert-butoxyethanol share common fragmentation pathways. According to the labelling experiments and energetics, it is proposed that, although the distonic ion and neopentanol behave similarly, there has to be an intermediate ion to allow their interconversion. The ylid ion is proposed to be this key intermediate.

5.3.1 Labelling

Table V shows the various labelling results for the above three isomeric ions. It is clear from these results that the initial position of the label is not important i.e. for a certain number of label atoms the fragments retain the same amount of label irrespective of their initial position. This may be explained by proposing that randomization of label position is complete before dissociation takes place and that the non-random distribution in the products is kinetically controlled. This aspect will be discussed in section 5.3.4.

Table V H/D distribution (± 2%) among $[C_4H_8]^{+\bullet}$ ions produced from metastable D-labelled $[C_5H_{12}O]^{+\bullet}$ isomers. Numbers in parentheses are the random statistical ratios.

ION	LABEL POSITION	C_4H_8	C_4H_7D	$C_4H_6D_2$	$C_4H_5D_3$
$(CH_3)_3CCH_2OH^{+\bullet}$	-OD	56(33)	44(67)		
	$-CD_2OH$	28(9)	56(48)	16(43)	
	$-CH_2D$	55	45		
	$-CD_2OD$	12(2)	43(22)	37(51)	8(25)
$(CH_3)_2C(CH_2D)CD_2OH^{+\bullet}$		16	42	34	8
$(CH_3)_2{}^{\bullet}CCH_2{}^{+}O(H)CH_3$	-OD	58	42		
	$-OCD_3$	14	43	37	6
$(CH_3)_3C^{+}O(H)^{\bullet}CH_2$	-OD	56	44		
	$-CD_2$	29	53	18	

5.3.2 Interconversion of ions.

To explain the conversion of neopentanol into the key intermediate it is suggested that there is partial separation of the tert-butyl cation and the $^{\bullet}CH_2OH$ radical and once a critical extension has been exceeded, there is rotation of the hydroxymethyl fragment to produce the ylid ion (Figure 67).

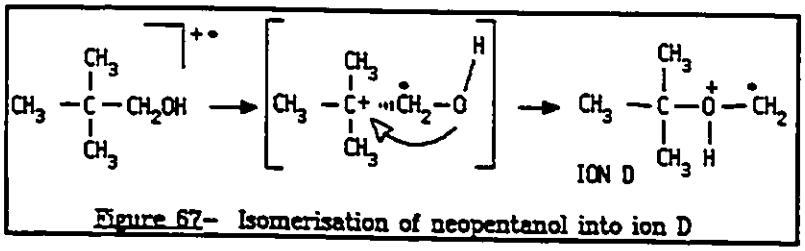

Figure 67– Isomerisation of neopentanol into ion D

This mechanism provides support for the original proposal of Hammerum and Audier[94] and shows similarities with the rearrangement of alkyl phenyl ether ions. The H/D exchange between the methyl groups and the methylene and between the methyl groups and the hydroxyl H can be explained via simple processes (Figure 68) involving 1,4-H shifts.

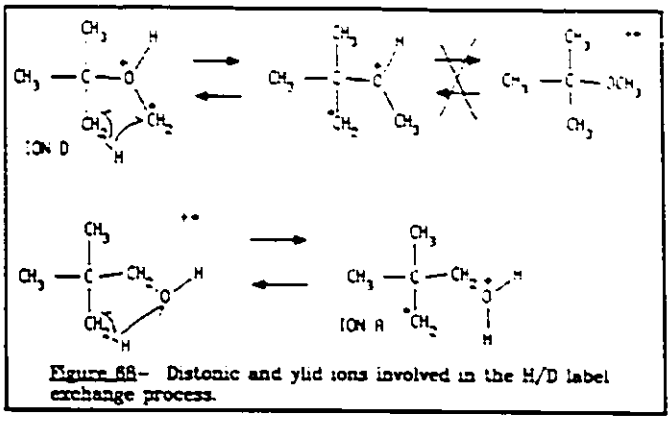

Figure 68– Distonic and ylid ions involved in the H/D label exchange process.

Note that the tert-butyl methyl ether ions showed no mixing upon metastable fragmentation. Therefore, the distonic or ylid ions shown in the above figure cannot be involved in the fragmentation of that ether.

The conversion of $(CH_3)_2\dot{C}CH_2{}^+O(H)CH_3$ to neopentanol ions was shown not to occur directly, therefore, the former should convert to the ylid ion. The mechanism is not clearly understood but a reversible methanol transfer to the radical site is a plausible mechanism to explain the exclusive $^{13}CH_3OH$ loss (Figure 69).

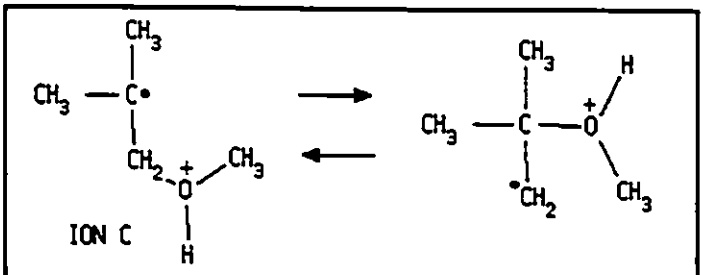

Figure 69– Isomerisation of ion C into a distonic ion which allows for H/D label exchange.

The above mechanisms clearly explain how the H/D label mixing occurs in each ion and also explain the behaviour of ^{13}C labelled ions.

5.3.3 Energetics

Figure 70 shows an energy diagram which illustrates the interconversion of the three ions. The dotted lines are estimated energies whereas the full lines were values from experiment. The transition state energy for the 1,4-H shifts has been set at 25 kJ/mol which is slightly below

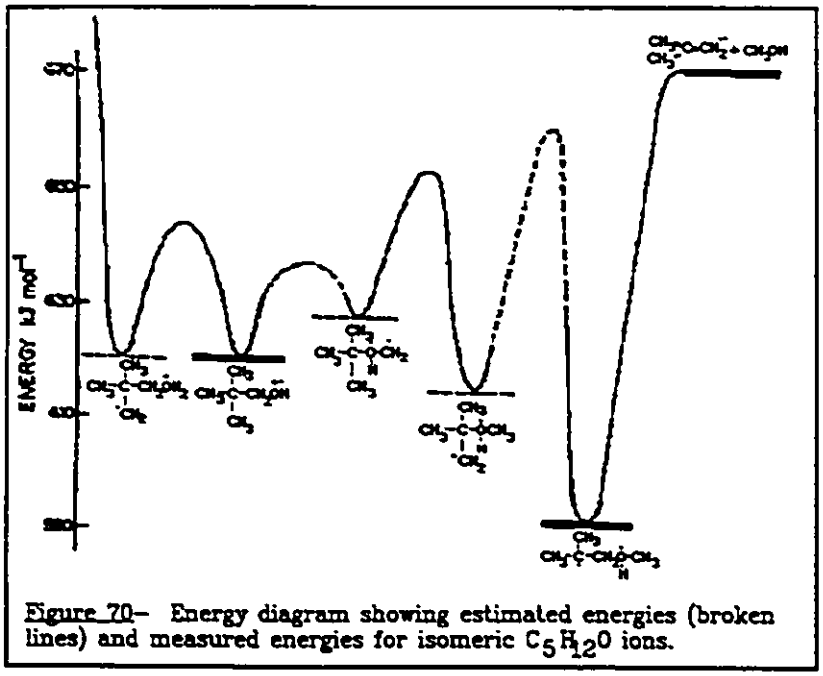

Figure 70– Energy diagram showing estimated energies (broken lines) and measured energies for isomeric $C_5H_{12}O$ ions.

that which has been measured for the 1,4-H transfer in the (smaller) propanol molecular ion (33 kJ/mol). The heat of formation of $(CH_3)_3C^{\cdot}C^{+}O(H)CH_3$=402 kJ/mol and D[$CH_2$-H]=431 kJ/mol, were estimated according to the method established in reference 38. The other transition state energies are not known and are only of qualitative significance in the diagram. The barrier for interconversion between ionized neopentanol and $(CH_3)_3C^{+}O(H)^{\cdot}CH_2$ is set as shown to allow for easy H/D exchanges. The metastable fragmentation to produce $C_4H_8^{+\cdot}$ and methanol takes place with a very small kinetic energy release and indicates a threshold dissociation i.e. no excess

energy barrier before obtaining the products. Thus, the $(CH_3)_2\dot{C}CH_2\dot{O}(H)CH_3$ ion is the key species from which the products are obtained and its ground state should lie in a deep energy well. The barrier between that ion and $(CH_3)_2(\dot{C}H_2)C\dot{O}(H)CH_3$ is set higher than that between $(CH_3)_3C\dot{O}(H)\dot{C}H_2$ and $(CH_3)_2(\dot{C}H_2)C\dot{O}(H)CH_3$ in order to allow for complete label exchange and rearrangements. The ion leading to the products, $(CH_3)_2\dot{C}CH_2\dot{O}(H)CH_3$, is proposed to rearrange into its final reacting configuration via a simple bond extension leading to an electrostatically bound complex between CH_3OH molecule and a methyl propene ion (Figure 45).

5.3.4 Isotope Effect.

That the same number of H and D atoms in all three ions produces the same distribution ratio of label in the fragments, independant of their initial position, (Table V) almost certainly results from H and D atoms losing their positional identity prior to metastable fragmentations. To obtain the observed ratios, and the observed excess of deuterium in the methanol produced can be rationalized by there being an isotope effect involved in the final separation of the products. This isotope effect produces the apparent non-randomization of the labels at longer lifetimes. This effect arises from the electrostatic bonding between CH_3OD and ionized methylpropene being weaker than for CH_3OH and methylpropene in that the density of states for the $CH_3OD\cdots C_4H_8^{+\cdot}$ complex will be smaller than for a $CH_2DOH\cdots C_4H_8^{+\cdot}$ ion. This is shown by the CIDI experiments where there is a clear preference for the label to be retained in the methanol (more specifically on the oxygen atom) rather than in the methyl propene fragment. This isotope effect thus governs the kinetics of the metastable decompositions and, depending

on the number of labels in the ion, the ion/molecule complexes dissociate at different rates.

Table VI H/D distribution (%) among $C_4H_8^{+\bullet}$ ions produced from labelled $C_5H_{12}O^{+\bullet}$ isomers, in different field free regions compared with predicted statistical ratios.

LABEL	ORIGIN	m/z 56	m/z 57	m/z 58	m/z 59
d_3	ZAB	13	43	37	7
	MS-9	11	33	44	12
	RANDOM	2	22	51	25
d_2	ZAB	28	56	16	
	MS-9	20	56	24	
	RANDOM	9	48	43	
d_1	ZAB	56	44		
	MS-9	47	53		
	RANDOM	33	67		

To prove this hypothesis, it should follow that at shorter lifetimes (higher internal energies) the labelled ions should produce fragments in abundance ratios closer to random, and so another experiment was performed. It consisted of measuring the relative ratios of the MI processes of variously labelled ions in the first field free region (1 FFR) of a mass spectrometer,

i.e. at shorter times than for the results shown in Table V. The experiments with the ZAB-2F show the 2 FFR MI processes whereas the MS-902S experiments were for the 1 FFR processes. In this first field free region, the ions have shorter lifetimes and the isotope effects are predicted to be smaller. Table VI shows the results obtained for d_1, d_2 and d_3 labelled ions where the results obtained with the MS-902S are compared with those from the ZAB-2F and with the random statistical ratios. The table clearly shows that at shorter lifetimes, MS-9 versus ZAB, the ratios tend towards complete randomization. Therefore, the hypothesis that there is complete H/D randomization prior to dissociation is strongly supported. It is possible to calculate the isotope effects according to the number of labels in the ions (see Appendix III).

5.4 C_5H_{11}-methyl ethers.

The behaviour of ionized neopentyl methyl ether was reported by Hammerum and Audier[94]. They observed extensive loss of H/D positional identity prior to metastable loss of C_2H_6O. The ion was briefly studied in this work to try to obtain information in relation with the behaviour of neopentanol. A quick glance at the metastable dissociation of t-amyl methyl ether, $CH_3CH_2C(CH_3)_2OCH_3$, was also made since its structure could permit a possible loss of methanol. This is described first.

5.4.1 1-Methoxy-1,1-dimethyl propane (t-amylmethyl ether).

The EI mass spectrum of this molecule shows no molecular ion (m/z 102). The base peak

is m/z 73 (loss $C_2H_5^{\cdot}$) with weaker signals at m/z 87 (34%), loss $CH_3^{\cdot}$, m/z 59 (17%), loss $C_3H_7^{\cdot}$, and m/z 55 (24%), loss of [$C_2H_5^{\cdot}$, H_2O]. The only true MI process is loss of C_2H_6 to give rise to a signal at m/z 72, the peak at m/z 70 in the MI mass spectrum arises from the ^{13}C contribution of the intense $C_6H_{13}O^{+}$ → m/z 69. There is no process which might relate to neopentanol. The only analogy which can be made is with t-butyl methyl ether which also loses an alkane fragment (CH_4). It could be predicted that the only metastable processes which would take place for R-$C(CH_3)_2OCH_3$ is loss of a R-H fragment.

5.4.2 Neopentyl Methyl Ether

The base peak in the EI mass spectrum is m/z 57 ($C_4H_9^{+}$) and the molecular ion, m/z 102, is of significant importance (20%). Other important peaks are m/z 56 (65%), loss of C_2H_6O, m/z 45 (47%), C_2H_5O, and m/z 87 (24%), loss of $CH_3^{\cdot}$. The MI mass spectrum displays only two peaks: m/z 56 ($C_4H_8^{+\cdot}$), 100% and m/z 70 (loss of CH_4O), 57%. The kinetic energy release measurements ($T_{0.5}$) for these peaks were 4.3 meV and 15.4 meV, respectively. Using the ΔH_f of the molecule, -299 kJ/mol, its IE (9.30 ± 0.05 eV) and the metastable AE values for m/z 70 (10.0 ± 0.1 eV) and m/z 56 (10.1 ± 0.1 eV), the energy diagram was constructed, Figure 71. The threshold for C_2H_6O elimination corresponds to loss of dimethyl ether and the ion m/z 70 was identified as the $(CH_3)_2C{=}CHCH_3^{+\cdot}$ ion. The latter has a ΔH_f=795 kJ/mol and its structure was confirmed by comparing its O_2 charge stripping (CS) mass spectrum with the results for other C_5H_{10} hydrocarbons[69]. Note that this isomer is the only one showing a significant peak at m/z $70^{+\cdot}$ and is therefore easily distinguishable.

Note also that although CH_3OCH_3 loss takes place at the thermochemical threshold the reaction leading to m/z 70, loss of CH_3OH has a considerable excess energy (50 kJ/mol), see Figure 71. This is quite unlike the behaviour of neopentanol. The He CA mass spectrum of neopentyl methyl ether shows that m/z 56 doubles in intensity upon introduction of the collision gas whereas m/z 70 was barely affected. Two other significant peaks appeared: m/z 47 and m/z 57 (both 14% of m/z 56). Therefore, one may conclude that the ion structure leading to m/z 70 is of lower abundance than that producing m/z 56; the latter behaves in a manner similar to neopentyl alcohol.

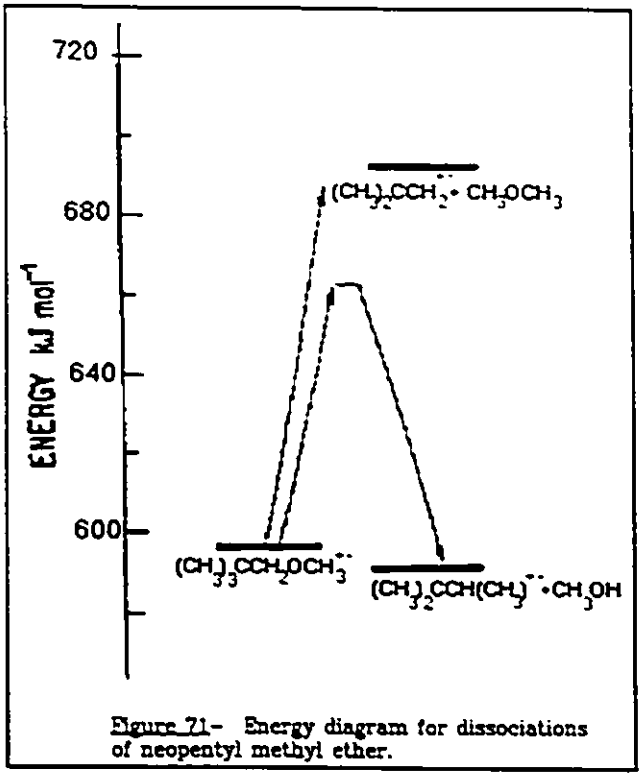

Figure 71- Energy diagram for dissociations of neopentyl methyl ether.

Three labelled compounds were studied. The MI mass spectrum of neopentyl ^{13}C-methyl ether showed only m/z 56 indicating that the label is always lost, and two peaks at m/z 71 and 70 of equal abundance indicating that the α-C and methyl-C atoms have equal chances of being lost (Figure 72). In the EI mass spectra of the labelled compounds, very little, if any H/D mixing before fragmentation was

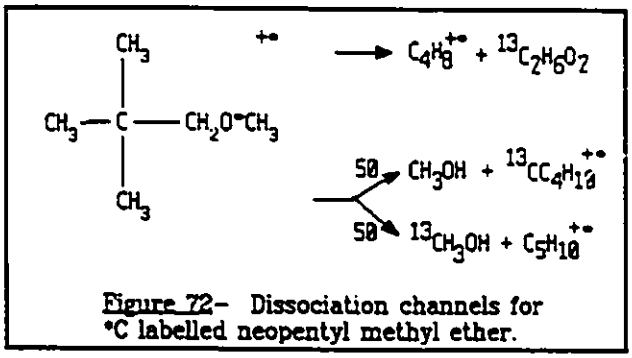

Figure 72- Dissociation channels for *C labelled neopentyl methyl ether.

observed. The labelling results for metastable ions are shown in Table VII.

Table VII H/D distribution (%) among $C_5H_{10}^{+\cdot}$ and $C_4H_8^{+\cdot}$ ions produced from metastable D-labelled neopentyl methyl ether ions. Numbers in parentheses are the random statistical ratios.

ION	C_5H_{10}	C_5H_9D	$C_5H_8D_2$	$C_5H_7D_3$	C_4H_8	C_4H_7D	$C_4H_6D_2$	$C_4H_5D_3$
$(CH_3)_3CCD_2$- -OCH_3	4	38	58		29	46	25	
RANDOM	7	44	49		16	53	31	
$(CH_3)_3CCH_2$- -OCD_3	4	12	46	38	11	42	39	8
RANDOM	1	17	49	33	6	33	46	15

The loss and retention of H/D among metastable ions is apparently not a random process and for the formation of C_4H_8 ions, there is greater retention of label in the neutral (as in neopentyl alchohol) whereas there is a different label retention for m/z 70 with results closer to random. The H/D randomization in m/z 70 may be expected since the ^{13}C labelled compound showed an exactly equal retention/loss behaviour.

To explain the metastable fragmentations of this ion, two mechanisms may be required.

The formation of the trimethylethene ion is explained by close analogy with the series of phenyl alkyl ethers[91] i.e. the methoxy radical-neopentyl cation pair separates sufficiently for the cation to isomerise to the tertiary amyl cation and a ß-H atom transfers from the ion to the radical to yield the products. The 70 kJ/mol of excess energy of the transition state above the products is typical of such reactions[91] in which the energy requirement for a secondary ß-H atom transfer has been reported to be 60 kJ/mol for the analogue reaction with neopentyl phenyl ether. In light of the results obtained with neopentyl alcohol and of the labelling results for metastable loss of C_2H_6O from neopentyl methyl ether, one can only speculate a reasonable mechanism in which the participation of an isobutene ion-dimethyl ether complex as the final reacting configuration is a plausible final intermediate.

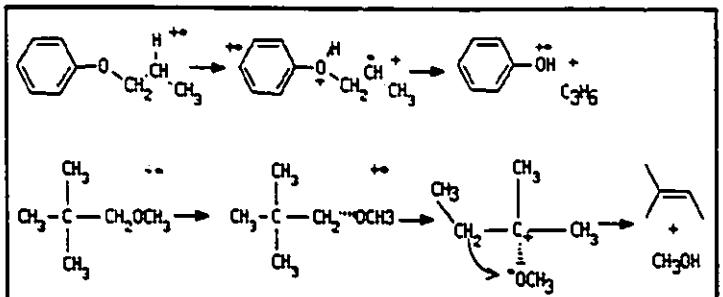

Figure 73- The formation of the trimethylethene ion can be explained by analogy with the formation of phenol ion.

5.5 Experimental

5.5.1 Chemicals

The α-CD_2 analogue of neopentyl alcohol was prepared by reduction of pivaloyl chloride with $LiAlD_4$ and the α-^{13}C compound came from a previous study[99]. The OD analogues for

alcohols were produced by exchange with D_2O. The tert-butyl methyl ether and its trideutero analogue were made by reaction of t-BuO$^-$ with CH_3I and CD_3I respectively. The labelled neopentyl methyl ethers were prepared similarly. The 1-Methoxy-2,2-dimethyl propanol was also prepared similarly from 2,2-dimethyl propanediol. The 2-t-butoxyethanol was synthesized by refluxing t-butyl chloride with an equimolar amount of sodium (dissolved in ethylene glycol) for 15 hours. The same reaction was performed with ethylene-d_2 glycol and ethylene-d_4 glycol to obtain respectively $(CH_3)_3CCCH_2CD_2OH$ and $(CH_3)_3COCD_2CD_2OH$. The $(CH_3)_2C(CH_2D)CD_2OH$ was made by reducing methyl (3-bromo-2,2-dimethyl) propionate with $LiAlD_4$ and $(CH_3)_2C(CH_2D)CH_2OH$ by a similar reduction with 3-bromo-2,2-dimethyl propanol. All other compounds were of research grade and were obtained from Aldrich Chemical Co Inc.

5.5.2 Experiments

All Electron Ionization (EI), Metastable Ion (MI), Collisional Activation (CA), Charge Stripping (CS), Collision Induced Dissociative Ionization (CIDI) and Neutralization-Reionization (NRMS) mass spectra were recorded using the VG Analytical ZAB-2F mass spectrometer described in chapter 2 of this thesis. In the experiments involving collision gases, the He or O_2 pressures were maintained such that the main beam's intensity was reduced by no more than 10% (essentially single collision conditions, see chapter 3). The Xe/O_2 NRMS were also recorded under single collision conditions. Except when kinetic energy releases were being determined, all energy resolving slits were wide open to avoid instrument discrimination effects.

Metastable peak AE values and first field free metastable abundance ratios were measured using the AEI MS-902S mass spectrometer described in chapter 2 of this thesis. The AE of the various compounds were obtained via comparison with the reference metastable loss of methyl from ionized diethyl ether.

Ionization Energy (IE) and other Appearance Energy (AE) values were measured with energy-selected electrons using an apparatus comprising an electrostatic electron monochromator with mini-computer data system[12].

CHAPTER 6

INVESTIGATION OF ISOMERIC $C_7H_5^+$ SPECIES IN THE GAS PHASE

6.1 Introduction

In this chapter $C_7H_5^+$ ions produced from various precursors were studied. The labelling technique, which was extremely useful in the previous chapter, was not applied to this system because of the prevalence of atom "scrambling" in aromatic ions[37]. Therefore, we will rely upon thermochemical information, metastable ion (MI), collision induced (CA) and charge stripping (CS) mass spectra to help to assign a structure to the various isomers.

Much interest has been shown in aryl cations because all attempts to generate them in the condensed phase by solvolysis of various precursors have failed[100]. It is known that the phenyl cation has a very low relative thermodynamic stability $\Delta H_f[C_6H_5^+]$= 269.6 kcal/mol. The 2-propenyl cation is one of the least stable vinyl cations produced by solvolysis but is, however, thermodynamically more stable than the phenyl cation by 27 kcal/mol (ab-initio calculations). At this point, it may be useful to define what is meant by stability. The stabilization of one even electron ion, A^+, relative to another, B^+, is often represented by the difference in the heterolytic bond dissociation energy $D[A^+\text{-}H^-] - D[B^+\text{-}H^-]$[101]. This energy can be estimated using the

following equation:

$$D(R^{+}\text{-}H^{\cdot}) = \Delta H_f(R^{+}) + \Delta H_f(H^{\cdot}) - \Delta H_f(\text{neutral}) \qquad [33]$$

Many experiments have been designed to find a substituted aryl cation more stable than the phenyl cation[100]. The conclusions were that substituents are not very effective in stabilizing singlet aryl cations. Ab-initio calculations have been performed to show two substitution patterns which stabilize the phenyl cation: the hyperconjugation between an empty 2p(C^{+}) orbital and -C-R bonds and hyperconjugation with high-lying strained C-C bonds. The major stabilizing interaction is between the empty 2p(C^{+}) orbital and the highest occupied Walsh orbital of a fused cyclopropane ring. This was calculated to stabilize the phenyl cation by ca 23 kcal/mol (38 kcal/mol if considering HBDE, see Figure 75). Other calculations[100] show that the 2-cyclopropaphenyl cation is more stable than $CH_2{=}C^{+}CH_3$ by 5 kcal/mol. However, estimates of the relative stability of D[R^{+}-$H^{\cdot}$] the phenyl cation, the 2-propenyl cation and the 2-cyclopropaphenyl via heterolytic bond strengths produced different numbers. Using the values shown in Figure 75, it is seen that the effect of the cyclopropane ring is to stabilize, not by 23 kcal/mol, but by 27 kcal/mol and that the 2-cyclopropaphenyl cation is stable by more than 5 kcal/mol i.e. 14 kcal/mol, relative to the 2-propenyl cation. Therefore, the 2-cyclopropaphenyl cation should be stable enough for it to be observed in a solvolysis experiment. Calculations comparing cyclopropabenzene and

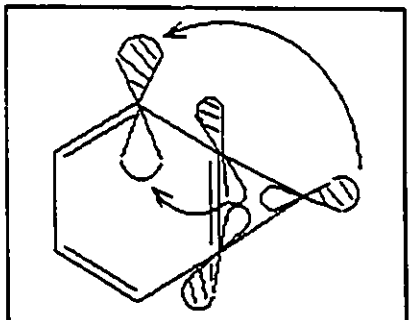

Figure 74- Stabilization of the cyclopropaphenyl cation.

cyclopropaphenyl cations showed that the C_1-C_6 bond is longer in the latter, thus releasing the strain in the cyclopropane ring.

Relative Stability, D(R⁺-H⁻)	
$D(R^+-H^-) = \Delta H_f(R^+) + \Delta H_f(H^-) - \Delta H_f(\text{neutral})$	
Benzene	$D(R^+-H^-) = \Delta H_f(C_6H_5^+) + \Delta H_f(H^-) - \Delta H_f(\text{benzene})$
	$D(R^+-H^-) = (269 + 34 - 20) = 283$ kcal/mol
2-Propene	$D(R^+-H^-) = \Delta H_f(C_3H_5^+) + \Delta H_f(H^-) - \Delta H_f(C_3H_6)$
	$D(R^+-H^-) = (231 - 34 - 4.8) = 270.2$ kcal/mol
cyclopropabenzene	$D(R^+-H^-) = \Delta H_f(C_7H_5^+) + \Delta H_f(H^-) - \Delta H_f(C_7H_6)$
	$D(R^+-H^-) = (311 - 34 - 89) = 256$ kcal/mol

Figure 75– Determination of heterolytic bond strength energies.

Experiments designed to study the cyclopropaphenyl cation (m/z 89) were recently reported by Uggerud et al[102]. The AE of the 2-cyclopropaphenyl cation obtained from the fragmentation of bromo-2-cyclopropabenzene was found to be 10.5 eV. By definition, the relative stabilization energy (S.E.) of compound (2) relative to (1) is given by the different between their respective AE (S.E.= AE(2)-AE(1)), see Figure 76. Using this relationship and a thermochemical cycle, the ΔH_f of the cyclopropaphenyl cation was calculated to be 311 kcal/mol. The most important factor to take into account when estimating the ΔH_f of cyclopropabenzene is the presence of two rings causing strain in the molecule. Thus, our estimate for ΔH_f(cyclopropabenzene) is probably an upper limit because it is assumed that the smaller ring is cyclopropene. If it were considered as a cyclopropane ring, the ΔH_f value would be smaller. Strangely enough, the value given in reference 9 is 89 kcal/mol. Therefore, it is possible that the value found in the literature for cyclopropabenzene is related to another C_7H_6 species.

This short project was conducted to see if the conclusions of Uggerud et al[102] were correct e.g. if the $C_7H_5^+$ ion generated from a wide variety of precursor molecules is a single species and/or if there is any evidence to suggest that the cyclopropaphenyl cation is actually generated by loss of $Br^\bullet$ from 2-bromocyclopropabenzene and with a $\Delta H_f(C_7H_5^+)$=309-312 kcal/mol. In the present thesis attempts have been made to generate the 2-cyclopropaphenyl cation and to perform a direct measurement of its heat of formation. Many aromatic compounds give rise to a significant peak at m/z 89 in their normal EI mass spectrum and the following were studied: benzyl formate, benzyl acetate, benzyl alcohol, 1,6-heptadiyne, 1,5-decadiyne and 2-bromo cyclopropabenzene.

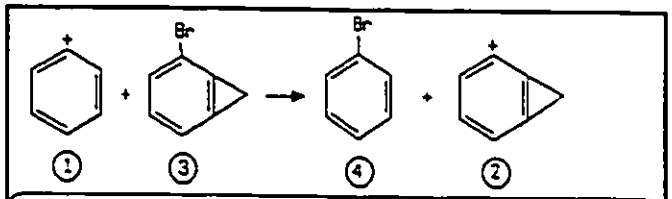

$AE(C_7H_5Br) = H_f(C_7H_5^+) - H_f(C_7H_5Br)$

$AE(C_8H_5Br) = H_f(C_8H_5^+) - H_f(C_8H_5Br)$

$S.E. = AE(2) - AE(1) = H_f(2) - H_f(3) - H_f(1) + H_f(4)$

$H_f(2) = AE(2) - AE(1) + H_f(1) + [H_f(3) - H_f(4)]$

$H_f(2) = 10.5\ eV - 11.7\ eV + 270\ kcal/mol + 67-70\ kcal/mol$

$H_f(2) = 309-312\ kcal/mol$

Figure 78- Determination of the heat of formation of 2-bromo cyclopropylbenzene using stabilization energies (S.E.)

6.2 What is known about these compounds?

The electron impact and chemical ionization mass spectra of benzyl acetate and benzyl formate have been recorded many times[103,104,105,106,107,108]. Surprisingly, m/z 90 is a

very intense fragment for both compounds. Emery[103] proposed that m/z 89 and m/z 90 arise both from loss of water from m/z 107 and m/z 108 respectively, and that the increase in intensity of the peaks from benzyl acetate relative to benzyl formate is due to the fact that the R group(CH_3 or H) is larger for benzyl acetate. However, the ion at m/z 90 does not arise from m/z 91, ($C_7H_7^+$), otherwise a peak at m/z 90 would be observed in the mass spectrum of toluene (in which m/z 91 is base peak), nor from m/z 108 because there is no m/z 90 in the mass spectrum of benzenemethanol (where m/z 108 a major peak).

Therefore, m/z 90 would arise from the loss of formic acid in the case of benzyl formate and acetic acid for benzyl acetate. Although losses of formic acid and acetic acid are energetically favored (ΔH_f(formic acid)=-378.8 kJ/mol and ΔH_f(acetic acid)=-418.1 kJ/mol), some aromatic stability must be involved to obtain such an intense peak at m/z 90.

The peak located at m/z 89 is also quite intense. From the observation of the normal mass spectrum, one may suggest that m/z 89 arises from loss of a hydrogen atom from m/z 90. According to the results obtained by Emery[103], there may even be a metastable peak (m*) for 90→89 ($m^*=M_2^2/M_1=89^2/90=88.1$), because a peak at m/z 88.3 was reported.

Many papers have described the mass spectrometry of benzyl acetate[103,104,105,106,107,108] but relatively few discuss the ion chemistry of benzyl formate[103,108]. Only the normal mass spectrum of benzyl formate has been described whereas benzyl acetate has been studied in more detail. The m/z 108 and m/z 91 fragments of benzyl acetate have been examined and it has been shown

that two forms of $C_7H_7^+$ ions are produced: tropylium and benzyl[105]. The conclusions of this study stated that tropylium is favored over benzyl at threshold energies. At higher energies, benzyl is the major fragment. Other work has shown that m/z 108 corresponds to ionized benzenemethanol[106].

The electron impact mass spectra of both benzyl acetate and benzyl formate have been studied by Corina et al.[108]. The observed peaks are m/z 108, 107, 91 and $M^{+\cdot}$-107 (m/z 43 for the acetate and m/z 29 for the formate). They concluded that major fragmentation processes for benzyl esters can take place via two routes: H-migration or, α or ß cleavage. Benzylic cleavage combined with H migration was found to compete with simple cleavage. Surprisingly, the peaks at m/z 90 and 89 which are as intense as m/z 107 in the normal electron impact mass spectrum, were not discussed.

6.3 Results and Discussion

In this section, the behaviour of various $C_7H_5^+$ ions produced from different precursors will be described from a thermochemical and dissociative point of view.

6.3.1 Benzyl Acetate

As mentioned in section 6.2, the EI mass spectrum of benzyl acetate shows a significant peak at m/z 89. Table VIII lists of the most intense fragments in the normal mass spectrum, the

numbers reported earlier for 70 eV EI mass spectrum by Emery[103] are also included.

Table VIII- Relative intensities of the peaks in the EI spectrum of benzyl acetate.

m/z	150	108	107	91	90	89	79	77	65	51	43
relative %	51	100	16	48	37	8	18	12	10	9	40
from ref 103	n/a	100	19	78	49	13	27	25	18	24	75

The peak at m/z 108 may arise from direct loss of 42 u, C_2H_2O. The peak at m/z 91 may be formed by direct cleavage, loss of CH_3COO. Subsequent losses of $H^{\cdot}$ and H_2 may give rise to m/z 90 and 89. The different mass spectra obtained in our experiment and that reported in reference 103 may be explained by at least two factors: a different instrument was used to record the spectra and the experimental (ion source) conditions may have been different.

The MI mass spectrum of the molecular ion of benzyl acetate (m/z 150) contains only one peak at m/z 108. This peak corresponds to the loss of a CH_2CO fragment to form $C_6H_5CH_2OH^{+\cdot}$ and with a kinetic energy release, $T_{0.5}$=12 meV. The He CA mass spectrum of m/z 150 shows peaks at m/z 108, 107, 91, 90, 89, 79, 77 and 43, reproducing the features of the EI mass spectrum.

The MI mass spectrum of m/z 108 was also recorded and apparently five metastable processes occur: m/z 107 (loss of $H^{\cdot}$), 98%, m/z 90 (loss of H_2O, 4%, m/z 80 (loss of CO), 5%,

m/z 79 (loss of HCO), 100% and m/z 78 (loss of CH_2O). However, the m/z 107, m/z 80, m/z 79 and part of m/z 78 arise from ^{13}C contribution from m/z 107. Thus, only H_2O and CH_2O losses produce true metastable peaks. The He CA mass spectrum of m/z 108 is not very intense; the peaks at m/z 78, 79 and 90 are not very sensitive to the collision gas, however, a new peak at m/z 77 appears, characteristic of the $C_6H_5^+$ fragment. The O_2 CIDI mass spectrum of m/z 108 shows peaks at m/z 30, 29 and 28 with a 18: 100: 15 ratio. This is in keeping with the presence of CH_2O, HCO and CO as neutral fragments. It also rules out the possibility that m/z 30 is C_2H_6, otherwise, a cluster of hydrocarbon peaks, m/z 24-30 would have appeared.

The peak of interest, m/z 89, was also studied. Its MI mass spectrum shows three processes: m/z 88 (loss of $H^{\cdot}$), 100%, m/z 87 (loss of H_2), <1% and m/z 63 (loss of C_2H_2), 9%. The kinetic energy releases ($T_{0.5}$ values), obtained for loss of $H^{\cdot}$ and loss of C_2H_2 were 26 ± 2 meV and 43 ± 3 meV respectively.

In the He CA mass spectrum of m/z 89, the m/z 88 and m/z 63 processes were both affected by the collision gas. Their relative ratios were 100:18 with a MI contribution of 70% for m/z 88 and 56% for m/z 63. Other fairly intense peaks are a cluster at m/z 84-87 indicating consecutive losses of H from the $C_7H_5^+$ ion and a peak at m/z 74 which provides some structural information i.e. the loss of $CH_3^{\cdot}$ from m/z 89 occurs easily upon introduction of the collision gas, and this loss may be indicative of structure in the m/z 89, $C_7H_5^+$ ion.

An attempt to measure the AE from m/z 89 was made but because of the intense peak

at m/z 90, only an estimate was possible, AE> 13 eV. The AE of the metastable peak m/z 90 → m/z 89 could not be measured because of the crossing of the curves (Fig 77). Ideally, the curves are parallel but in "real life" they often converge i.e. the distance between the curves at the top is larger than at the bottom. When normalizing the observations it is customary[11] to multiply one of the curves by a certain factor to obtain parallel curves, but when the curves cross, even the use of a large multiplying factor will never lead to parallel curves. The energetics of $C_7H_5^+$ ions will be discussed in length in section 6.4.

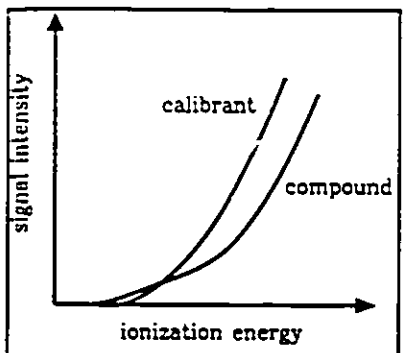

Figure 77- Crossing of the calibrant and compound curves.

6.3.2 Benzyl Formate

Table IX gives a list of the most intense fragments in the normal mass spectrum of benzyl formate as well as values taken from reference 103. The loss of CO gives rise to m/z 108 and the direct bond cleavage at the CH_2-O site, to lose the oxygen atom, produces m/z 91. The peaks at m/z 107, 90 and 89 arise from consecutive losses of H from m/z 108 and m/z 91 respectively.

Only one metastable peak occurs from the molecular ion, m/z 136. It is loss of a CO fragment to form an ion at m/z 108 with a very large kinetic energy release of ca 800 meV. The He CA mass spectrum of m/z 136 shows very weak peaks and does not provide any valuable structural information.

Table IX- Relative intensities of the peaks in the EI spectrum of benzyl formate.

m/z	136	135	108	107	91	90	89	79	77	65	43
relative %	8	81	44	31	100	79	17	32	28	22	40
from ref 103	n/a	n/a	35	30	100	80	19	39	36	26	75

The same metastable processes as for benzyl acetate occur from m/z 108 i.e. loss of water and loss of CH_2O in a 1:4 ratio. The He CA mass spectrum of m/z 108 is very similar to that of benzyl acetate and so one can conclude that the m/z 108 ions from the acetate and the formate indeed have the same structure.

The m/z 89 ion from the formate shows only two major metastable processes: m/z 88 and m/z 63 in a respective ratio of 100:9. The $T_{0.5}$ values obtained were 23 and 45 meV respectively. The MI data are thus in excellent agreement with the results obtained with benzyl acetate, and so, it can confidently be concluded that both m/z 89 ions have the same structure. The similarity of both CA mass spectra confirms this hypothesis. Again, because of the high intensity of the peaks near m/z 89 in the EI spectrum, it was not possible to perform any thermochemical measurements.

6.3.3 Benzyl Alcohol

The EI mass spectrum of benzyl alcohol has its base peak at m/z 79 (loss of CHO), a very

intense molecular ion (93%), strong peaks at m/z 107 (loss of $H^{\cdot}$), 67% and m/z 77 ($C_6H_5^+$), 57% and weaker processes at m/z 91 (loss of OH), 17%, m/z 90 (loss of H_2O), 9% and m/z 89 (loss of H_2O and $H^{\cdot}$), 8%. The MI mass spectrum of m/z 108 shows only peaks at m/z 90 and 78 with a ratio of 1:4 therefore allowing one to conclude that the m/z 108 ions obtained from benzyl acetate and benzyl formate also have the structure $C_6H_5CH_2OH^{+\cdot}$. The He CA mass spectrum of benzyl alcohol also shows the same characteristics as for the compounds discussed in sections 6.3.1 and 6.3.2.

The MI mass spectrum of m/z 89 shows two intense metastable peaks at m/z 63 (28%) and m/z 88 (100%) and a weaker process at m/z 87 (<1%). The $T_{0.5}$ values obtained for m/z 88 and m/z 63 are respectively 22 meV and 39 meV. Although the intensity of the m/z 63 is a little higher than for benzyl formate and benzyl acetate, the similarity in $T_{0.5}$ values and of the HeCA mass spectra, lend support to the conclusion that benzyl alcohol, benzyl acetate and benzyl formate give rise to $C_7H_5^+$ ions of the same structure. As a reminder, the He CA mass spectra shows a peak at m/z 74 indicating a facile loss of $CH_3^{\cdot}$ from $C_7H_5^+$. The O_2 charge stripping (CS) mass spectra of the m/z 89 ion from these three precursors were recorded and for benzyl alcohol, the O_2 charge stripping spectrum of m/z 89 showed peaks at m/z 85^{++}, 86^{++}, 87^{++}, 88^{++} and 89^{++} in a ratio of 5: 80: 24: 30: 100. These numbers will be compared with other data in section 6.5 where the various $C_7H_5^+$ ion structures are discussed in more detail.

Some thermochemical data were also obtained for benzyl alcohol. The AE for the m/z 90→89 process could be measured and was found to be 13.82 eV. A table containing the heats

of formation of the various $C_7H_5^+$ ions is shown in section 6.4.

6.3.4 2-Bromocyclopropabenzene.

The EI mass spectrum of 2-bromocyclopropabenzene shows a pair of fairly intense molecular ion peaks at m/z 168/170 (41% and 43% of the base peak). The base peak, m/z 89, corresponds to loss of $^{79}Br^{\bullet}$ and $^{81}Br^{\bullet}$. Another important peak is at m/z 63 and very probably arises by C_2H_2 loss from the m/z 89 fragment. All other peaks in the mass spectrum are less than 10% of the base peak. As expected, the MI mass spectrum of m/z 168 shows a unique process giving rise to m/z 89 with a kinetic energy release of 64 meV, evaluated from the half height width of the Gaussian metastable peak.

The MI mass spectrum of m/z 89 displays peaks at m/z 88 and 63 (ratio 20:100), a different ratio from that obtained for benzyl alcohol (see table X). There is also a weak but significant peak at m/z 87 (3%). These two metastable processes occur with $T_{0.5}$ = 22 meV for m/z 88 and $T_{0.5}$ = 37 meV for m/z 63.

The He CA mass spectrum of m/z 89 from 2-bromocyclopropabenzene shows similar features to that of benzyl alcohol except that loss of $H^{\bullet}$ is the most intense process in benzyl alcohol (intensity of m/z 88 from benzyl alcohol doubles upon introduction of collision gas). All collision induced fragments are very weak in the bromo compound, possibly indicating a very stable structure for m/z 89 i.e. possibly the cyclopropaphenyl cation.

The O_2 charge stripping mass spectrum displays peaks at m/z 85^{++}-89^{++} in the following ratios 2: 70: 26: 24: 100 (see table XII).

The IE of 2-bromocyclopropabenzene was measured using energy selected electrons and a value of 10.02 eV was obtained. The AE of the metastable peak for m/z 168→89 was also measured and gave a value of 10.5 eV, significantly above the result using energy selected electrons, 10.15 eV. These observations will be discussed later.

6.3.5 1,6-heptadiyne

The EI mass spectrum of 1,6-heptadiyne displays a small peak for the molecular ion, m/z 92 (8% of the base peak, m/z 91). All other peaks in the spectrum are fairly weak (less than 5%) except for m/z 65 which is 9% of the base peak's intensity.

The MI mass spectrum of m/z 92 displays a pair of peaks at m/z 65 and m/z 66 but the latter is due to ^{13}C contribution from m/z 91 and part of m/z 65 (75%) is due to that isotopic interference also. The MI mass spectrum of m/z 89 shows the same two peaks which seem to be characteristic of m/z 89 ions i.e. m/z 88 and m/z 63, and there is also a peak at m/z 87 which is fairly intense; the peaks appear in a ratio 100: 70: 22. The kinetic energy release values were found to be $T_{0.5}$ = 13 meV for m/z 88, $T_{0.5}$ = 32 meV for m/z 63 and for the weaker m/z 87, only an estimate could be obtained, $T_{0.5}$ ≈ 260 meV.

The He CA mass spectrum of m/z 89 shows the same peaks as for the other m/z 89 ions but in different ratios. The intensity of the m/z 88 peak relative to the subsequent H losses is different from that in the benzyl alcohol and bromo compounds. The CA mass spectrum may indicate an easier loss of C_2H_2 fragment because of the increase in intensity of the m/z 63 peak with introduction of the collision gas. It could perhaps arise from a structure which can lose C_2H_2 with minimum rearrangement.

The O_2 charge stripping mass spectrum displays the same five doubly charged ions in the 42.5-45.5 region in a ratio of 5: 94: 28: 31: 100 (see table XII).

The AE of the metastable peak for the m/z 91→m/z 89 process was also measured and a value of 11.46 eV was obtained.

6.3.6 1,5-decadiyne.

The base peak in the EI mass spectrum of 1,5-decadiyne (m/z 134) is m/z 91 and corresponds to loss of $CH_3CH_2CH_2^{\bullet}$. Other important peaks are m/z 119 (loss of $CH_3^{\bullet}$), 23%, m/z 105 (loss of $C_2H_5^{\bullet}$), 36%, m/z 95 (loss $C_3H_3^{\bullet}$), 38% and m/z 92 (loss of C_3H_6), 34%.; The peak at m/z 89 is only 2% of the base peak. The MI mass spectrum of m/z 89 shows the same three processes as for the previous molecules but in a completely different ratio. The ratios for m/z 88/87/63 are 9: 100: 5. The $T_{0.5}$ values are respectively 26 meV, 12 meV and 51 meV. In the He CA mass spectrum of m/z 89, the peak at m/z 87 is almost unaffected by the collision gas.

There is only a small increase in intensity for m/z 63 and m/z 88.

The O_2 CS mass spectrum also shows a series of doubly charged peaks at m/z 85^{++}-89^{++} in the following ratios: 6: 100: 54: 32: 97. Thermochemical information was also obtained for the m/z 89 ion from 1,5-decadiyne. The AE of the metastable peak 91→89 was measured to be 11.38 eV.

The following two sections will discuss the thermochemistry related to the various m/z 89 ions and will compare the information available. Finally, an attempt will be made to assign a structure to each m/z 89 ion.

6.4 Thermochemistry

As discussed in chapter 3, knowledge of the thermochemistry related to ions in the gas phase is very important when trying to identify and compare a series of ions. Table X contains measured AE values and ΔH_f values for m/z 89 ions from each precursor.

The heats of formation of the neutral precursors were obtained using Benson's additivity[19] method and the following equation was used to estimate ΔH_f of all the ions

$$AE = \Sigma\Delta H_f \text{ (products)} - \Sigma\Delta H_f \text{ (reactant)} \qquad [34]$$

Table X- Thermochemical data related to the various $C_7H_5^+$ ions.

PRECURSOR	PROCESS	AE (eV) ± 0.05	$\Delta H_{f(ion)}$ ±2 kcal/mol	$\Delta H_f(n)$ ±1 kcal/mol
Benzyl Formate	loss CH_2O loss OH 90→89	14.04	298	-61
Benzyl Alcohol	loss H_2O 90→89	13.82	301	-24
2-bromocyclopropabenzene	168→89	m* 10.5 (10.15)	309 (302)	94
1,6-heptadiyne	loss H 91→89	11.46	307	95
1,5-decadiyne	loss $C_3H_7^{\cdot}$ 91→89	11.38	313	75

According to Table X, benzyl alcohol and benzyl formate may yield the same ion since they have a similar value for the heat of formation. Furthermore, as seen in section 6.3, the dissociative behaviour is also similar. Unfortunately, thermochemical data was not obtainable for benzyl acetate, but its dissociative behaviour was very similar to benzyl alcohol. By comparing ΔH_f(ions) in Table X, one can say that there are three ions produced; a first ion with

ΔH_f=300±2 kcal/mol, another one with ΔH_f=307 kcal/mol and a last one with ΔH_f=313 kcal/mol.

6.5 Comparison of Information

From Table X, one can propose that at least three different m/z 89 ions may have been identified. Using the results of sections 6.3 and 6.4, it was proposed that benzyl acetate, benzyl formate and benzyl alcohol produce the same $C_7H_5^+$ ion, therefore, only benzyl alcohol will be discussed hereafter. However, the results found in Table XI suggest the existence of four different structures since all the results are clearly different from one another.

Table XI- Metastable peaks for $C_7H_5^+$ ions ($T_{0.5}$ values (±2 meV) are in brackets).

PRECURSOR	m/z 88	m/z 87	m/z 63
Benzyl Alcohol	100 (22)	<1	28 (39)
2-bromocyclopropabenzene	20 (22)	3	100 (37)
1,6-heptadiyne	100 (13)	22 (260)	70 (32)
1,5-decadiyne	9 (26)	100 (12)	5 (51)

The CS mass spectra were not sufficiently different to be structure diagnostic (refer to Table XII below).

Table XII- O_2 charge stripping spectra for $C_7H_5^+$ ions.

PRECURSOR	85^{++}	86^{++}	87^{++}	88^{++}	89^{++}
Benzyl Alcohol	5	80	24	30	100
2-bromocyclopropabenzene	2	70	26	24	100
1,6-heptadiyne	5	94	28	31	100
1,5-decadiyne	6	100	54	32	97

Ion structures which should be considered must be those whose ΔH_f values can reasonably be expected to lie within the range 295-315 kcal/mol. The following figure represents some of the possible structures for m/z 89 ions. As mentioned earlier, isotopic labelling of the precursors (especially the hydrocarbons) was considered unlikely to provide any valuable information since a lot of scrambling occurs with hydrocarbons. Therefore, the structure assignment must be made with the information available. Ions capable of resonance structures should be considered first, e.g. the various substituted allyl cations, $C_7H_5^+$, ions 2 to 5 in figure 78.

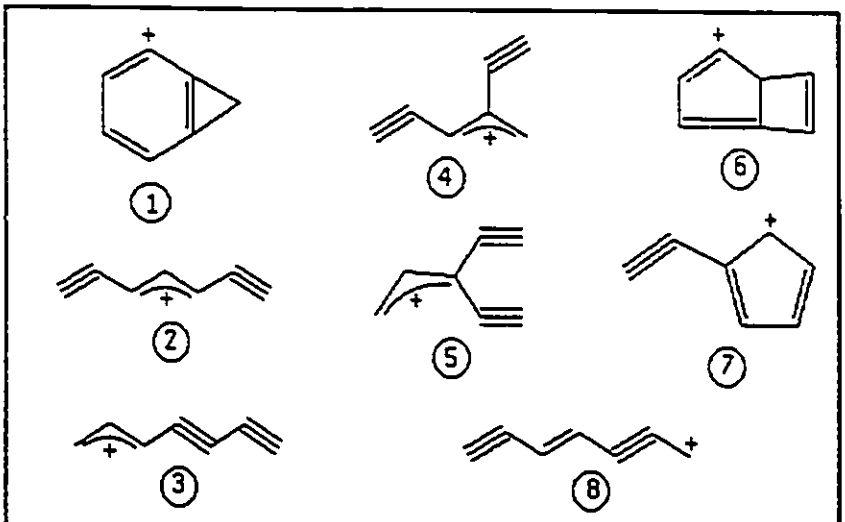

Figure 78- Possible structures for m/z 89 ions.

The difficulty resides in the estimation of ΔH_f(ions). A graphical method developed by Lossing and Holmes[109] can be used to estimate the heats of formation of ions. A ΔH_f(ion) versus log(n) plot can be made (where n is the total number of atoms in the ion) using variously substituted allyl species (Figure 79) ions which will be stabilized by resonance.

The value obtained for ΔH_f(2) is 308 kcal/mol making it a plausible structure for one of the present $C_7H_5^+$ ions. In general, the positional effect of substituents in an allyl ion is very small[2] i.e. whether they are at the same or opposite ends of the allyl cation does not affect the ΔH_f value. In other words, the heats of formation of ions 2 and 5 should be quite similar; the same applies to ethynyl substitution at the middle of the allyl ion (as in ion 4).

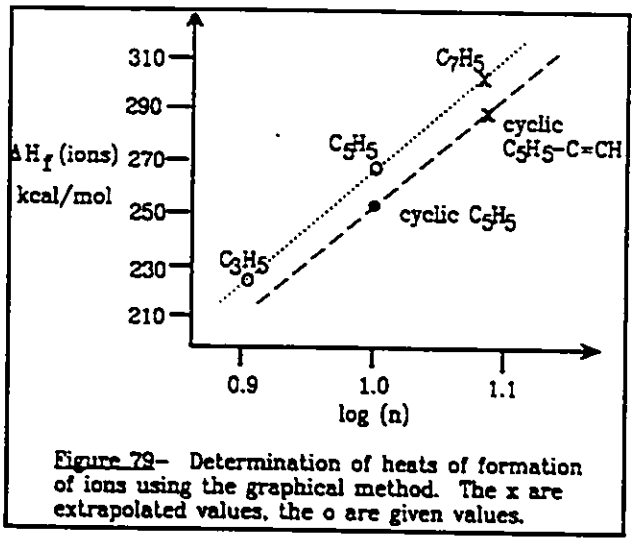

Figure 79– Determination of heats of formation of ions using the graphical method. The x are extrapolated values, the o are given values.

Ions 3 and 8 can also be written as resonance species, however the ΔH_f values are difficult to estimate. They are considered as substituted allene and propargyl ions (which have higher heats of formation than the allyl ion) and, therefore are unlikely to have a ΔH_f value lower than ions 2, 4, and 5.

Ion 6 is subject to ring strain in the cyclobutene moiety making its ΔH_f certainly larger than aliphatic ions. The ΔH_f of ion 7 can also be estimated using the graphical method; a value

$\Delta H_f(7)$=292 kcal/mol was obtained.

Supposing that 2-bromocyclopropabenzene dissociates into a bromine atom and cyclopropaphenyl ion (**1**), and using the measured AE values (10.15 and 10.5 eV), $\Delta H_f(C_7H_5^+)$ is estimated to be 301-313 kcal/mol.

$$AE = \Delta H_f(C_7H_5^+) + \Delta H_f(Br^\cdot) - \Delta H_f(C_7H_5Br) \qquad [35]$$

$$\Delta H_f(C_7H_5^+) = 301 \text{ (AE=10.15 eV) or } 313 \text{ kcal/mol (AE=10.5 eV)}$$

Table XIII- Estimated ΔH_f values and heterolytic bond dissociation energies (HBDE) for ions **1, 2, 4, 5, 7.**

ION	ΔH_f(ion) kcal/mol	ΔH_f(neutral) kcal/mol ± 2 kcal/mol	HBDE kcal/mol ± 2 kcal/mol
1	301-313	89	247-259
2	308	120	222
4	<308	120	222
5	308	120	222
7	292	90	237

In terms of heterolytic bond dissociation energies, ions **1, 2, 4, 5, 7** can be considered to be quite stable species.

6.5.1 2-bromocyclopropabenzene

Structure 1 of the previous figure may be assigned to the m/z 89 ion from the bromo compound since it would be formed by a simple bond cleavage between the bromine atom and the ring (Figure 80).

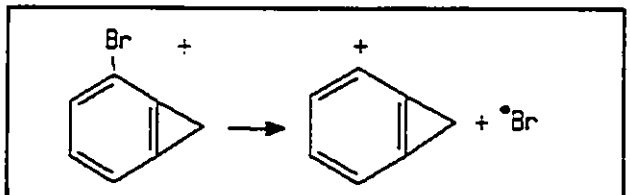

Figure 80- Formation of m/z 89 ion from 2-bromo cyclopropabenzene.

The CA mass spectrum showing very little fragmentation upon introduction of gas indicating that this structure does not fragment easily. The aromaticity of the ion makes it quite difficult to lose only one hydrogen. The loss of C_2H_2 is the major metastable process occurring from this ion, and it appears to be unique among the ions studied in terms of the relative abundance of peaks in the MI mass spectrum (Table XI).

6.5.2 1,6-heptadiyne

The next ion which can be "easily" identified by its heat of formation and fragmentation characteristics is that from 1,6-heptadiyne, where consecutive loss of H_2 and H˙ or of 3 H˙ would lead directly to structure 2.

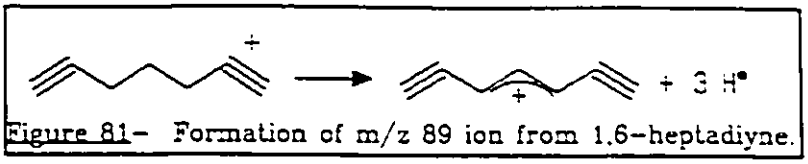

Figure 81- Formation of m/z 89 ion from 1,6-heptadiyne.

If these hydrogen losses occur so easily, it may explain why the most intense process for metastable m/z 89 from 1,6-heptadiyne is loss of H. Furthermore, the loss of H_2 or 2 H• to produced m/z 87 can also be explained with this structure. The loss of C_2H_2 could also take place via a simple bond cleavage followed by a H transfer.

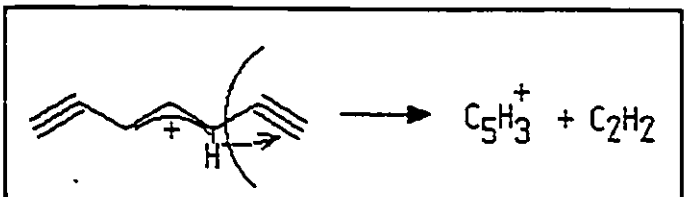

Figure 82- Dissociation of m/z 89 ion from 1,6-heptadiyne.

6.5.3 1,5-decadiyne

For the m/z 89 ion from 1,5-decadiyne, structure 8 can be proposed since it already contains two triple bonds separated by three single bonds. To obtain that structure from 1,5-decadiyne, a bond cleavage followed by two H losses is required. The loss of H_2 can occur easily from the CH_2 site. The loss of C_2H_2 does not take place so easily either because it would involve appreciable rearrangement of structure 8.

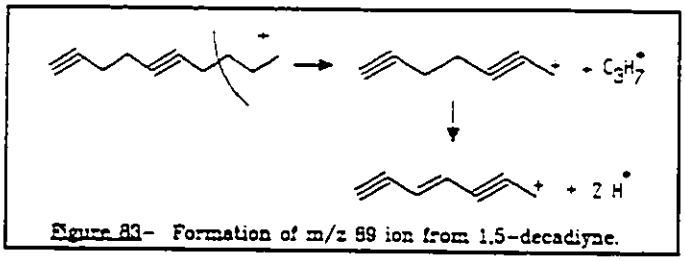

Figure 83- Formation of m/z 89 ion from 1,5-decadiyne.

6.5.4 Benzyl Alcohol

The structure of the m/z 89 ion from this compound is the most difficult one to assign. Structure 4 is quite plausible, its formation could involve a ring opening followed by a H transfer. The terminal H may be easily lost and that is why m/z 88 is the most metastable process. The loss of C_2H_2 is not so intense because it again involves a rearrangement. Furthermore, the structure can yield a $CH_3^{\bullet}$ fragment by a simple H transfer confirming the hypothesis made from the He CA results.

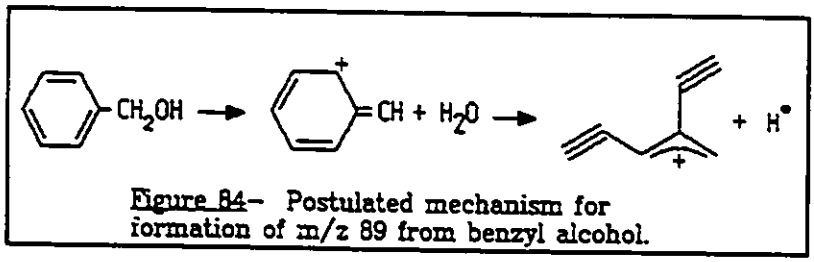

Figure 84- Postulated mechanism for formation of m/z 89 from benzyl alcohol.

6.5.5 Summary

1. At least three different $C_7H_5^+$ ions were identified using thermochemistry and dissociation characteristics.

2. However, the available information does not allow one to make unequivocal structure assignments. Nevertheless, there is no evidence to suggest that the cyclopropaphenyl ion does not exist as a stable species in the gas phase.

3. We were not able to explain in detail explicitly the behaviour of these ions but it was possible to determine what does not happen i.e. the ions do not interconvert because of their specific characteristics.

Historically, attempts to identify aromatic ions using isotopic labelling failed because of major atom scrambling. Indeed, benzyl and tropyl ions can only be identified from minor peaks in their CA mass spectra.

6.6 Experimental

6.6.1 Experiments

Electron Ionization (EI), Metastable Ion (MI), Collision Induced Dissociation (CA), Collision Induced Dissociative Ionization (CIDI) and Charge Stripping (CS) mass spectra were recorded using a VG Analytical ZAB-2F mass spectrometer, modified as described elsewhere. In all experiments, collision gas pressures (He or O_2) were adjusted such that the main ion beam's intensity was reduced by no more than 10%, i.e. essentially single collision conditions. Except when kinetic energy releases were being determined, all energy slits were wide open to

avoid instrument discrimination effects.

Metastable peak AE values and first field free metastable abundance ratios were measured using the AEI MS-902S mass spectrometer described in chapter 2 of this thesis. The AE of the various compounds were obtained via comparison with the reference metastable loss of methyl from diethyl ether.

Ionization Energy (IE) and other Appearance Energy (AE) values were measured with energy-selected electrons using an apparatus comprising an electrostatic electron monochromator with mini-computer data system[12].

6.6.2 Chemicals

The 2-bromocyclopropabenzene was synthesized according to the method described in reference [11]. Benzyl acetate was synthesized by refluxing benzyl alcohol with an excess of acetic anhydride in pyridine for 4 hours. Benzyl formate was made by refluxing benzyl bromide in an excess of formic acid in DMF for 4 hours. Benzyl alcohol, 1,5-decadiyne and 1,6-heptadiyne were of research grade and obtained by Aldrich Chemical Co.

APPENDIX I

MASS SPECTRA - CHAPTER 5

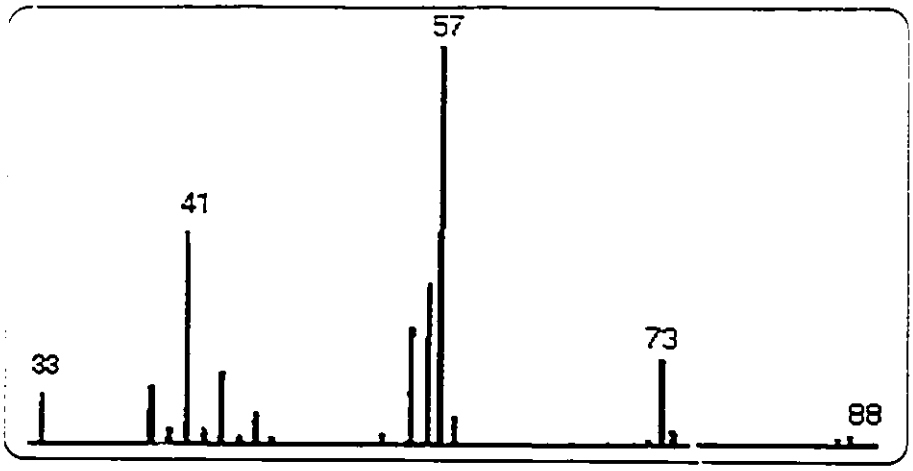

S1- Electron Impact mass spectrum of neopentanol.

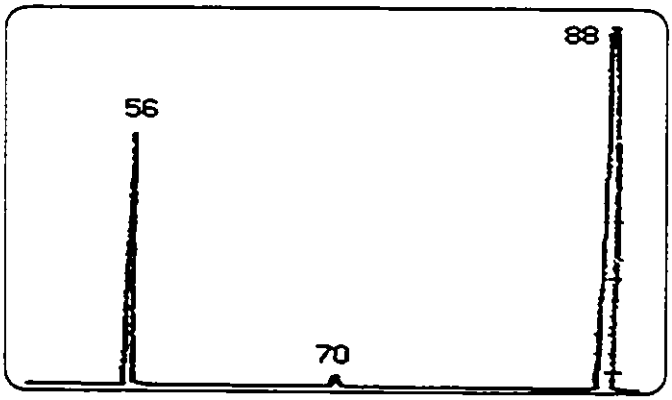

S2- MI mass spectrum of m/z 88 from neopentanol.

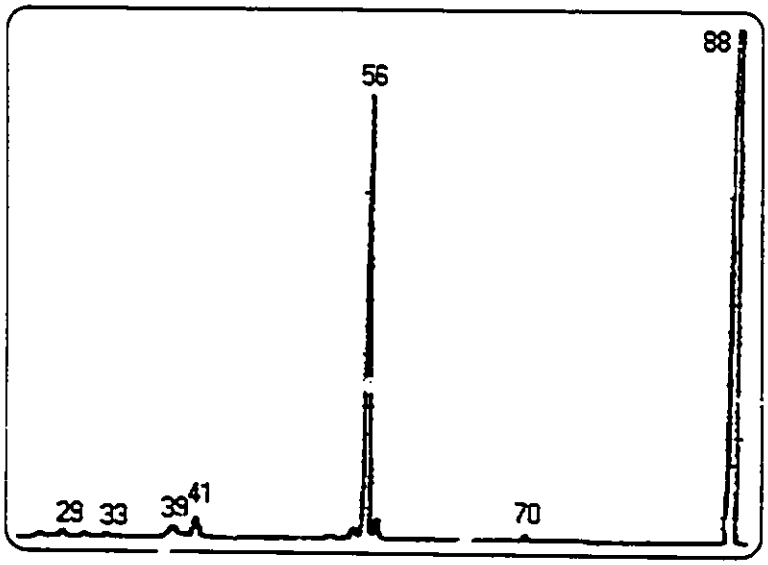

S3- He CA mass spectrum of m/z 88 from neopentanol.

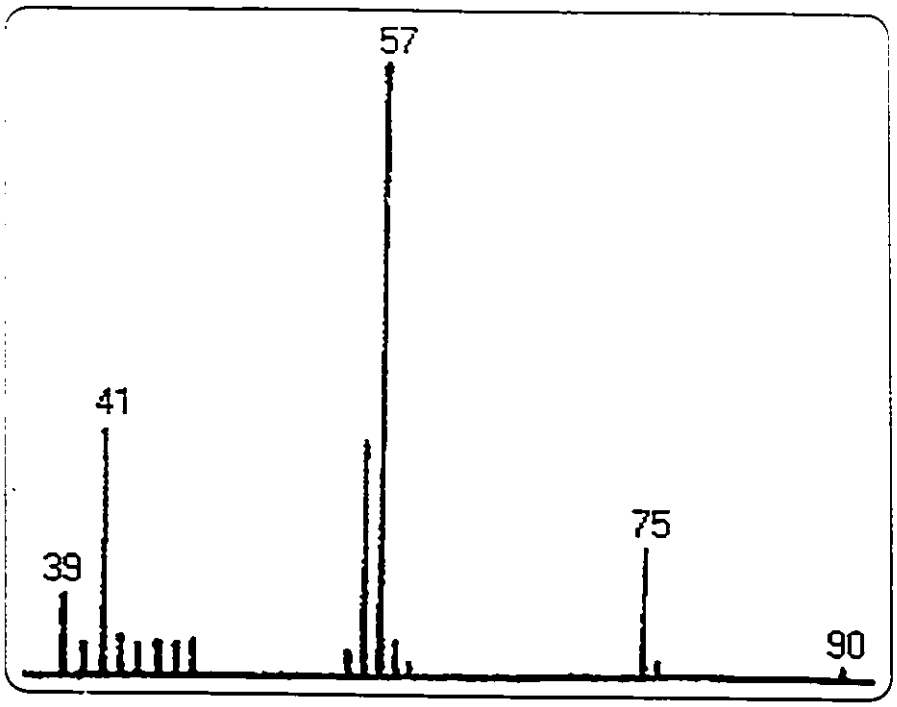

S4- Electron Impact mass spectrum of CD2-neopentanol.

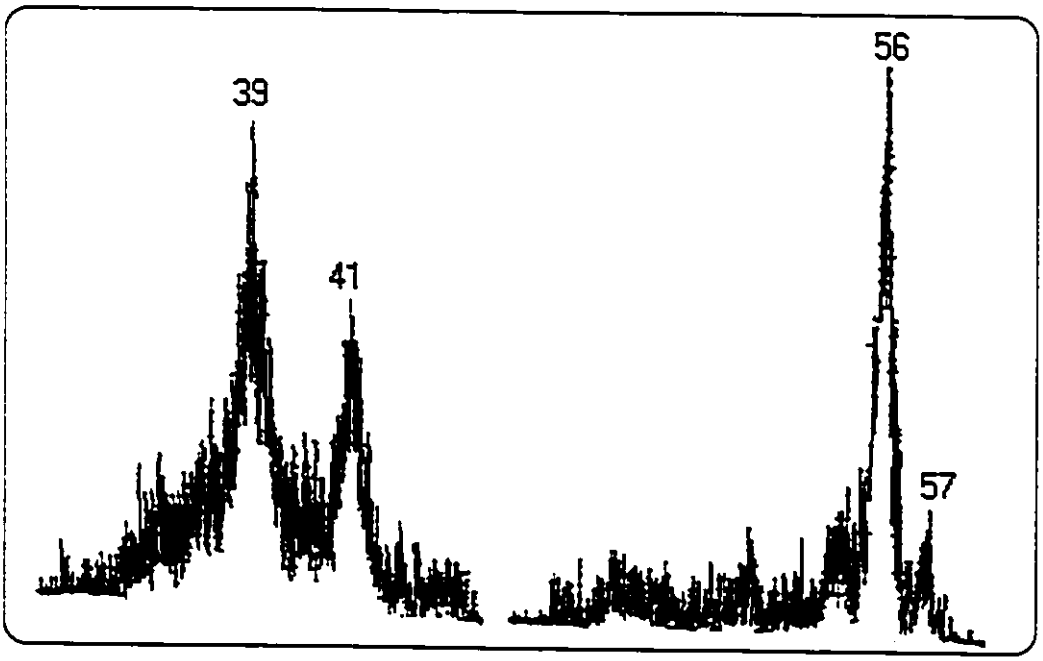

S5- NR mass spectrum of m/z 88 from neopentanol.

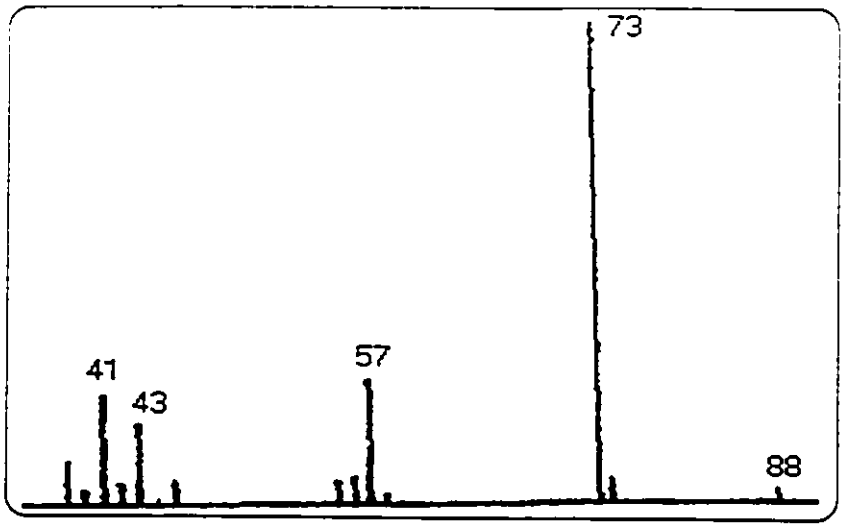

S6- Electron Impact mass spectrum of methyl-t-butyl ether.

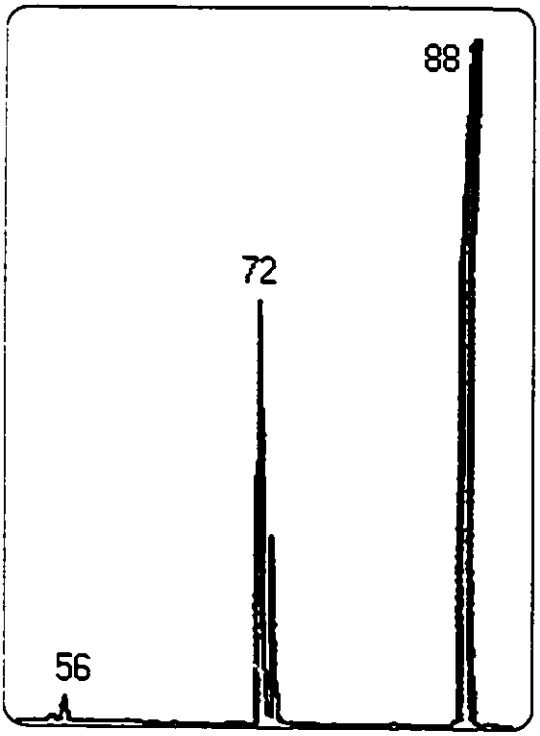

S7- MI mass spectrum of m/z 88 from methyl-t-butyl ether.

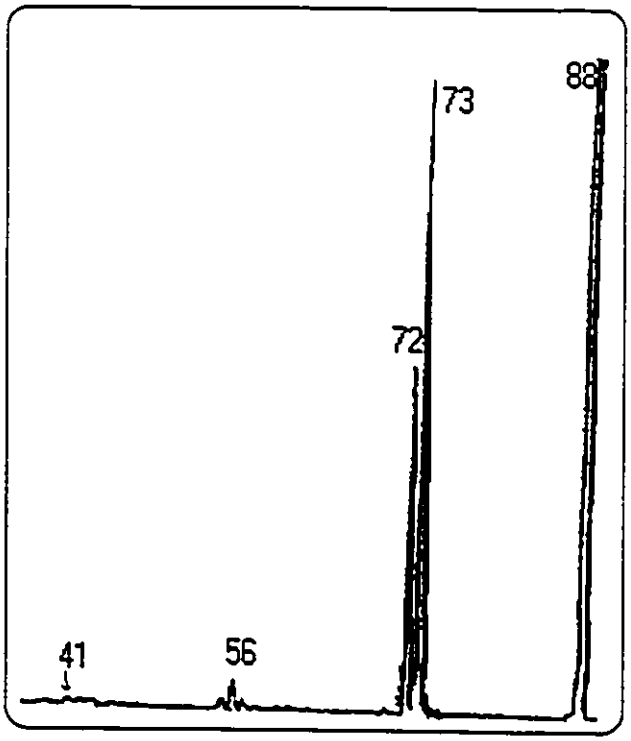

S8- He CA mass spectrum of m/z 88 from methyl-t-butyl ether.

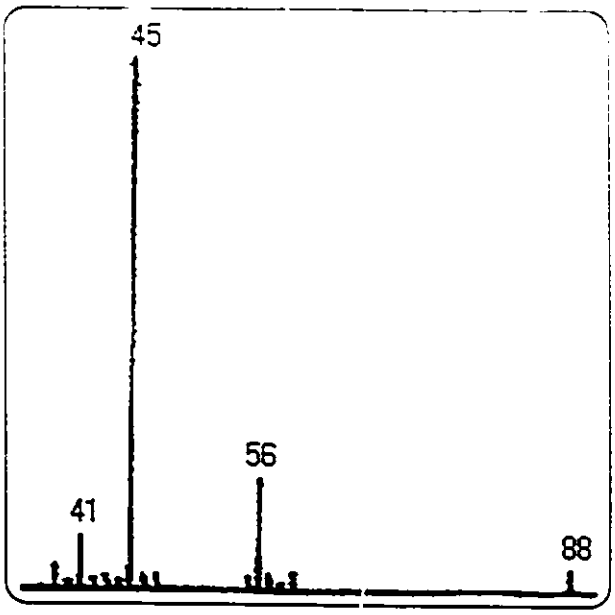

S9- Electron Impact mass spectrum of methyl-n-butyl ether.

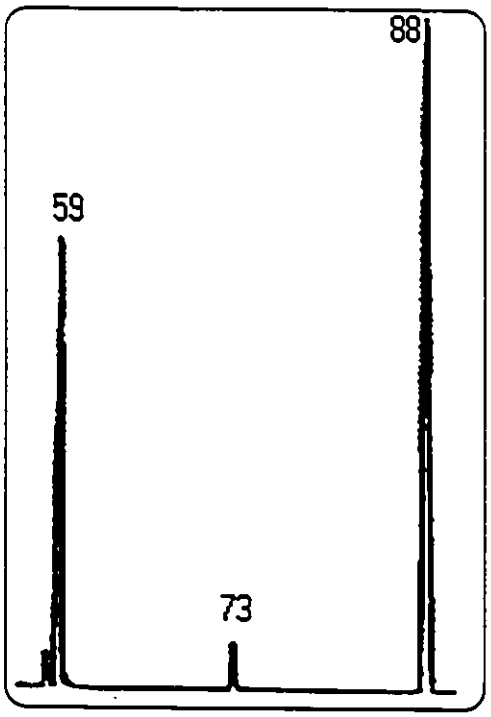

S10- MI mass spectrum of m/z 88 from methyl-n-butyl ether.

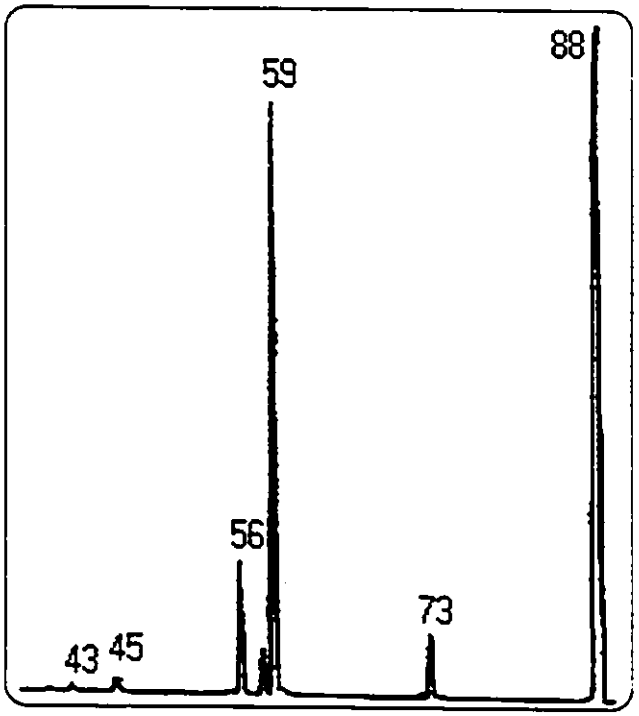

S11- He CA mass spectrum of m/z 88 from methyl-n-butyl ether.

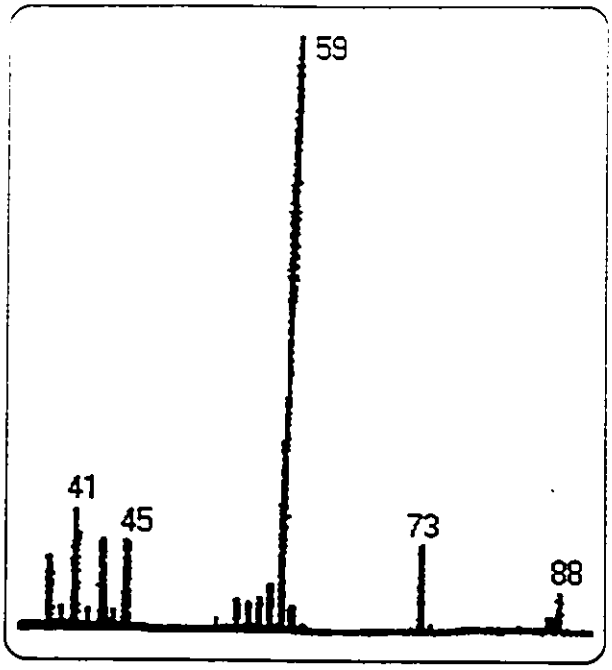

S12- Electron Impact mass spectrum of 2-methoxy butane.

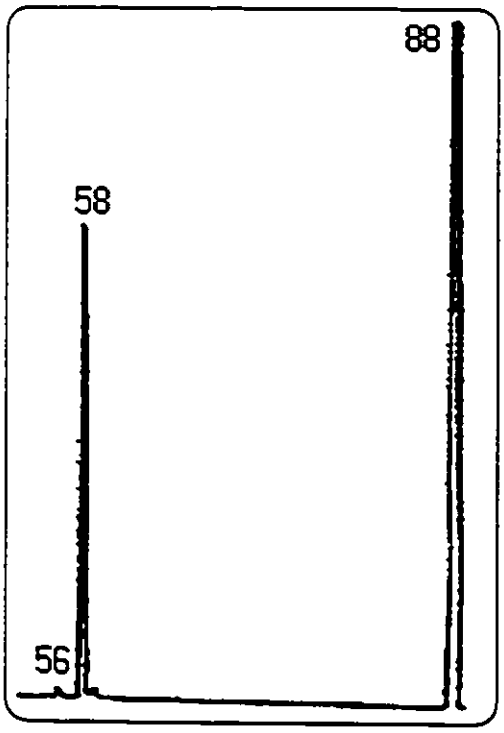

S13- MI mass spectrum of m/z 88 from 2-methoxy butane.

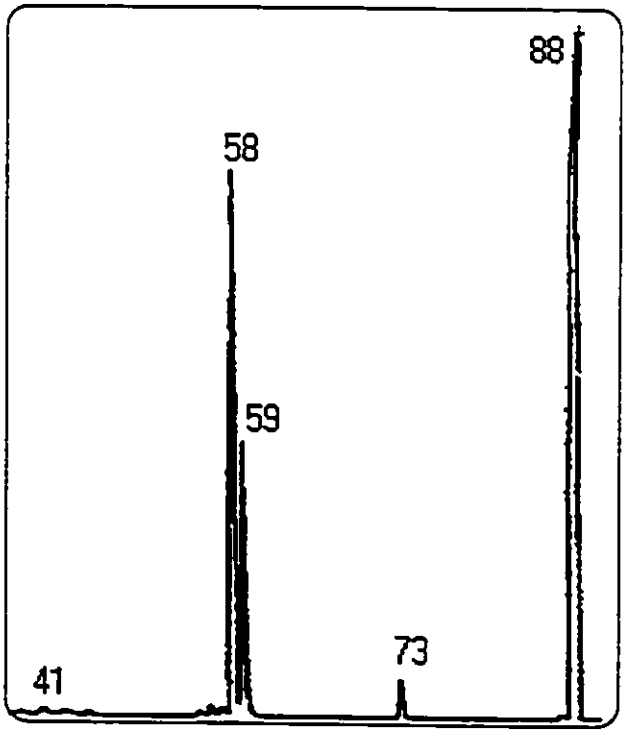

S14- He CA mass spectrum of m/z 88 from 2-methoxy butane.

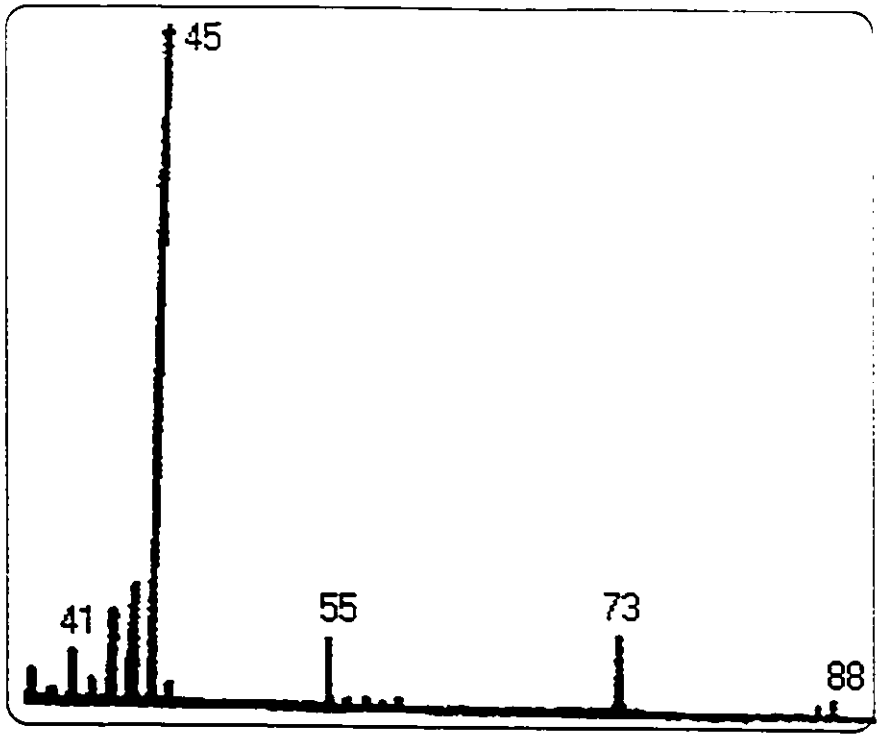

S15- Electron Impact mass spectrum of 3-methyl-2-butanol.

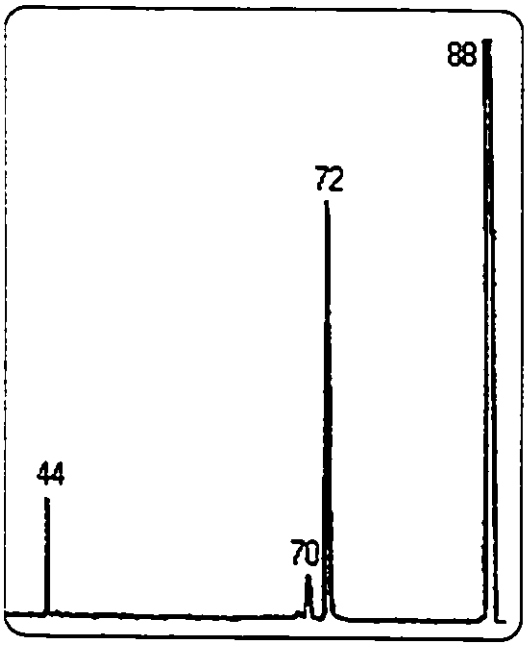

S16- MI mass spectrum of m/z 88 from 3-methyl-2-butanol.

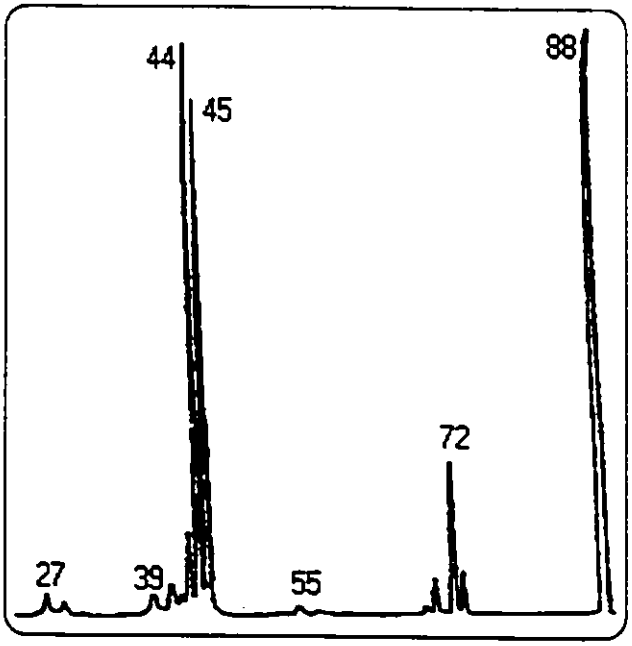

S17- He CA mass spectrum of m/z 88 from 3-methyl-2-butanol.

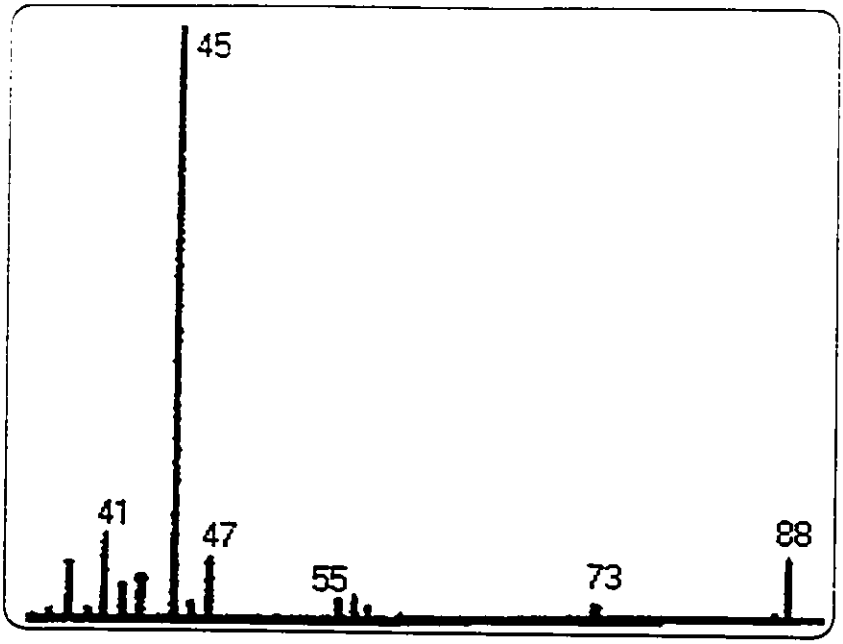

S18- Electron Impact mass spectrum of methyl isobutyl ether.

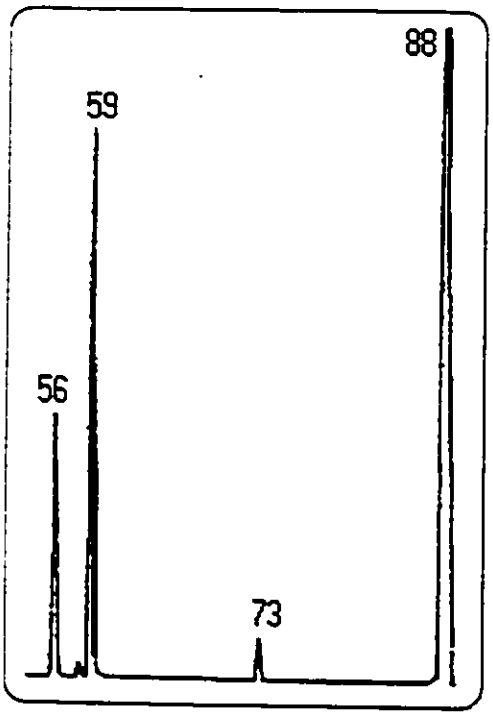

S19- MI mass spectrum of m/z 88 from methyl isobutyl ether.

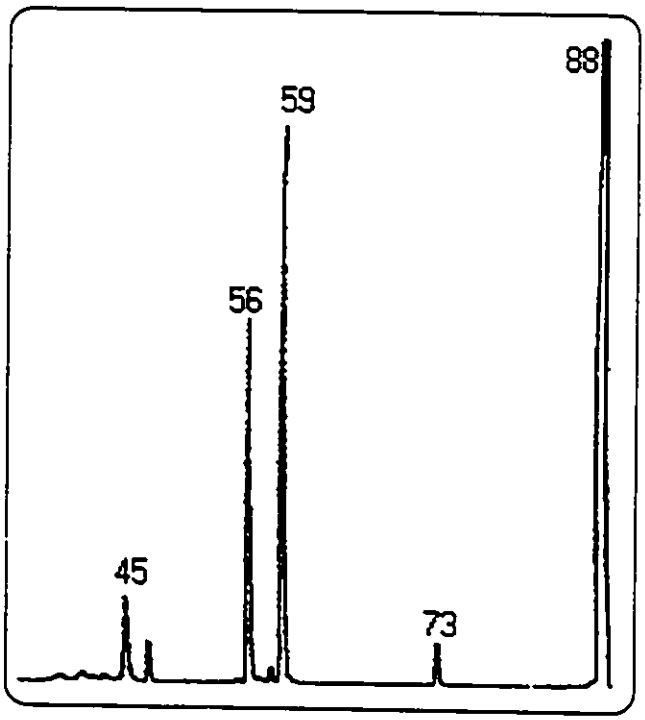

S20- He CA mass spectrum of m/z 88 from methyl isobutyl ether.

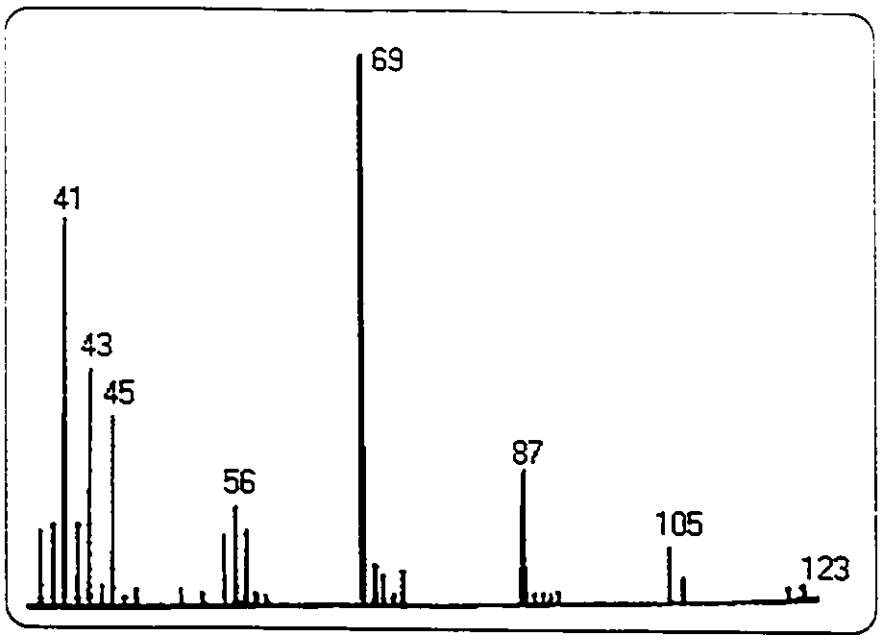

S21- Electron Impact mass spectrum of 3-chloro-2,2-dimethyl propan-1-ol.

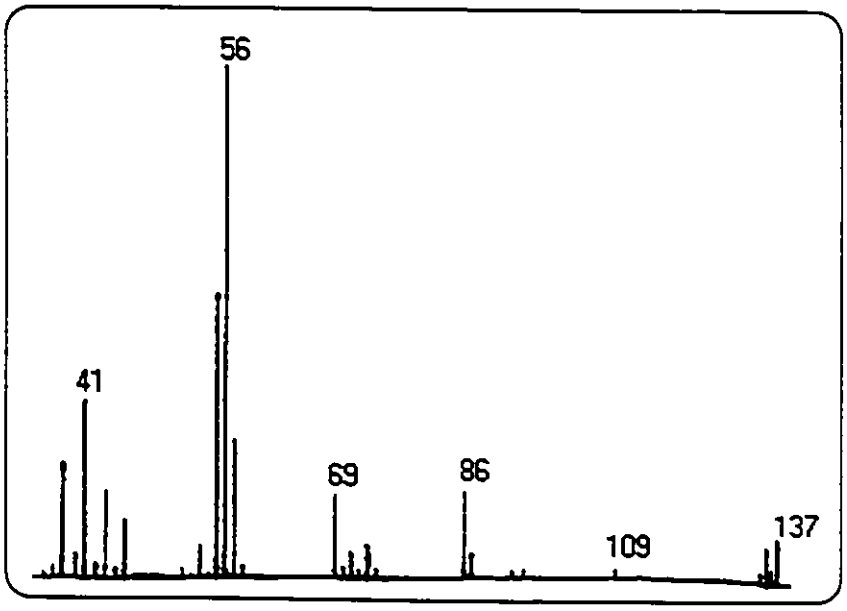

S22- Electron Impact mass spectrum of 3-bromo-2,2-dimethyl propan-1-ol.

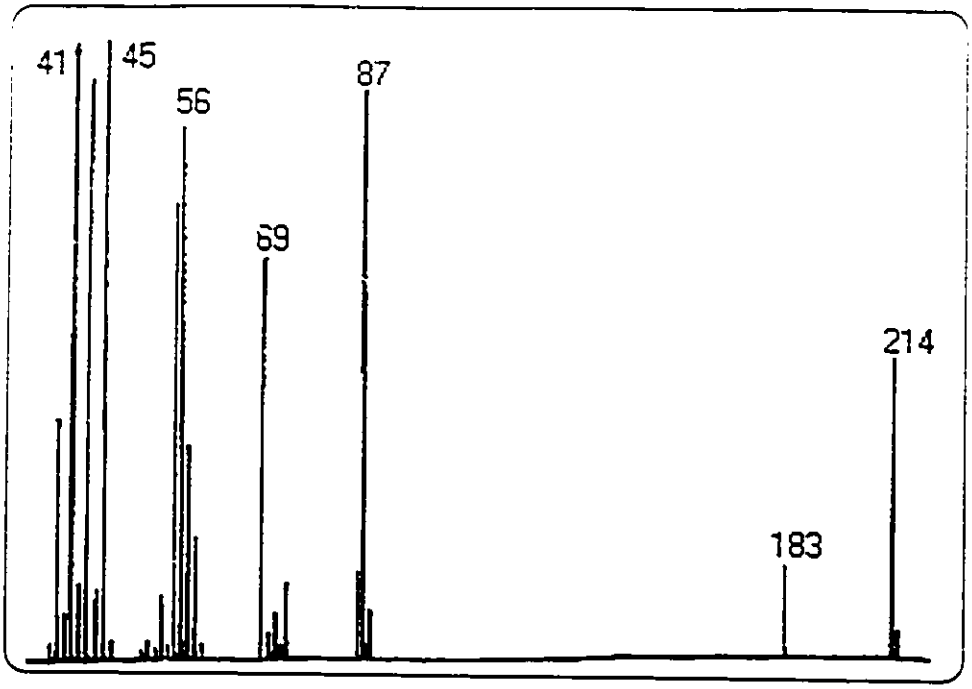

S23- EI mass spectrum of 3-iodo-2,2-dimethyl propan-1-ol.

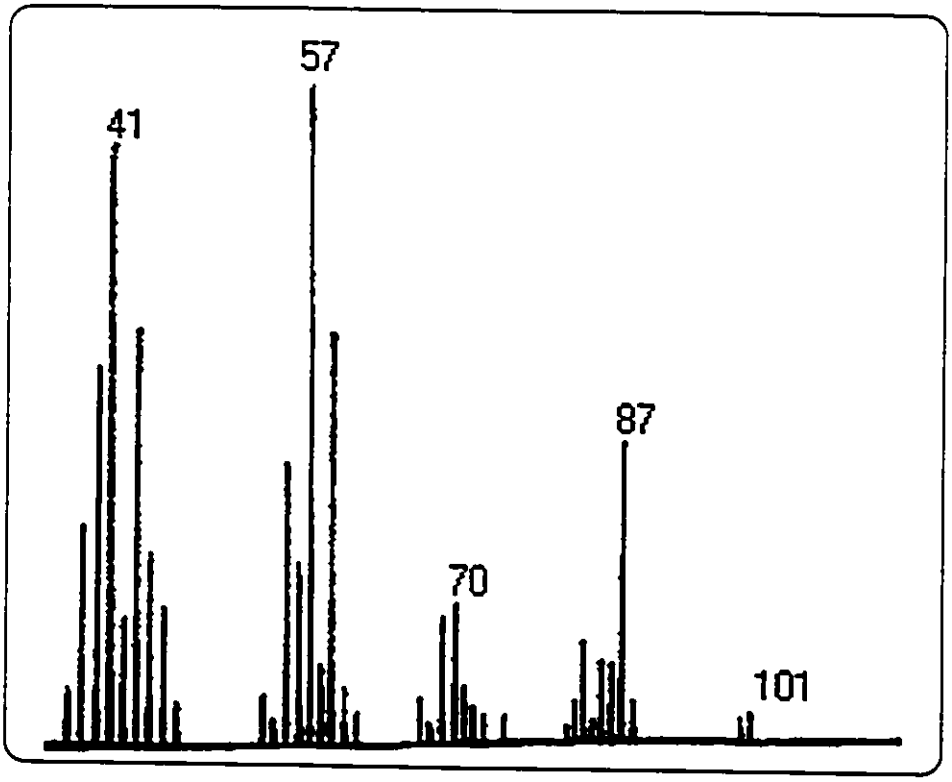

S24- EI mass spectrum of 3,3-dimethyl butan-1,2-diol.

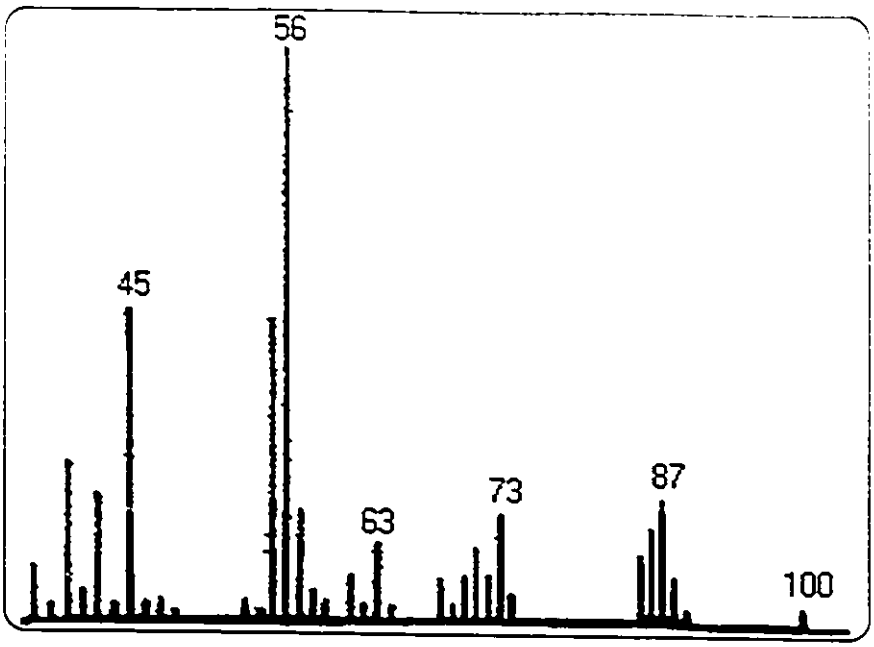

S25– EI mass spectrum of 3–methoxy–2,2–dimethyl propanol.

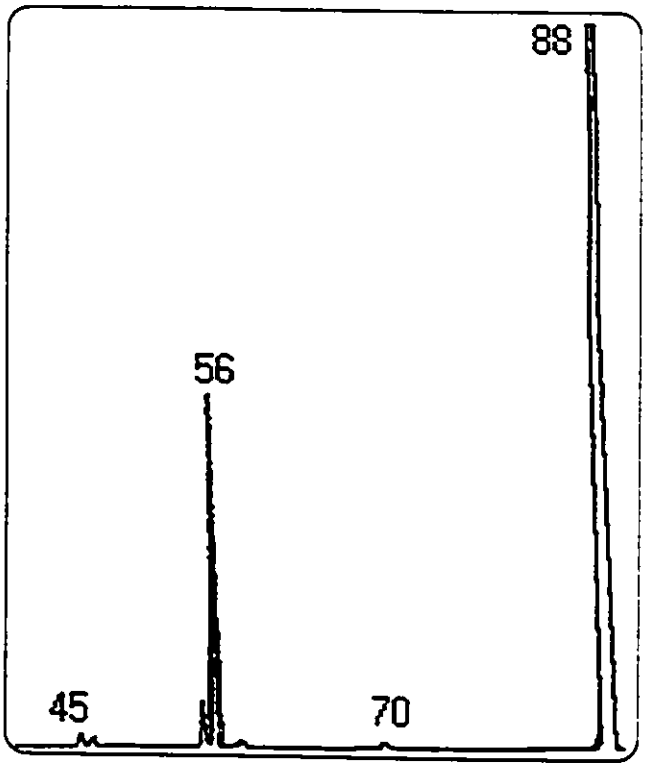

S26– MI mass spectrum of m/z 88
from 3–methoxy–2,2–dimethyl propanol.

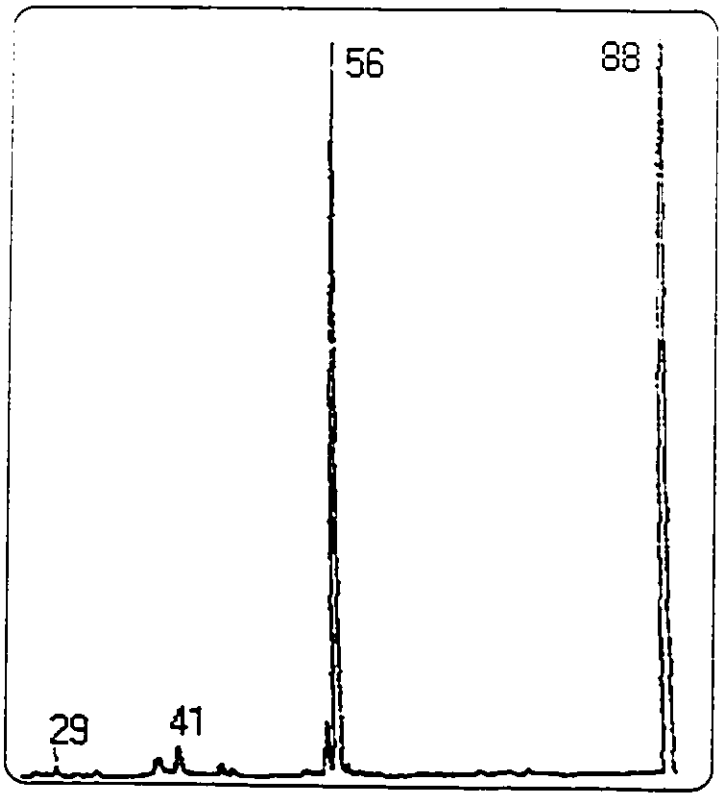

S27- He CA mass spectrum of m/z 88 from 3-methoxy-2,2-dimethyl propanol.

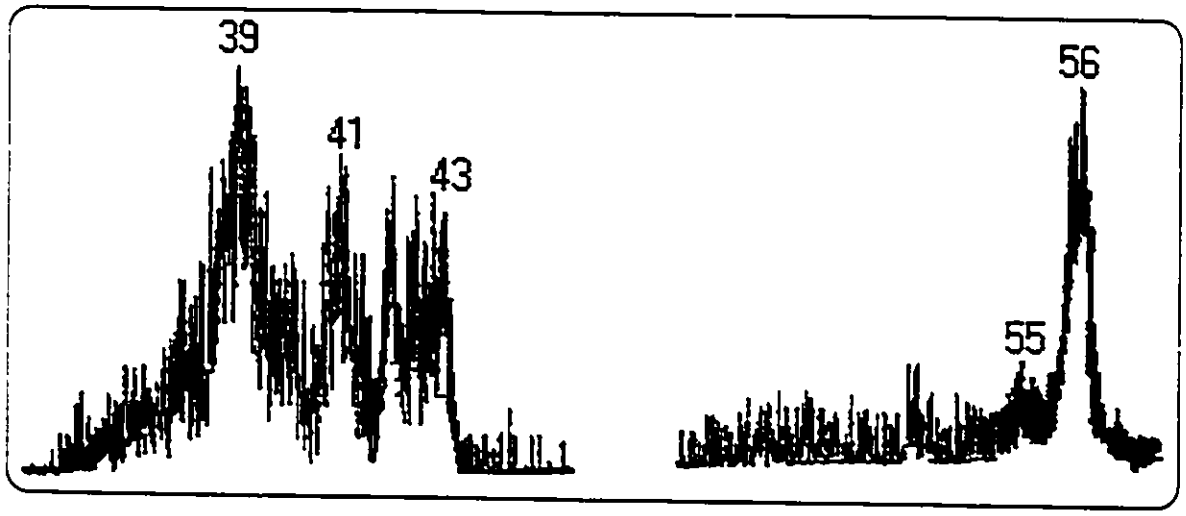

S28- NR mass spectrum of m/z 88 from 3-methoxy-2,2-dimethyl propanol.

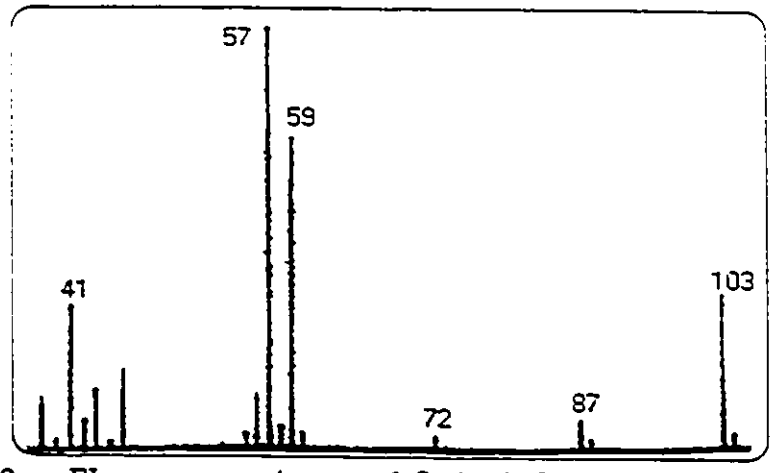

S29- EI mass spectrum of 2-tert-butoxyethanol.

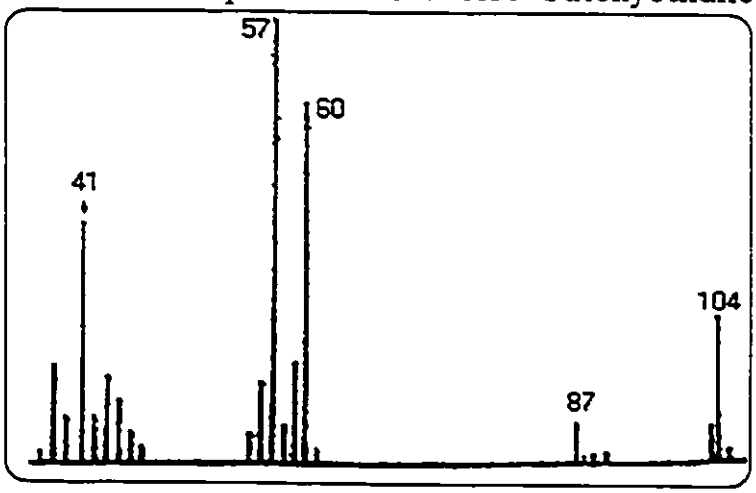

S30- EI mass spectrum of OD 2-tert-butoxyethanol.

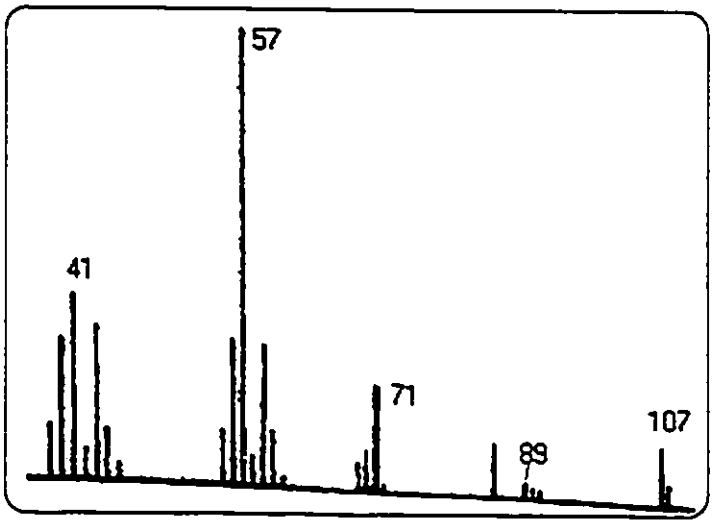

S31- EI mass spectrum of CD2CD2 2-tert-butoxyethanol.

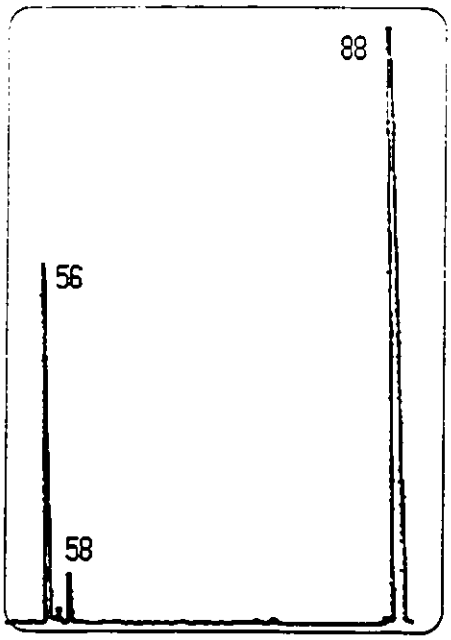

S32- Mi mass spectrum of m/z 88 from 2-tert-butoxyethanol.

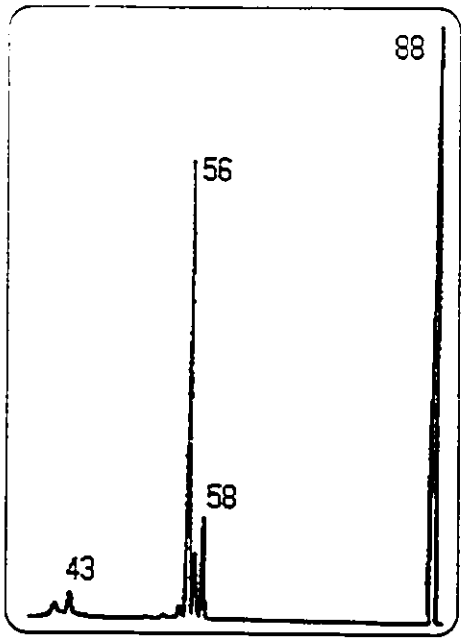

S33- He CA mass spectrum of m/z 88 from 2-tert-butoxyethanol.

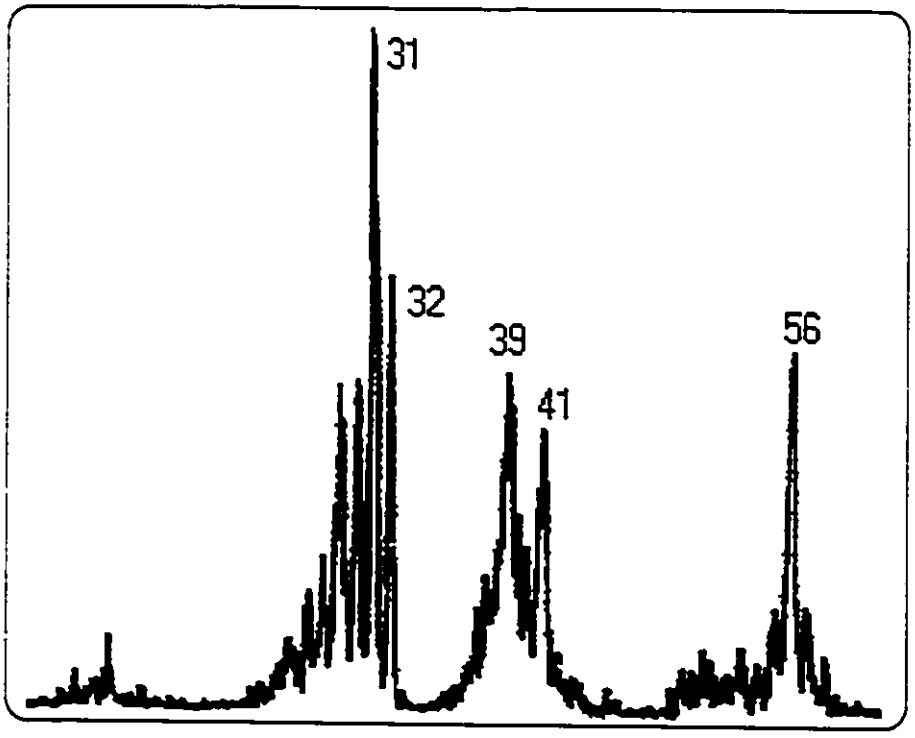

S34- NR mass spectrum of m/z 88 from 2-tert-butoxyethanol.

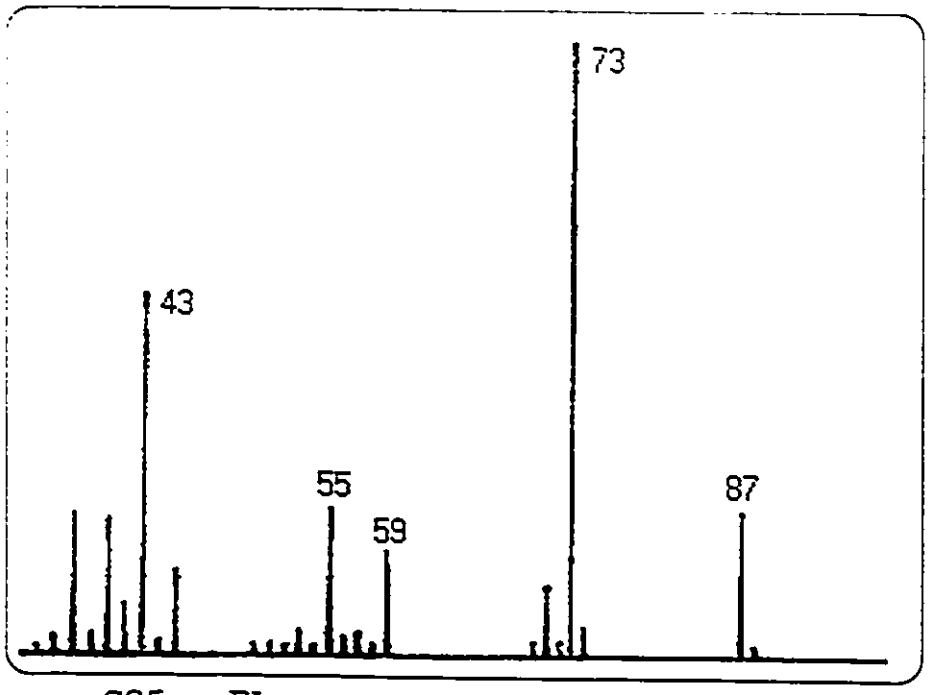

S35- EI mass spectrum of
1-methoxy-1,1-dimethyl propanol.

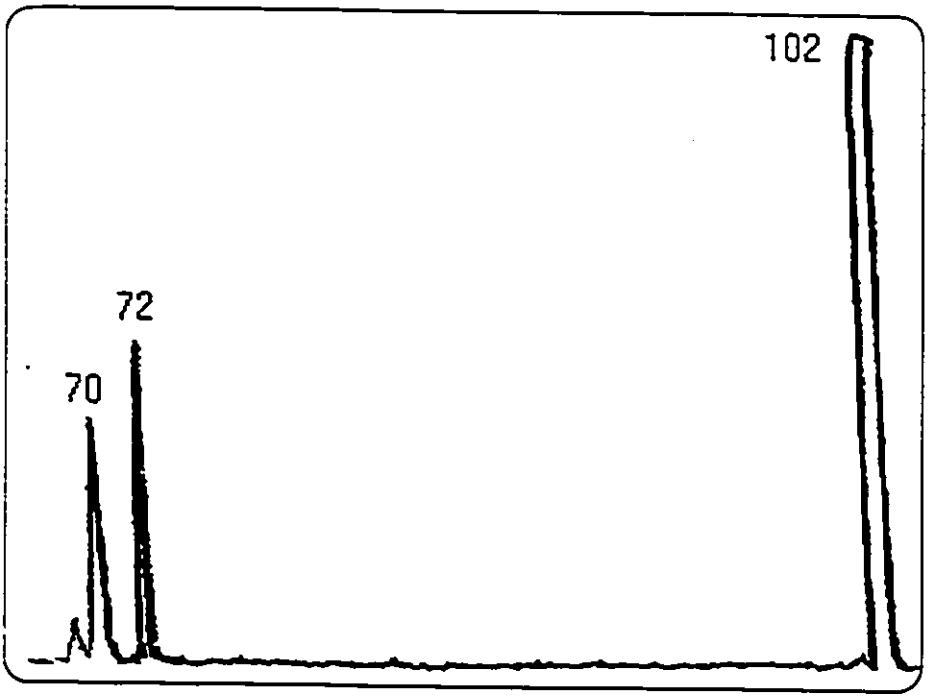

S36- MI mass spectrum of m/z 88 from
1-methoxy-1,1-dimethyl propanol.

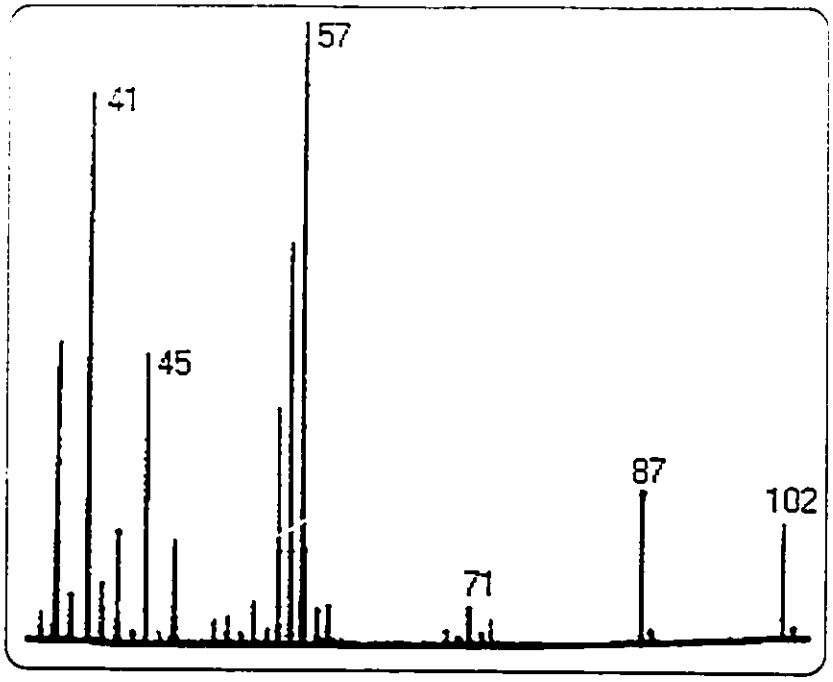

S37- EI mass spectrum of neopentyl methyl ether.

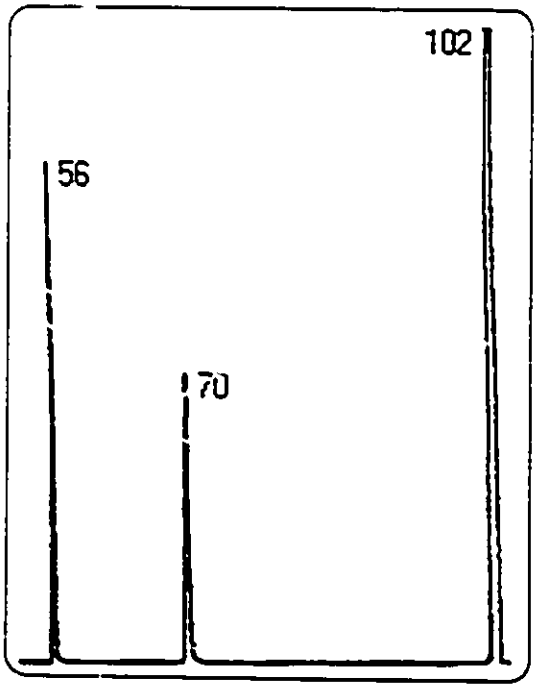

S38- MI mass spectrum of m/z 102 from neopentyl methyl ether.

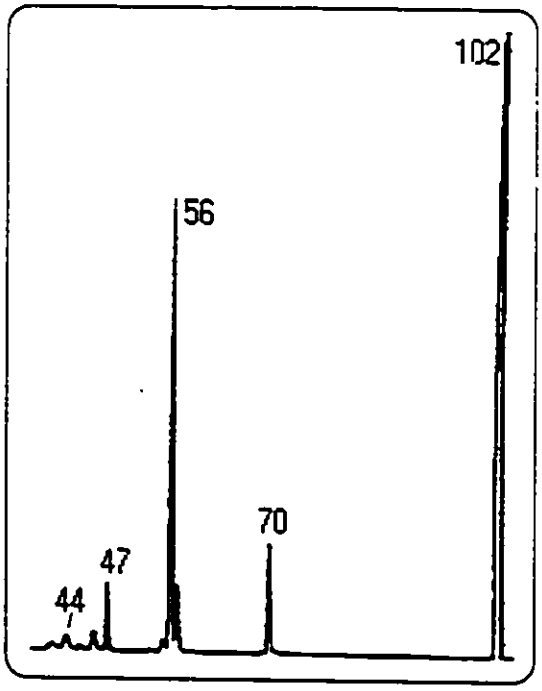

S39- He CA mass spectrum of m/z 102 from neopentyl methyl ether.

APPENDIX II

MASS SPECTRA - CHAPTER 6

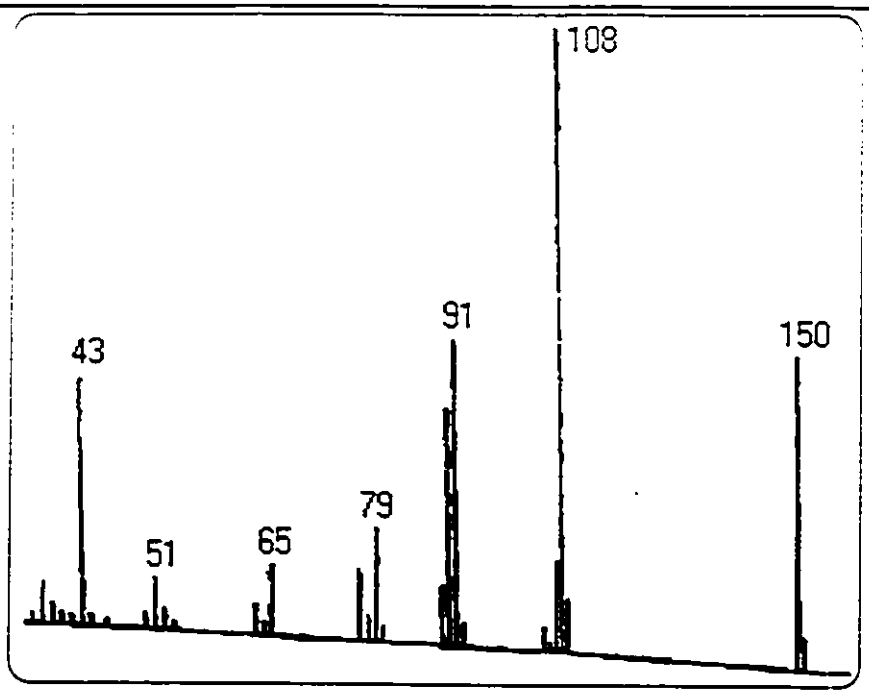

S40- Electron impact mass spectrum of benzyl acetate.

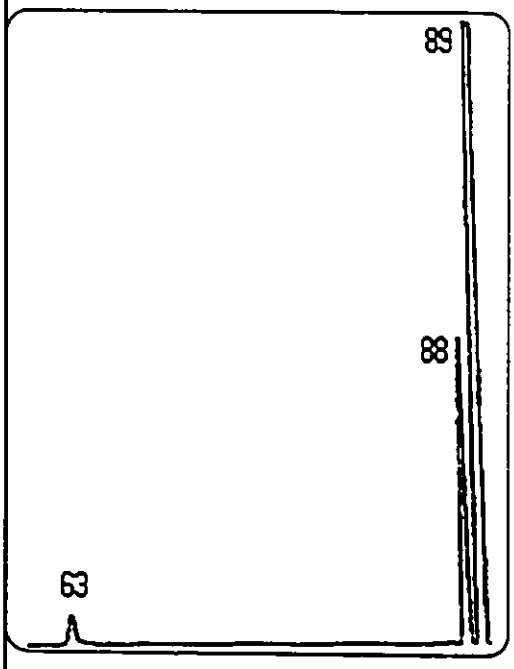

S41- MI mass spectrum of m/z 89 from benzyl acetate.

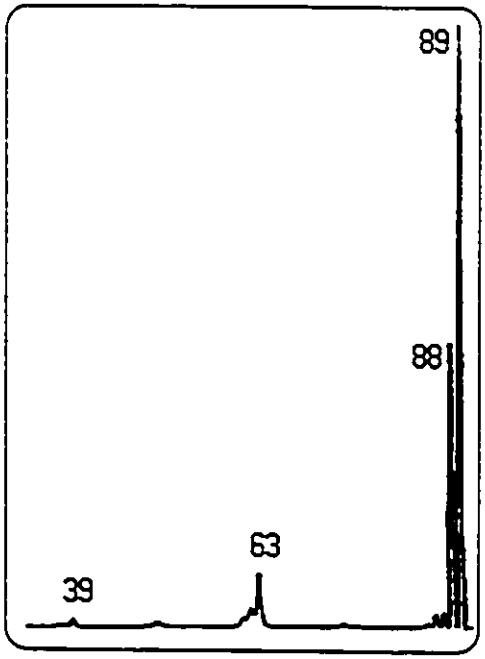

S42- He CA mass spectrum of m/z 89 from benzyl acetate.

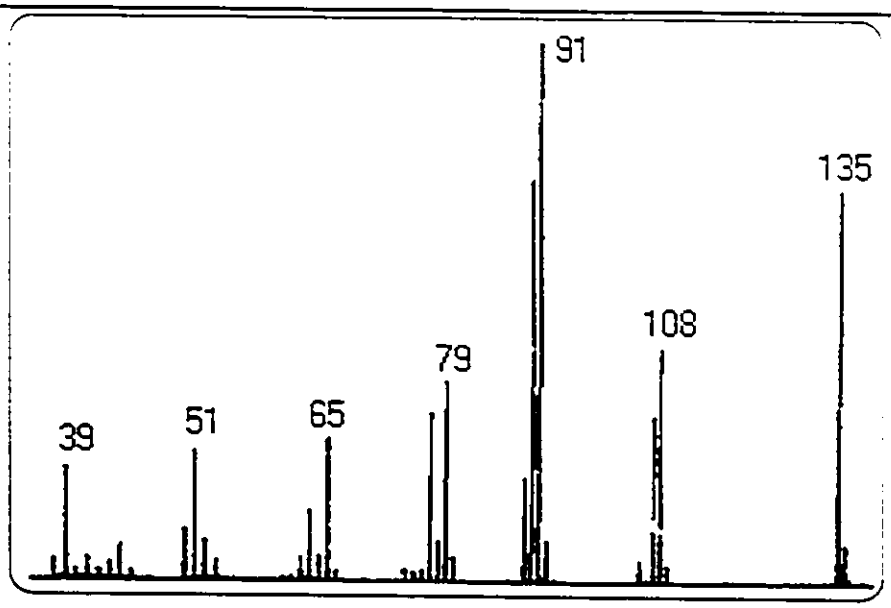

S43- Electron Impact mass spectrum of benzyl formate.

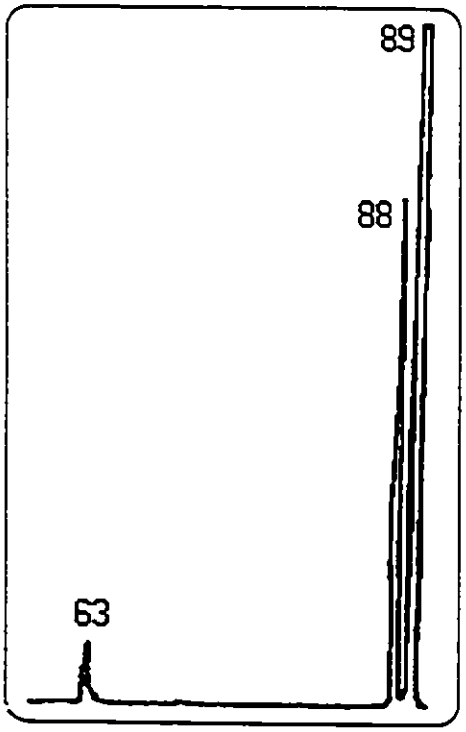

S44- MI mass spectrum of m/z 89 from benzyl formate.

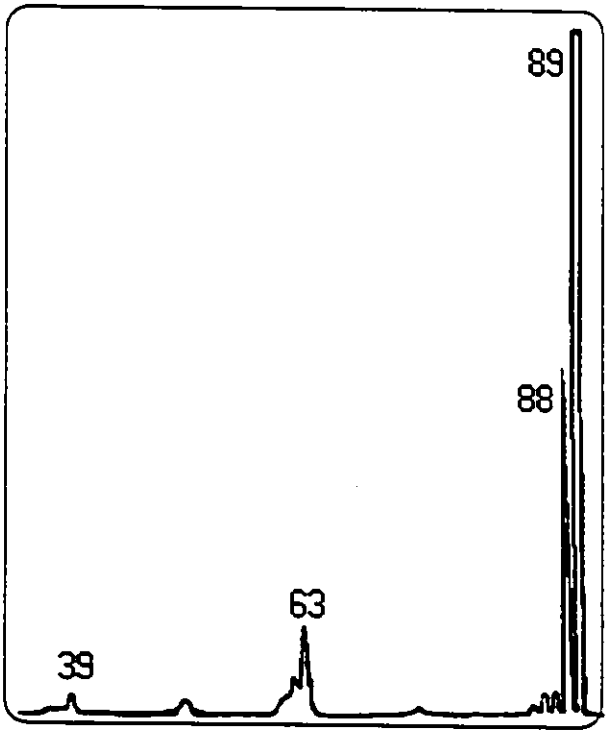

S45- He CA mass spectrum of m/z 89 from benzyl formate.

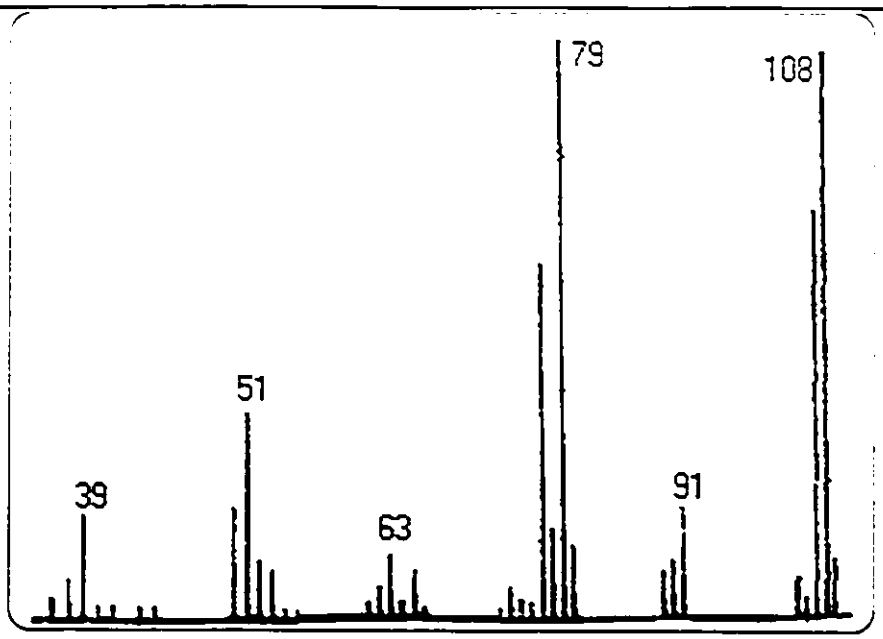

S46- Electron Impact mass spectrum of benzyl alcohol.

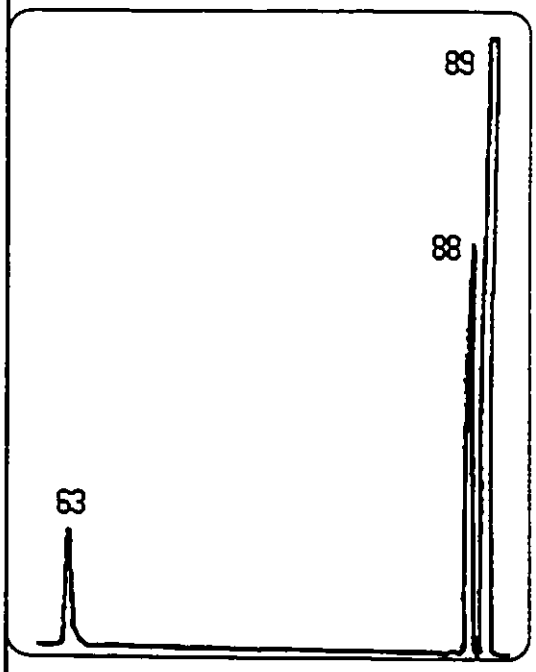

S47- MI mass spectrum of m/z 89 from benzyl alcohol.

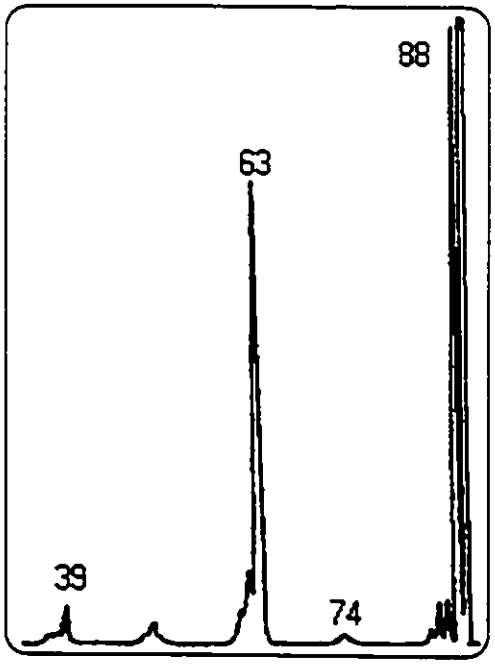

S48- He CA mass spectrum of m/z 89 from benzyl alcohol.

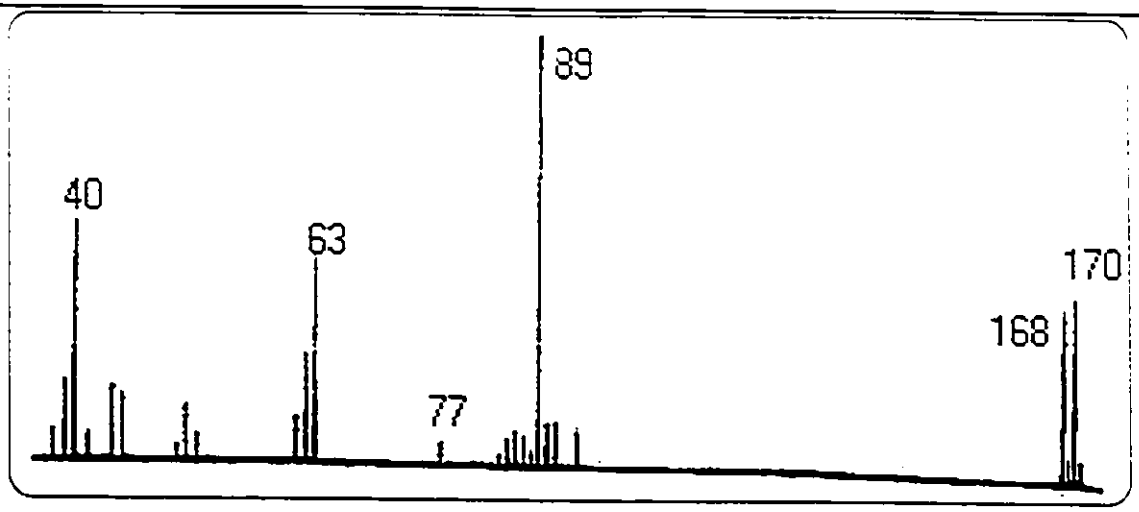

S49- EI mass spectrum of 2-bromocyclopropabenzene.

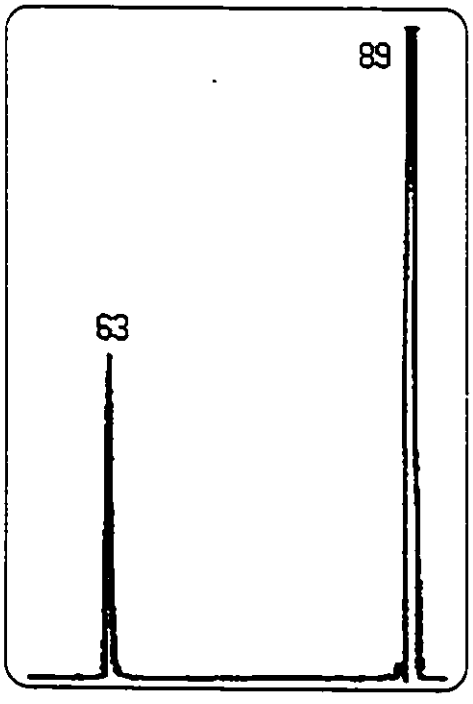

S50- MI mass spectrum of m/z 89 from 2-cyclopropabenzene.

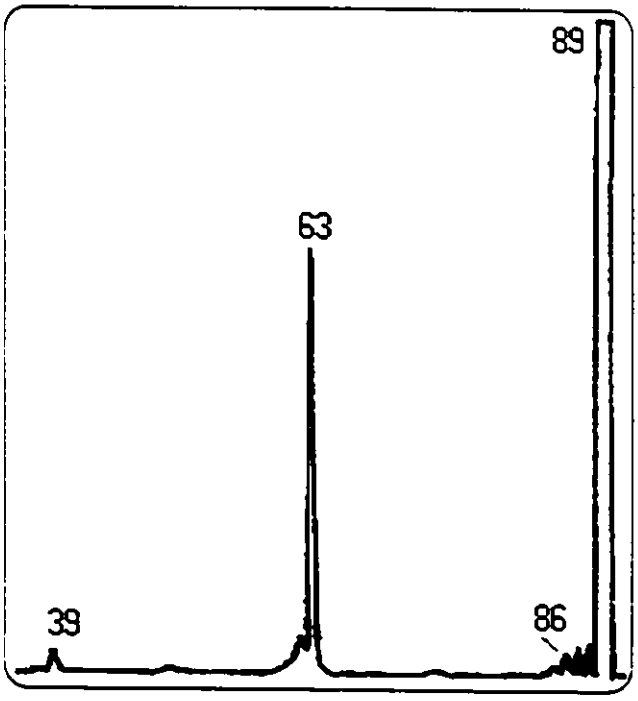

S51- He CA mass spectrum of m/z 89 from 2-cyclopropabenzene.

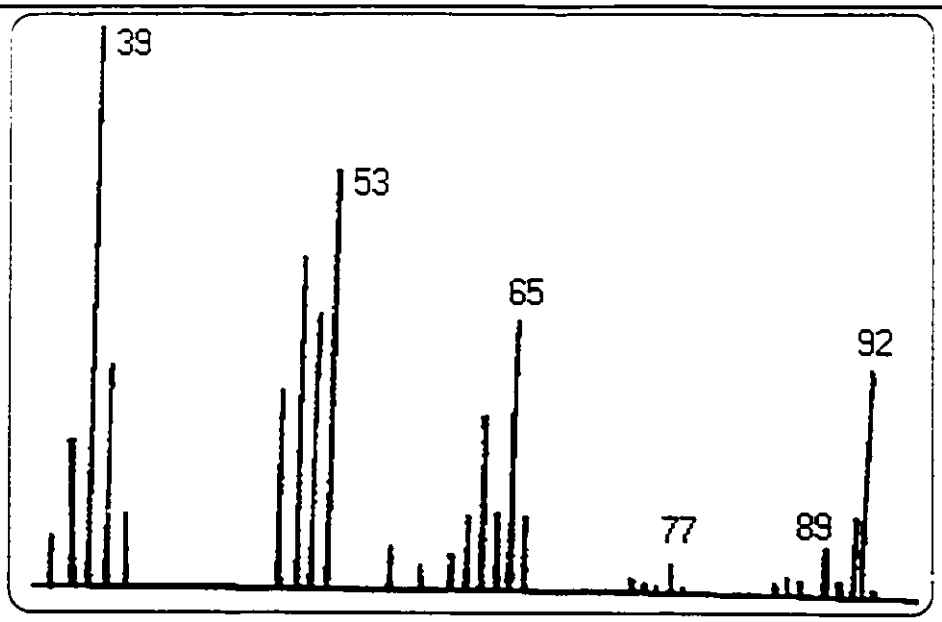

S52- Electron Impact mass spectrum of 1,6-heptadiyne.

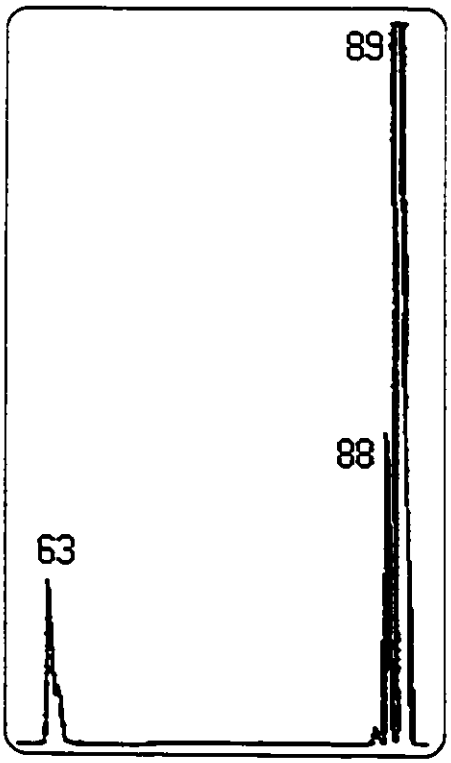

S53- MI mass spectrum of m/z 89 from 1,6-heptadiyne.

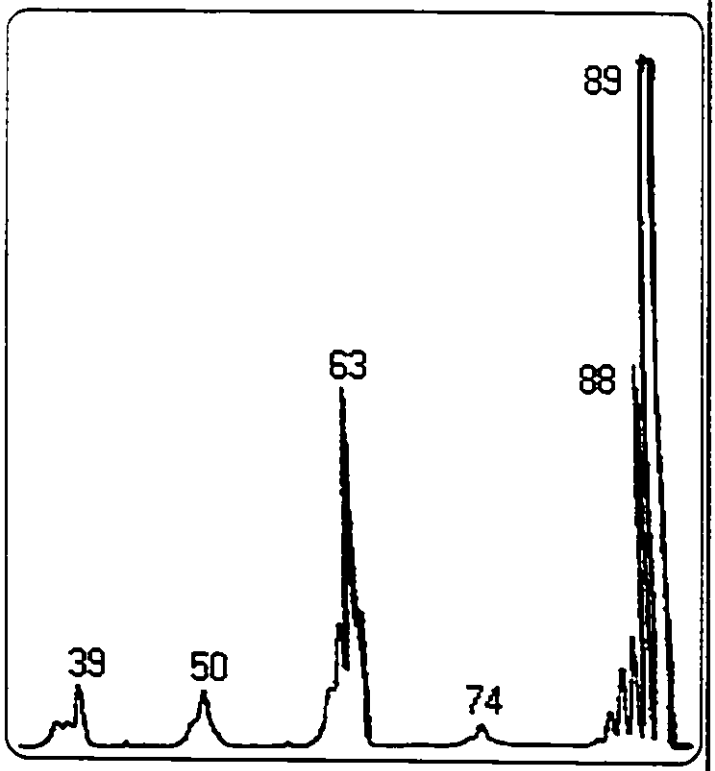

S54- He CA mass spectrum of m/z 89 from 1,6-heptadiyne.

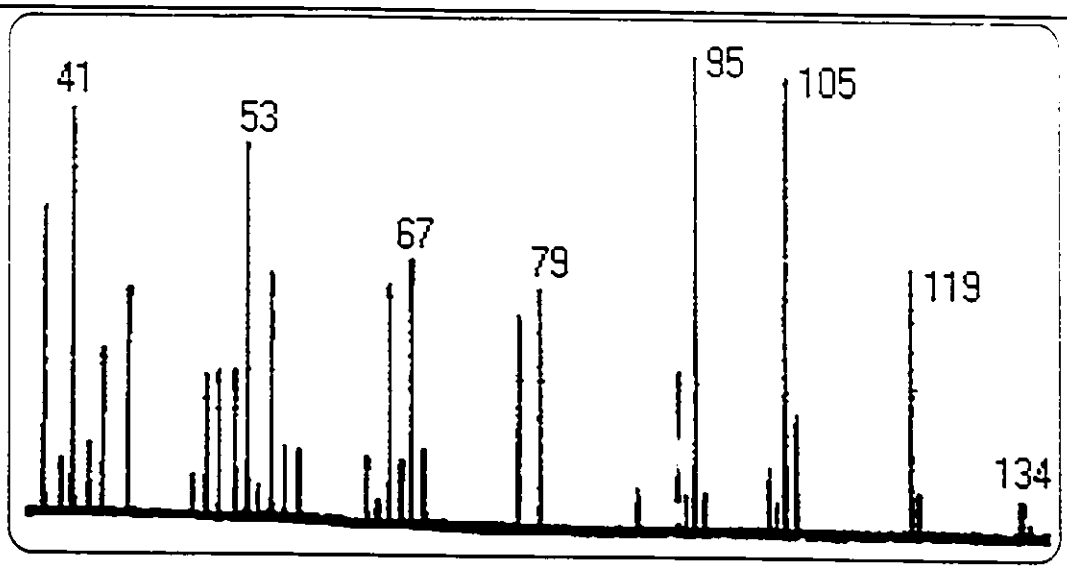

S55- Electron Impact mass spectrum of 1,5-decadiyne.

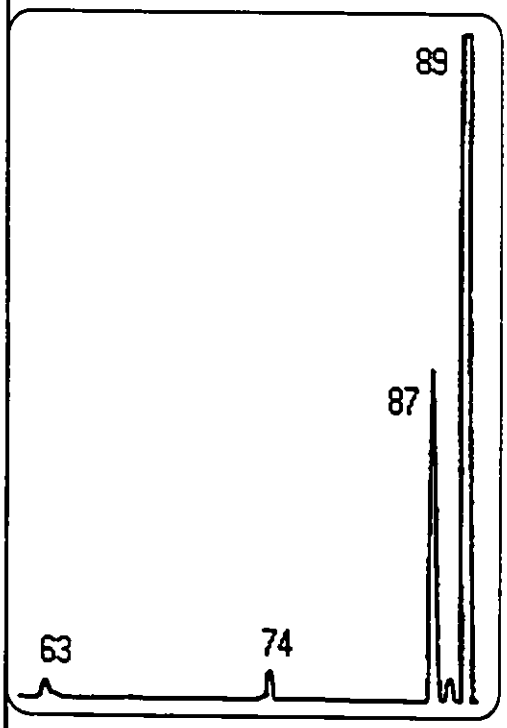

S56- MI mass spectrum of m/z 89 from 1,5-decadiyne.

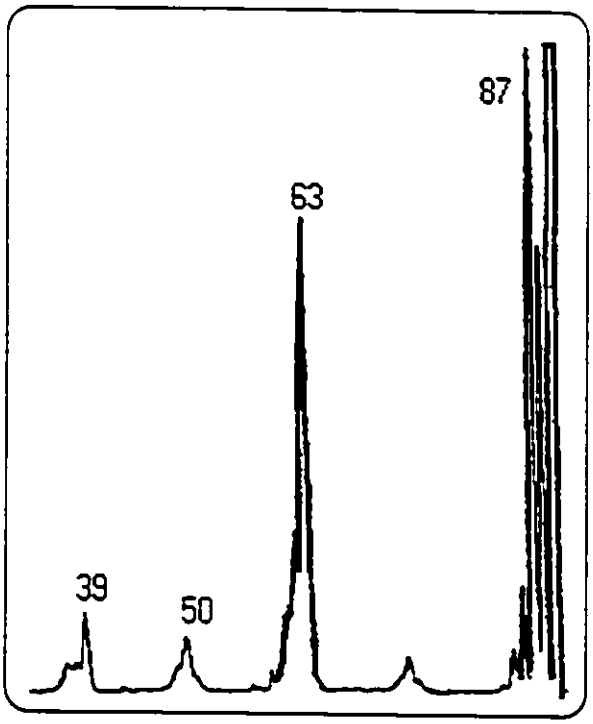

S57- He CA mass spectrum of m/z 89 from 1,5-decadiyne.

APPENDIX III

ISOTOPE EFFECTS - CHAPTER 5

ESTIMATION OF ISOTOPE EFFECTS

The isotope effect will be different depending whether 0, 1 or 2 D atoms are present in the fragment produced.

ONE D

	CH_4O	CH_3DO
Random	66.6	33.3
Observed	44	56

Therefore, $0.44 = 66.6/(66.6 + 33.3\ i_1)$, where i_1 is the isotope effect when only one D atom is involved. Solve for i_1: 2.55.

TWO D

	CH_4O	CH_3DO	CH_2D_2O
Random	42.4	48.5	9.1
Observed	17	55	28

Therefore, $0.17 = 42.4/(42.4 + 48.5\ i_1 + 9\ i_2)$, where i_2 is the isotope effect when two D atoms are involved. Replace i_1 and solve for i_2: 9.14.

To check, $y = x/(42.4 + 48.5\ i_1 + 9.1\ i_2)$, where x is the random ratio and y should correspond to the observed ratio.

For 0 D atom: 17.0 For 1 D atom: 49.6 For 2 D atoms: 33.4

Thus, i_1 is too small and i_2 is too large. By "playing" with the numbers, we can obtain more satisfactory values with a smaller error of ± 1.2.

So, for i_1=3.05 and i_2=8.55, we obtain 15.8, 55.2 and 29.0 for 0, 1 and 2 D atoms respectively.

THREE D

	CH_4O	CH_3DO	CH_2D_2O	CHD_3O
Random	25.5	50.9	21.8	1.8
Observed	8	37	43	12

Therefore, $0.37 = 50.9i_1/(25.5 + 50.9\ i_1 + 21.8\ i_2 + 1.8\ i_3)$, where i_3 is the isotope effect when 3 D atoms are involved. Replace i_1=3.05 and i_2=8.55 and solve for i_3: 29.2.

To check, $y = x/(25.5 + 50.9i_1 + 21.8i_2 + 1.8i_3)$.

For 0 D atom: 6.1 For 1 D atom: 37.0

For 2 D atoms: 44.4 For 3 D atoms: 12.5

This i_3 number produces values very close to the observed values (± 2). By "playing" with the numbers (decreasing i_2 and i_3), very little improvement is obtained.

Therefore, the isotope effects for 0,1 and 2 deuterium atoms are i_1=3.05, i_2=8.55 and i_3=29.2 respectively. Although this may not have any real significance, note that the isotope effects increase approximately according to 3^{n-1}, where n=number of D atoms.

REFERENCES - CHAPTER 2

1. R.W. Kiser, Introduction to Mass Spectrometry and its Applications, Prentice Hall, N.J., (1965).

2. J. Roboz, Introduction to Mass Spectrometry, Instrumentation and Techniques, John Wiley and Sons, N.Y., (1968).

3. E. Goldstein, Berl. Ber., **39**, 691, (1886).

4. a) W. Wien, Wied. Ann., **65**, 440, (1898) b) Ann. Physik, **8**, 244, (1902).

5. S. Meyerson, Org. Mass Spectrom., **21**, 197, (1986).

6. R.P. Morgan, J.H. Beynon, R.H. Bateman and B.N. Green, Int. J. Mass Spectrom. Ion Phys., **28**, 171, (1978).

7. J.L. Holmes, A.A. Mommers, J.K. Terlouw and C.E.C.A. Hop, Int. J. Mass Spectrom. Ion Proc., **68**, 249, (1986).

8. M.C. Blanchette, J. Bordas-Nagy, J.L. Holmes, C.E.C.A. Hop, A.A. Mommers and J.K. Terlouw, Org. Mass Spectrom., **23**, 804, (1988).

9. S.G. Lias, J.E. Bartmess, J.F. Liebman, J.L. Holmes, R.D. Levin, W.G. Mallard, J. Phys. Chem. Ref. Data, **17**, Suppl. 1, (1988).

10. M.C. Blanchette, M.Sc. Thesis, University of Ottawa, (1987).

11. P.C. Burgers and J.L. Holmes, Org. Mass Spectrom., **17**, 123, (1982).

12. K. Maeda, G.P. Semeluk and F.P. Lossing, Int. J. Mass Spectrom. Ion Phys., **1**, 395, (1968) and F.P. Lossing and J.C. Traeger, idem, **19**, 9, (1976).

13. R.G Cooks, J.H. Beynon, R.M. Caprioli and G.R. Lester, Metastable Ions, Elsevier Scientific Publishing Co., Amsterdam, (1973).

14. P. Longevialle, Principes de la Spectrométrie de Masse des Substances Organiques, Masson, Paris, (1980).

15. M. Sirois, J.L. Holmes and C.E.C.A. Hop, Org. Mass Spectrom., **25**, 167, (1990).

16. H.M. Rosenstock and M. Krauss, Mass Spectrometry of Organic Ions, F.W. McLafferty ed, Academic Press, New York, (1963).

REFERENCES - CHAPTER 3

17. Kartsen Levsen, Fundamental Aspects of Organic Mass Spectrometry, vol 4, New York, (1978).

18. J.B. Pedley, R.D. Naylor and S.P. Kirby, Thermochemical Data of Organic Compounds, 2nd Ed, London, N.Y., Chapman and Hall, (1986).

19. S.W. Benson, Thermochemical Kinetics, 2nd Ed, Wiley-Inter Science, New York, (1976).

20. a) J.L. Holmes and F.P. Lossing, J. Am. Chem. Soc., **102**, 1591, (1980). b) J.L. Holmes and F.P. Lossing, J. Am. Chem. Soc., **104**, 2648, (1982).

21. J.C. Traeger and R.G. McLoughlin, Int. J. Mass Spectrom. Ion Phys., **27**, 319, (1978).

22. M.C. Blanchette, J.L. Holmes and F.P. Lossing, Org. Mass Spectrom., **22**, 701, (1987).

23. J.L. Holmes, Org. Mass Spectrom., **20**, 169, (1985).

24. P.C. Burgers and J.L. Holmes, Int. J. Mass Spectrom. Ion Proc., 58, 15, (1984).

25. P.C. Burgers, A.A. Mommers and J.L Holmes, J. Am. Chem. Soc., **105**, 5976, (1983).

26. J.L. Holmes, M. Fingas and F.P. Lossing, Can. J. Chem., **59**, 80, (1981).

27. J.L. Holmes and F.P. Lossing, the uses of gas phase ion thermochemistry

28. F.P. Lossing, J. Am. Chem. Soc., **99**, 7526, (1977)

29. J.L. Holmes, F.P. Lossing and R.A. MacFarlane, Int. J. Mass Spectrom. Ion Proc., **86**, 209, (1988).

30. J.L. Holmes and F.P. Lossing, Can. J. Chem., **60**, 2365, (1982).

31. F.P. Lossing and J.L. Holmes, J. Am. Chem. Soc., **106**, 6917, (1984).

32. J.L. Holmes, P.C. Burgers, J.K. [redacted]ouw, H. Schwarz, B. Ciommer and H. Halim, Org. Mass Spectrom., **18**, 208, (1983).

33. C. Lifshitz, P. Gotchiguian and R. Roller, Chem. Phys. Letters, **95**, 106, (1983).

34. P.C. Burgers, J.L. Holmes, A.A. Mommers, J.E. Szulejko and J.K. Terlouw, Org. Mass Spectrom., **19**, 442, (1984).

35. J.L. Holmes, F.P. Lossing and Allan Maccoll, J. Am. Chem. Soc., **110**, 7939, (1988).

36. J.L. Holmes and F.P. Lossing, J. Am. Chem. Soc., **110**, 7943, (1988).

37. J.L. Holmes and F.P. Lossing, Int. J. Mass Spectrom. Ion Proc., 92, 111, (1989).

38. E. Buncel, C.C. Lee, Isotopes in Organic Chemistry, Elsevier, (1975), Chapter 3 by J.L. Holmes.

39. J.A. Hipple and E.U. Condon, Phys. Rev., 29, 54, (1945).

40. T.W. Shannon and F.W. McLafferty, J. Am. Chem. Soc., 88, 5021, (1966).

41. J.L. Holmes and J.K. Terlouw, Org. Mass Spectrom., 15, 3838, (1980).

42. Ch. Ottinger, Phys. Letters, 17, 269, (1965).

43. E.G. Jones, L.E. Bauman, J.H. Beynon and R.G. Cooks, Org. Mass Spectrom., 7, 185, (1973).

44. H.M. Rosenstock, V.H. Dibeler and F.N. Harllee, J. Chem. Phys., 40, 591, (1964).

45. H.D. Smyth, Phys. Rev., 25, 452, (1925).

46. K.R. Jennings, Int. J. Mass Spectrom. Ion Phys., 1, 227, (1968).

47. W.F. Haddon and F.W. McLafferty, J. Am. Chem. Soc., 90, 4745, (1968).

48. P.O. Danis, R. Feng, F.W. McLafferty, Anal. Chem., 58, 355, (1986).

49. P.J. Todd and F.W. McLafferty, Int. J. Mass Spectrom. Ion Phys., 38, 371, (1981).

50. F.W. McLafferty, P.F. Bente, III, R. Kornfeld, S. Tsai and I. Howe, J. Am. Chem. Soc., 95, 2120, (1973).

51. F.W. McLafferty, R. Kornfeld, W.F. Haddon, K. Levsen, I. Sakai, P.F. Bente III, S. Tsai and H.D.R. Shuddemage, J. Am. Chem. Soc., 95, 3886, (1973).

52. J.L. Holmes, A.A. Mommers, J.E. Szulejko and J.K. Terlouw, J. Chem. Soc, Chem. Commun., 165, (1984).

53. J.K. Terlouw, W. Heerma and G. Dijkstra, Org. Mass Spectrom., 16, 326, (1981).

54. P.C. Burgers, J.L. Holmes, J.K. Terlouw and B. van Baar, Org. Mass Spectrom., 20, 202, (1985).

55. J.L. Holmes and A.A. Mommers, Org. Mass Spectrom., 19, 460, (1984).

56. P.C. Burgers, J.L. Holmes, A.A. Mommers and J.K. Terlouw, Chem. Phys. Letters, 102, 1, (1983).

57. R. Clair, J.L. Holmes, A.A. Mommers and P.C. Burgers, Org. Mass Spectrom., 20, 207, (1985).

58. C.A. Lieder and J.I. Brauman, J. Am. Chem. Soc., **96**, 4028, (1974).

59. P.O. Danis, C. Wesdemiotis and F.W. McLafferty, J. Am. Chem. Soc., **105**, 7454, (1983).

60. C. Wesdemiotis and F.W. McLafferty, Chem. Rev., **87**, 485, (1987) and references therein.

61. J.L. Holmes, Mass Spectrom. Rev., **8**, 513, (1989) and references therein.

62. G.I. Gellene and R.F. Porter, Acc. Chem. Res., **16**, 200, (1983).

63. P.O. Danis, R. Feng and F.W. McLafferty, Anal. Chem., **58**, 348, (1986).

64. J.K. Terlouw, W.M. Kieskamp, J.L. Holmes, A.A. Mommers and P.C. Burgers, Int. J. Mass Spectrom. Ion Proc., **64**, 245, (1985).

65. J.L. Holmes and M. Sirois, Org. Mass Spectrom., **25**, 481, (1990).

66. J.L. Holmes, F.P. Lossing, J.K. Terlouw and P.C. Burgers, J. Am. Chem. Soc., **104**, 2931, (1982).

67. R.G. Cooks, J.H. Beynon and T. Ast, J. Am. Chem. Soc., **94**, 1004, (1972).

68. J.L Holmes, J.K. Terlouw, P.C. Burgers and R.T. Rye, Org. Mass Spectrom., **15**, 149, (1980).

69. D. Harnish, J.L. Holmes, F.P. Lossing, A.A. Mommers, A. Maccoll and M.N. Mruzek, Org. Mass Spectrom., **25**, 381, (1990).

70. J.H. Vajda, A.G. Harrison, A. Hirota and F.W. McLafferty, J. Am. Chem. Soc., **103**, 36, (1981).

71. C. Wesdemiotis, R. Csencsits and F.W. McLafferty, Org. Mass Spectrom., **20**, 98, (1985).

72. J.K. Terlouw, J.L. Holmes and P.C. Burgers, Int. J. Mass Spectrom Ion Proc., **66**, 239, (1985).

73. J.L. Holmes, C.E.C.A. Hop and J.K. Terlouw, Org. Mass Spectrom., **21**, 777, (1986).

74. N. Heinrich, H. Schwarz, J. Schmidt and Y. Apeloig, J. Am. Chem. Soc., **109**, 1317, (1987).

75. B.L.M. van Baar, P.C. Burgers, J.L. Holmes and J.K. Terlouw, Org. Mass Spectrom., **23**, 355, (1988).

REFERENCES - CHAPTER 4

76. P.C. Burgers and J.K. Terlouw, Specialist Periodical Reports: Mass Spectrometry, ed. M.E. Rose, The Royal Society of Chemistry, London, 1989, **10**, Chapter 2.

77. a) A-M. Dommröse and H.F. Grützmacher, Org. Mass Spectrom., **22**, 437, (1987). b) R. Wolf, A-M. Dommröse and H.F. Grützmacher, Org. Mass Spectrom., **23**, 26, (1988).

78. J.L. Holmes, Ion Stuctures paper

79. J.W. Larson and T.B. McMahon, J. Am. Chem. Soc., **106**, 1257, (1984).

80. M. Meot-Ner, J. Am. Chem. Soc., **106**, 1257, (1984).

81. R. Postma, P.J.A. Ruttink, F.B. van Dijneveldt, J.K. Terlouw and J.L. Holmes, Can. J. Chem., **63**, 2798, (1985).

82. P.C. Burgers, J.L. Holmes, C.E.C.A. Hop, R. Postma, P.J.A. Ruttink and J.K. Terlouw, J. Am. Chem. Soc., **109**, 7315, (1987).

83. P.C. Burgers, J.L. Holmes, C.E.C.A. Hop and J.K. Terlouw, Org. Mass Spectrom., **21**, 549, (1986).

84. S. Hammerum, J. Chem. Soc. Chem. Commun., 858, (1988).

85. D.J. McAdoo, Mass Spec. Reviews, **7**, 363, (1988).

86. H. Schwarz and D. Stahl, Int. J. Mass Spectrom. Ion Phys., **36**, 285, (1980).

87. R.D. Bowen, D.H. Williams, J. Chem. Soc. Chem. Commun., 836, (1981).

88. a) D.J. McAdoo, J.C. Traeger, C.E. Hudson and L.L. Griffin, J. Chem. Phys., **92**, 1524, (1988) b) J.C. Traeger, C.E. Hudson and D.J. McAdoo, preprint.

89. J.L. Holmes, P.C. Burgers, M.Y.A. Mollah and P. Wolkoff, J. Am. Chem. Soc., **104**, 2879, (1982).

90. S. Hammerum and P.J. Derrick, J. Chem. Soc. Perkin Trans. II, 1577, (1986).

91. M.C. Blanchette, J.L. Holmes and F.P. Lossing, Org. Mass Spectrom., **24**, 673, (1989).

92. T. Weiske, S. Akkök and H. Schwarz, Int. J. Mass Spectrom. Ion Proc., **76**, 117, (1987).

REFERENCES - CHAPTER 5

93. T.H. Morton, Org. Mass Spectrom., **26**, 1, (1991).

94. S. Hammerum and H.E. Audier, J. Chem. Soc. Chem. Commun., 860, (1988).

95. J. Parker, personal communication.

96. M. George and J.L. Holmes, Org. Mass Spectrom., **25**, 605, 1990.

97. D.J. McAdoo, W. Farr and C.E. Hudson, J. Am. Chem. Soc., **102**, 5165, (1980).

98. S.G. Lias, J.F. Liebman, R.D. Levin, J. Phys. Chem. Ref. Data, **13**, 695, (1984).

99. J.L. Holmes, D.C.M. Tong and R.T.B. Rye, Org. Mass Spectrom., **6**, 897, (1972).

REFERENCES - CHAPTER 6

100. Y. Apeloig, D. Arad, J. Am. Chem. Soc., **107**, 5285, (1985).

101. F.P. Lossing and J.L. Holmes, J. Am. Chem. Soc., **106**, 6917, (1984).

102. E. Uggerud, D. Arad, Y. Apeloig, H. Schwarz, J. Chem. Soc. Chem. Commun., 1015, (1989).

103. E.M. Emery, Anal. Chem., **32**, 1495, (1960).

104. P.C. Price, H.S. Swofford Jr and S.E. Buttrill Jr, Anal. Chem., **50**, 1127 (1978).

105. F.W. McLafferty and F.M. Bockhoff, J. Am. Chem. Soc., **101**, 1783, (1979).

106. D. Cameron and R.G. Cooks. J. Am. Chem. Soc., **101**, 3162, (1979).

107. D.J. Burinsky, R.G. Cooks, E.K. Chess and M.L. Gross, Anal. Chem., **54**, 295, (1982).

108. D.L. Corina, J.N. Wright and K.E. Ballard, Org. Mass Spectrom., **18**, 60, (1983).

109. F.P.L. Lossing, J.L.H. Holmes, J. Am. Chem. Soc., **107**, 5285, (1985).

110. B. Halton, C.J. Randall, G.J. Gainsford and W.T. Robinson, Aust. J. Chem., **106**, 6917, (1984).